~~CONFIDENTIAL~~

COPY NO. 22

SNAP 27/ALSEP SAFETY EVALUATION REPORT

February 28, 1969

~~GROUP 4~~

~~Downgraded at 3 year intervals; declassified after 12 years.~~

~~DEFENSE INFORMATION~~

~~This material contains information affecting the national defense of the United States within the meaning of the espionage laws, Title 18, U.S.C., Secs. 793 and 794, the transmission or revelation of which in any manner to an unauthorized person is prohibited by law.~~

~~CONFIDENTIAL~~

~~CONFIDENTIAL~~

SNAP 27/ALSEP SAFETY EVALUATION REPORT

RECD:9520 3-6-69
CODE
9521
9522
1 Action Reply
2. Note & Forward
3. See Me
4. Note & File
5. Destroy

February 28, 1969

Prepared by:

SNAP 27/ALSEP INTERAGENCY SAFETY EVALUATION PANEL

AEC PANEL MEMBERS	NASA PANEL MEMBERS	DoD PANEL MEMBERS
G. P. Dix, SNS	T. B. Kerr, HQ	M. MacWilliams, AFINS
T. J. Dobry, SNS	E. Katzen, ARC	G. Stewart, AFINS
C. Richmond, DBM	J. Hallissy, LaRC	P. Zigman, NRDL
J. Holland, DBM	S. Fellows, MSFC	G. Crane, AFSC
C. Osterberg, DBM	C. Barnes, MSC	D. Livermore, AFINS
I. Van der Hoven, ESSA	C. Weaver, USPHS	
R. Miller, ALO	C. Overbey, KSC	

The appendices list names of other contributors in specialized areas.

~~This material contains information affecting the national defense of the United States within the meaning of the espionage laws, Title 18, U.S.C., Secs. 793 and 794, the transmission or revelation of which in any manner to an unauthorized person is prohibited by law.~~

~~GROUP 4~~

~~DOWNGRADED AT 3 YEAR INTERVALS; DECLASSIFIED AFTER 12 YEARS~~

~~CONFIDENTIAL~~

TABLE OF CONTENTS

		Page No.
I.	INTRODUCTION	1
	A. General	1
	B. Mission Plan	1
	C. Interagency Safety Review Panel	1
	D. Scope of the Review	2
II.	SNAP 27/ALSEP	3
	A. Application	3
	B. Launch Site	3
	C. Meteorology of Site Environs	5
	D. Apollo Launch Vehicle	5
	E. Graphite LM Fuel Cask (GLFC)	6
	F. Secondary Thermal Shield	7
	G. Fuel Capsule Assembly (FCA)	7
	H. Fuel	8
III.	DESCRIPTION OF POTENTIAL ACCIDENTS	10
	1. Phase Description	10
	2. Accidents Postulated and SNAP 27 Response	10
	3. Likelihood and Severity of Accidents	10
	A. Prelaunch and Launch Phase	11
	1. Phase Description	11
	2. Accidents Postulated and SNAP 27 Response	11
	a. Shock Overpressure and Impulse	13
	b. Fragments	14
	c. Fireball and Afterfire	16
	d. Impact	18
	3. Likelihood and Severity of Prelaunch and Launch Accidents	19
	B. Early Ascent Phase	21
	1. Phase Description	21
	2. Accidents Postulated and SNAP 27 Response	21
	3. Likelihood and Severity of Early Ascent Accidents	22

TABLE OF CONTENTS
Continued

	Page No.
a. Fuel Release in Firestream	22
b. Impact	22
c. Marine Releases	22
C. Suborbital Phase	23
1. Phase Description	23
2. Accidents Postulated and SNAP 27 Response	23
a. Reentry Failure of GLFC	24
b. Impact of GLFC	24
3. Likelihood and Severity of Suborbital Accidents	25
a. Reentry Failure of GLFC	25
b. Impact Failure of GLFC	25
D. Orbital Phase	26
1. Phase Description	26
2. Accidents Postulated and GLFC Response	26
a. Reentry Failure of GLFC	26
b. Explosion	26
c. Impact of GLFC	27
3. Likelihood and Severity of Orbital Accidents	27
a. Reentry Failure of GLFC	27
b. Explosion	27
c. Impact Failure of GLFC	27
E. Superorbital Phase	28
1. Phase Description	28
2. Accidents Postulated and GLFC Response	28
a. GLFC Ablator Failure	29
b. Explosion	29
c. Impact of GLFC	29

TABLE OF CONTENTS
Continued

	Page No.
3. Likelihood and Severity of Superorbital Accidents	30
a. Reentry Failure of GLFC	30
b. Explosion	30
c. Impact Failure of GLFC	30
IV. EVALUATION OF POTENTIAL ACCIDENTS	31
A. Prelaunch and Launch Phase	33
1. Prompt Release	34
a. Source Term	34
b. Areal Extent of Lung Burdens and Ground Concentrations	35
2. Delayed Release	35
a. Source Term	35
b. Areal Extent of Lung Burdens and Ground Concentrations	36
3. Point Source Release (Impact)	36
a. Source Term	36
b. Areal Extent of Lung Burdens and Ground Concentrations	37
B. Early Ascent Phase	37
1. Source Term	37
2. Areal Extent of Lung Burdens and Ground Concentrations	38
C. Reentry Phase	38
1. Source Term	38
2. Areal Extent of Lung Burdens and Ground Concentrations	39

TABLE OF CONTENTS
Continued

	Page No.
V. SUMMARY EVALUATION OF RISK	41
A. Risk Criteria	41
1. Radiation Criteria	41
2. Meteorological Conditions	41
3. Probabilistics	41
4. Contingency Plans	41
B. Accident Evaluation	42
1. Potential Accidents	42
2. Population-at-Risk	42

TABLE I - Probability Estimates for Fuel Release SNAP 27 Apollo Mission

TABLE II - Evaluation of Potential Accidents

FIGURE 1 - Apollo Lunar Surface Experiment Package with SNAP 27 Radioisotope Electric Generator

FIGURE 2 - Map of John F. Kennedy Space Center

FIGURE 3 - Cape Kennedy & Merritt Island Launch Area

FIGURE 4 - Saturn V/Apollo Configuration

FIGURE 5 - Graphite LM Fuel Cask (GLFC)

FIGURE 6 - Fuel Capsule Assembly (FCA)

FIGURE 7 - Fuel Vaporization

APPENDIX A - Report of SNAP 27/ALSEP Range Safety Working Group for SNAP 27 Interagency Safety Review Panel

APPENDIX B - Report of SNAP 27 Reentry Working Group for SNAP 27 Interagency Safety Review Panel

APPENDIX C - Report of the Meteorological Working Group SNAP 27 Safety Review Panel

APPENDIX D - Review of the Marine Aspects of SNAP 27 Safety Analysis Report

APPENDIX E - Biomedical Hazard Evaluation of SNAP 27/ALSEP

SNAP 27/ALSEP SAFETY EVALUATION REPORT

I. INTRODUCTION

A. General

This report documents the independent nuclear safety evaluation of the SNAP 27/ALSEP mission conducted by the Interagency Safety Review Panel. It provides the Agency Heads of NASA, AEC, and DoD with a common nuclear safety basis for their recommendations regarding flight approval. Since the launch involves "a major nuclear system," the NASA, as the action agency will seek presidential approval through the National Aeronautics and Space Council (NASC). The report was prepared by the Panel and delineates the Panel's assessment of risks involving nuclear health and safety in potential mission aborts. It summarizes the supporting safety documentation submitted to the Panel for review, as well as information introduced by the Panel and independent tests and analyses conducted by the Panel and its consultants during the course of the review.

B. Mission Plan

Deployment of the Apollo Lunar Surface Experiments Package (ALSEP) will be the primary scientific objective of the second lunar landing mission. SNAP 27 is designed to provide continuous, reliable, long-lived electric power for ALSEP. The first launch of SNAP 27/ALSEP is scheduled for the 3rd quarter of 1969 and is expected to be followed by additional SNAP 27/ALSEP flights spaced at approximately three month intervals.

C. Interagency Safety Review Panel

The safety review was conducted from early September, 1968 through February, 1969 by the Panel and its working groups. Because of the large volume of data to be digested, five discipline-oriented working groups were utilized: Range Safety, Reentry, Meteorology, Oceanography, and Biomedical. Approximately one hundred varied scientific and engineering specialists from a number of government agencies, laboratories, and universities comprised the five working groups and effectively brought the best available expertise to bear for the review. Appendices A thru E contain the working group reports.

The working groups reviewed SNAP 27/ALSEP safety documentation submitted by the General Electric Company, prime contractor for SNAP 27, and performed their own independent calculations and tests, when required.

The Interagency Panel was convened from December 9-13, 1968, to discuss the safety considerations of SNAP 27. At this meeting each working group presented its findings to the Panel, supported by expert testimony of key scientific and engineering specialists in the group.

D. Scope of the Review

This report provides an assessment of the nuclear risk to operations personnel and the general population and considers a spectrum of postulated accidents. The accidents considered were categorized by the following mission phases: Prelaunch and Launch, Early Ascent, Suborbital, Orbital, and Superorbital. During these phases the SNAP 27 Fuel Capsule Assembly (FCA) is contained in the Graphite LM Fuel Cask (GLFC) installed on the Lunar Module Descent Stage. After lunar descent SNAP 27 poses no potential risk to the earth's population.

Section II is a description of SNAP 27/ALSEP. The risk assessment is conducted sequentially by mission phase. Section III identifies and describes the mission phases, postulated accidents and SNAP 27 response, and considerations bearing on the probability of the accidents. It treats the range safety and reentry aspects of various Saturn V/Apollo aborts. Section IV presents an evaluation of the radiological source term, its transport in the environment, and the resultant lung doses and ground concentrations. Section V summarizes the combined probabilities and consequences of the various postulated accidents.

Storage, transportation, and ground handling accidents at Cape Kennedy are not discussed at length in this report. The Panel does not consider them to be significant because: (1) It is unlikely that a fuel release could occur during this phase of operation; and (2) The operations will be accomplished within existing AEC radiation safety guidelines and under established storage, handling, and radiological control procedures. The Panel does recommend, however, that SNAP 27/ALSEP storage and handling procedures, radiological control plans, and contingency plans be prepared, reviewed, and approved by appropriate NASA, AEC, and DoD officials responsible for SNAP 27/Apollo operations.

II. SNAP 27/ALSEP

A. Application

ALSEP will employ a SNAP 27 system as a source of electric power for the lunar surface experiments. This application will mark the first use of nuclear electric power on the moon and is designed to provide continuous power throughout the extremes of temperature of the lunar nights and days. The ALSEP package consists of the $_{238}$Pu fueled SNAP 27, scientific instruments and supporting equipment for performing lunar experiments and provision for transmitting data back to earth for a period of at least a year. The use of nuclear power for the experiments is the culmination of three and one-half years of effort on the part of the AEC and NASA. Its use is considered essential to the success of the scientific experiments because of its unique ability to produce continuous power for extended periods during the extremes of lunar temperature and long periods of darkness.

Instruments, support equipment, and crew handling tools are transported to the moon in two major instrument subpackages. Both subpackages are stored inside the LM descent stage. The Graphite LM Fuel Cask (GLFC) containing the SNAP 27 fuel capsule is mounted on the external surface of the LM descent stage where it is accessible to the astronauts on the lunar surface. Subpackage 1 contains the scientific instruments and data transmission equipment. Subpackage 2 contains geological equipment, the SNAP 27 generator assembly and associated electrical power system equipment.

The ALSEP is inoperative during the trip to the moon. After the LM vehicle lands on the moon, a crew member will remove the subpackages from the equipment bay, remove the SNAP 27 fuel capsule from the reentry body, insert it into the generator assembly, and deploy the experiments and power system. Figure 1 illustrates the experiment layout on the lunar surface.

B. Launch Site

Figure 2 shows the Cape Kennedy region and specifically the NASA Kennedy Space Center (KSC) located on Merritt Island Launch Area (MILA). MILA is located on the East Coast of Florida, 150 miles south of Jacksonville, immediately northwest of and adjacent to Cape Kennedy Air Force Station. MILA is located in the northeast section of Brevard County which has a total population of about 250,000. Most of the county population is concentrated along the coast south from Titusville which is 12 miles west of the launch site. Other adjacent population centers are Orlando (metropolitan area - 200,000), 50 miles west, and Daytona Beach (65,000), 50 miles north.

Figure 3 shows the detailed chart of MILA and environs. MILA is an irregularly shaped area about 34 miles long and 5 to 10 miles wide. It is generally a flat, level area of sandy soil only a few feet above sea level (less than 8 feet). It is bound by shallow tidewater river basins from several hundred feet to several thousand feet wide, except to the north, where it adjoins marshy, uninhabited land. Pad A of Launch Complex 39 is assumed to be the pad from which the SNAP 27/ALSEP will be launched although launch can occur from Pad A or B. It is located in the extreme northeast corner of MILA adjacent to a controlled beach and Atlantic Ocean to the east.

The normal daytime population of MILA is about 15,000 most of which are centered in the industrial and administrative area about six miles southwest of the launch area; however, about 3500 people are located within a five-mile radius of the launch pad on an average work day. About 6000 people are normally located on the Cape Kennedy Air Force Station from 5 - 12 miles southeast of the launch complex. During a launch additional people are located in the Vehicle Assembly Building (VAB), at the press site, and in the Launch Control Center (LCC) about three miles west of the pad. Also during Apollo launches large numbers of spectators are located at the site boundary. All personnel within about an eight-mile radius of the pad are under administrative control of the range authority. A stringent exclusion area is maintained within a two-mile radius of the pad during launch operations from which all personnel are excluded except a few essential operational people who are protected in bunkers.

The Saturn V/Apollo vehicle, after assembly, is transported from the VAB with the Mobile Launcher by the Crawler-Transporter and placed on one of the Launch Complex 39 pads for final preparations. The center elevation of the concrete pad is 48 feet above sea level. The Mobile Service Structure which services the Saturn for launch is about 400 feet high and is moved 7000 feet from the pad at launch. The Umbilical Tower of the Mobile Launcher remains at the pad thru launch. Propellant storage facilities for LOX, RP-1, and LH_2 are located 1500 feet from the launch pad. Two holding ponds to retain RP-1 and/or potentially contaminated effluent spilled in the flame bucket are capable of holding the entire RP-1 load of a Saturn V vehicle. The water deluge system is capable of spraying the pad area with water at the rate of 50,000 gpm.

C. Meteorology of Site Environs

The atmospheric diffusion conditions in the MILA area have been considered in assessing the meteorological transport of potential radioactive effluents. For the ground level conditions the more stable atmospheric conditions (slow vertical and horizontal diffusion rates) result in higher effluent downwind surface air concentrations. For the elevated source conditions (above 1000 meters), the controlling meteorological situation is rapid downward diffusion as typified by unstable atmospheric conditions. This will maximize the local surface effluent air concentrations. The stable condition, on the other hand, will tend to keep the elevated source from diffusing to the ground until several tens of miles downwind and consequently will allow more time for the cloud to diffuse. This will result in lower effluent concentrations over a larger area.

Based on data from the 200 foot meteorological tower between Air Force Launch Complexes 15 and 16, it can be concluded that in the first few hundred feet above the ground, the atmosphere is generally stable at night (2000-0700 hours) and unstable during the daytime. Seasonally, the unstable condition is maximized in the summer and the stable condition is most intense and persistent in the winter. On an annual basis, stable conditions occur about 47 percent of the time.

For effluent releases above 1000 meters, atmospheric conditions ranging from moderately unstable to slightly stable usually occur. Unstable conditions predominate in the lower layers during the daytime hours. During the night, conditions tend to be neutral to slightly stable at this height and the more stable layers near the ground will tend to inhibit the elevated effluent from reaching the ground.

Wind directions, especially in the warmer half of the year, follow a diurnal cycle with flow from the sea during the day and weaker flow to the sea at night up to about 5000 feet altitude. In the period November through January, winds prevail from the northwest with no appreciable diurnal cycle.

D. Apollo Launch Vehicle

The SNAP 27/ALSEP is transported to the lunar surface on the descent stage of the Apollo Spacecraft Lunar Module (LM). The spacecraft is boosted through the translunar injection phase by the three stage Saturn V launch vehicle shown in Figure 4. The combined system is about 360 feet high on the pad with the SNAP 27

located at about the 280 foot level. The spacecraft is composed of the Command Module (CM) with its Launch Escape System (LES), the Service Module (SM), the LM Adapter (SLA), and the Lunar Module (LM). The SM holds about 39,000 pounds of hypergolic propellant and the LM holds about 22,000 pounds. Propellant for both is a 50/50 mixture of hydrazine (N_2H_4) and unsymmetrical dimethylhydrazine (UDMH), with nitrogen tetroxide (N_2O_4) as oxidizer.

The Saturn V first stage, S-IC, has a propellant capacity of 4,723,000 pounds of LOX and RP-1. The second stage, S-II, has a propellant capacity of about 985,000 pounds of LOX and LH_2. The S-IVB third stage contains about 230,000 pounds of LOX and LH_2. The total propellant aboard the Apollo/Saturn V system at launch is, therefore, about 6,000,000 pounds of hypergolics, LOX, RP-1, and LH_2. Figure 4 summarizes data on each stage. After attaining earth orbit, the S-IVB is restarted when over Houston, Texas, and boosts the spacecraft to translunar injection at 35,600 ft/sec and about 160 miles altitude before it is separated.

E. Graphite LM Fuel Cask (GLFC)

The Graphite LM Fuel Cask (GLFC), shown in Figure 5 contains the Fuel Capsule Assembly (FCA) during the operational mission from launch up to lunar surface deployment. In the event of an abort of the spacecraft, the GLFC is designed to provide reentry protection and containment for the fuel. It is mounted on the outside of the LM descent stage inside the Spacecraft LM Adaptor (SLA). The FCA is removed from the GLFC on the lunar surface by an astronaut and installed in the SNAP 27 generator.

The GLFC is a cylindrical container with hemispherical ends which consists of a primary heat shield, Secondary Thermal Shield (STS), and fuel capsule support structure. The outside container with end caps is the primary heat shield made of Hitco Pyrocarb graphite. The cylinder wall is 0.35 inches thick and the end cap wall is 0.7 inches thick. The overall length is 23 inches and the diameter is 8 inches. The GLFC, with the FCA inserted, weighs about 40 pounds and is mounted on the LM by a titanium support structure supplied by Bendix Corporation.

The primary heat shield is designed to protect the fuel capsule during reentry by heat sink, reradiation, and ablation methods. In normal vacuum operations, heat rejected by the FCA is transmitted through the STS and absorbed by the primary heat shield where it is both reradiated to the external environment and conducted to the GLFC support structure. During pad operations up to lift-off the NASA specification for the surface of the GLFC is air cooling to

less than 350°F which is below the spontaneous ignition temperature of the hypergolic fuel in air. Qualification tests indicate that the GLFC will actually be about 220°F when air cooled on the vehicle.

F. Secondary Thermal Shield

The Secondary Thermal Shield (STS) is a beryllium cylindrical barrel 4.13 inches outside diameter, 0.565 inches thick, and 13.7 inches long. It contains the fuel capsule inside the GLFC to provide additional thermal protection, along with the supporting structure, for the FCA.

The beryllium is coated with successive layers of silver, gold, rhodium, and radifax to provide oxidation resistance and a high emissivity surface to promote radiant heat transfer. While the FCA is in the GLFC, when the FCA temperature is higher than ambient, the STS conducts and reradiates heat from the FCA to the GLFC from which it is radiated to space. When the ambient temperature is higher than the FCA temperature, the STS and the internal supporting structure for both it and the FCA provide a heat sink which retards transfer to the FCA. The melting temperature of the Be is about 2330°F and specific heat is 0.45 BTU/lb°F.

The Be sleeve and the supporting structure are designed to provide an integral STS structure for continuing thermal protection of the FCA. A titanium thermal cap or dome is attached over the forward support structure to provide heat transfer from the fuel capsule end to the Be sleeve for cooling purposes and to provide thermal protection when exposed to high external temperatures. The melting point of this particular titanium alloy is 3100°F. The FCA back plate and insulating plug provide thermal protection at the aft end of the integral STS structure. The high specific heat of the Be sleeve and the high temperature and strength properties of the titanium (melting point 2800-3100°F) and Inconel (melting point 2540-2600°F) supporting structure offer protection for the FCA for thermal pulses, fragments and impulsive loads.

G. Fuel Capsule Assembly (FCA)

The Fuel Capsule Assembly (FCA) provides about 1480 watts of thermal energy for the SNAP 27 generator assembly. Figure 6 shows the various components and configuration of the FCA. It fits into the STS and is secured to the integral STS structure by a Haynes-25 latching mechanism on the back plate.

The FCA is comprised of two half capsule assemblies, each separately sealed and containing approximately equal amounts of PuO_2 microspheres. The fuel in each half capsule is sealed in an annulus between inner and outer Haynes-25 liners. The annular configuration greatly enhances containment in case of impact of the FCA since the center void provides low resistance space for compressive distortion of the fuel and liners with minimum stress exerted on the external containment. Each sealed liner assembly containing the fuel is further clad with Haynes-25 to form the half capsules. The half capsules are joined end to end by flange extensions of the cladding to form the FCA such that an independently sealed compartment is created at the mid-plane. This flanged mid-plane cladding section is deliberately undercut to be thinner than the rest of the cladding so as to create a zone of weakness to cause a preferential break during impact and/or vent internal pressure from each half capsule.

Impact energy absorption is enhanced by foamed Haynes-25 spacers in the end of each half capsule and in the mid-plane space. An insulating plug of Min-K-2000 is mounted on the aft end of the FCA, next to the back plate, to offer thermal protection in a high temperature environment when the FCA is in the STS structure.

Helium formed from $_{238}Pu$ decay fills the space between the fuel microspheres and the center void of the sealed fuel annulus thus minimizing internal pressure build-up under normal operation. The helium is further vented to the mid-plane space via a Haynes-25 filter in the end cladding of each half capsule which will not pass particulate matter. In case of failure at the undercut mid-plane cladding due to impact or internal pressure, the fuel could still be contained. Rupture discs in the mid-plane end of the half capsule liner assembly are designed to break after capsule fabrication is complete but before liner distortion can occur.

The overall dimensions of the FCA are 16.5 inches long by 2.5 inches diameter. The fueled zone in each half capsule is a 6.88 inch long annulus. The fuel thickness is 0.407-0.475 inches. The total FCA weight is 14.8 pounds of which 8.36 pounds are fuel.

H. Fuel

The FCA is fueled with PuO_2 microspheres 50 to 250 microns in diameter. The size selection of 50 microns minimum was made to preclude inhalation of fuel particles. The total fuel weight is 8.36 pounds of PuO_2, containing 44,500 curies of $_{238}Pu$, having a half life of 87.5 years. There are about 10^9 microspheres in the

FCA, and the fines (particles less than 47 microns) are estimated to be $<10^{-3}$ weight percent of the fuel. $_{238}PuO_2$ is characterized by a 5.49 Mev alpha, a 17 Kev X-ray, and 0.5 - 4.4 Mev neutrons from the (α, n) reaction with light elements. The total source of neutrons (2.4×10^4 n/gm - second) is generated by spontaneous fission and α - n reactions. The nominal dose rate from the side of the bare FCA at 1 meter is 92 mrem/hr with 86 mrem/hr from neutrons and 6 mrem/hr from photons.

III. DESCRIPTION OF POTENTIAL ACCIDENTS

This section identifies and describes potential nuclear accidents postulated for the prelaunch and launch, early ascent, suborbital, orbital, and superorbital phases of the mission. Appendices A (Range Safety) and B (Reentry) provide the primary sources of detailed information in support of this section. Since there has not been an abort of a Saturn V/Apollo vehicle, the Panel used experimental data, theoretical analyses, expert opinions, and experience from analogous events to postulate and describe potential accidents involving SNAP 27. The following information is presented for each phase:

1. Phase Description

   The spatial, temporal, and operational factors germane to the postulation of nuclear accidents are described.

2. Accidents Postulated and SNAP 27 Response

   The accident is postulated, the accident environment vis à vis the GLFC is described, and judgments are made regarding the response of the GLFC, STS, and FCA. These are based upon analyses and tests applicable to Saturn V/Apollo and SNAP 27 hardware.

3. Likelihood and Severity of Accidents

   The Panel sought to quantify the likelihood and severity of accidents in the various operational phases. In estimating the likelihood of aborts, the Panel used calculated NASA probability values on Saturn V/Apollo vehicle failures of all kinds and specifically those failures resulting in vehicle explosions and fires for each mission phase. These input values, though exclusive of human error and ground support equipment failures, are characteristic of those used for non-nuclear risk assessments by the aerospace community and are based on component, structural, subsystem, and system reliability tests and analyses.

   Given Saturn V/Apollo failures, order-of-magnitude-type engineering estimates were made on the probabilities of fuel release as a result of various aborts. It is emphasized that these estimates are judgmental and are not corroborated by statistically-founded confidence levels such as those derived from large samples of test results.

Table I presents the NASA Saturn V/Apollo accident probabilities and overall estimates of fuel release probabilities to provide a relative measure of accident probability and severity for each mission phase.

A. Prelaunch and Launch Phase

1. Phase Description

The prelaunch and launch phase is defined as the time interval between T - 12/24 hours, when the FCA is put on-board to T + ~20 seconds, when the vehicle reaches 2000 feet altitude. This is a nominal altitude and varies with S-IC engine performance. During the latter part of the prelaunch period cryogenic propellants are on-board the vehicle (See Figure 4). The nominal launch procedure calls for S-IC engine ignition at T - 8.9 seconds with verification of thrust at T - 1.5 seconds. Prior to lift-off the vehicle is constrained by four hold-down arms and the S-IC engines are shut down in the event of a propulsion malfunction. After nominal lift-off the vehicle clears the launch tower reaching an altitude of 600 feet in ~10 seconds and reaches 2000 feet in ~20 seconds of flight over the launch site.

The primary safety consideration is crew safety, and an automatic Emergency Detection System or manual means are used to actuate the Launch Escape System (LES) in the event of an abort. The thrust termination function and Propellant Dispersion System (PDS) is operative at T - 17 seconds through hard-line to the GSE prior to lift-off. There is an independent PDS on each stage which is a dual channel, parallel redundant system designed to terminate thrust, scatter the S-IC, S-II, and S-IVB oxidizers and fuels in different directions, and thereby minimize their energy yields. After lift-off the range safety officer can send two commands separately or simultaneously: "Arm" which results in thrust cut-off and "Destruct" which opens the tank walls by actuating the PDS. A four second delay time between "Arm" and "Destruct" is programmed to assure that the crew is clear of the vehicle at the time of destruct and also to permit charging of the destruct units.

2. Accidents Postulated and SNAP 27 Response

It was postulated that the Saturn V/Apollo could explode, burn, and impact the launch area during this phase.

The types of failure modes or events which were analyzed include: (1) Failures Prior to Engine Ignition, (2) Vehicle Tipover, (3) Vehicle Fallback, (4) Tower Collision, and (5) S-IVB Intact Impact on the Earth.

(1) An explosion prior to S-IC engine ignition could occur as a result of tank rupture of any propellant tank from overpressurization, or structural failure of a tank or a pressure bottle which in turn ruptures a propellant tank. A propellant tank rupture from overpressurization is unlikely since it requires a combination of several independent failures (e.g., failure of ground pressurization system plus failure of relief valves). Tank rupture as a result of structural failure is equally unlikely since this would require nominal working pressures to exceed the structural integrity of the particular component.

(2) The possibility of the Saturn V Launch Vehicle tipping over on the pad before S-IC ignition has been studied and there does not exist any known failure mode of significance. Analysis indicates that in the event of a hold down arm failing to release, the launch vehicle would proceed through the hold down arm and continue the mission. Further, redundancies incorporated in the hold down system make the probability of this failure on the order of 10^{-7}.

(3) Failures in the S-IC propulsion system are the only contributing factors leading to vehicle fallback. Liftoff cannot occur unless all engines are operating and thrust verified. Beyond less than one second after liftoff it would require failure of more than one engine to experience a fallback. The predicted probability of an engine failure resulting in a fallback is considered to be less than 1×10^{-6}.

(4) Failures leading to tower collision are primarily S-IC propulsion system failures requiring No. 1 or No. 2 engine failure prior to 4.5 seconds after liftoff, a plus yaw saturated signal before 2.3 seconds after liftoff or a minus yaw saturated signal before 5.2 seconds. These failure modes have been thoroughly analyzed and the probability of occurrence is considered to be less than 4×10^{-6}.

(5) The only postulated malfunction of significance which could lead to earth impact of an intact S-IVB is control signal saturation and loss of vehicle control. The probability of signal saturation occurring is less than 4×10^{-6}. To reach the earth intact after loss of vehicle control the S-IVB would need to survive the probable structural failure of the vehicle, possible tower collision, or command destruct action.

Although it is recognized that LM propellants next to the GLFC above the S-IVB, and propellants of the S-IC and S-II stages below the S-IVB could contribute to the below environments, the S-IVB containing 230,000 pounds of LOX and LH_2 was considered by the Panel to predominate because of its energy potential and proximity to the GLFC. Appendix A treats this subject in detail.

The following environments could be experienced by the GLFC in the event of an explosion and fire: (a) Shock overpressure and impulse, (b) Fragment flux, (c) Thermal transient from fireball and afterfire, and (d) Impact on vehicle parts or the earth.

a. Shock Overpressure and Impulse

A centerline explosion of the S-IVB is defined as one occurring at the center of the common bulkhead of the LOX/LH_2 tanks. An explosion at this point gives the greatest calculated shock overpressure and impulse to the GLFC for a given yield since it is nearer the GLFC than other potential S-IVB explosion centers. However, analysis indicates that an explosion center at this point is unlikely. The common bulkhead is structurally stronger than the sidewalls and, therefore, the more probable failure point is at the juncture of the common bulkhead and the sidewall, placing the explosion center further from the GLFC at a point in a torus outside the common bulkhead and sidewall juncture. The yield from a centerline explosion is postulated to be greater than for an explosion centering outside the vehicle since some propellant mixing could take place within the confines of the tank outer wall prior to ignition. An explosion centering outside the vehicle would not be expected to have a yield much greater than that resulting from a command destruct explosion because the failure modes are similar and little confined propellant mixing would be anticipated prior to ignition.

Although considered highly improbable, should the S-IVB impact the earth intact, the yield (30-60%) could be postulated to be considerably higher than for an "air burst" explosion if it is assumed that optimum mixing takes place on impact prior to ignition.

The table below lists failure modes of the S-IVB, the energy yields postulated from the failure mode explosion expressed in terms of TNT equivalent, and the calculated resultant shock overpressure at the GLFC. The data are based on failure mode analysis and yields from experiments involving 200 to 25,000 pounds of LOX/LH_2.

Failure Mode	Maximum Yield (% TNT)	Static Overpressure at GLFC (PSI)
Command Destruct	1	95
Tank Sidewall (Off-Center)	1-10	95-240
Common Bulkhead (Centerline)	4-20	240-530
S-IVB Impact (100 fps)	30	680 (GLFC Test Point)
S-IVB Impact (138 fps)	60	910

A full scale GLFC was tested in the Sandia shock tube under overpressure and impulse conditions simulating a 30% TNT equivalent yield for the S-IVB. The GLFC was mounted at an angle of 13° to the long axis on a Bendix LM attachment structure and heated to operating temperature. The measured incident static overpressure was 680 psi and the impulse was 2.7 psi-seconds. The experimental conditions (30% yield) were 50% greater than the high yield conditions (20% yield) and comparable to an S-IVB free fall intact impact explosion.

The graphite shattered and was completely stripped from the STS which was damaged but remained integral. The beryllium cylinder contained a crack running down the side of the cylinder. It was not deemed detrimental to the ability of the STS to provide thermal protection for the FCA. The FCA was wedged in the STS and some difficulty was encountered in removing it from the STS for examination. The 27 pound STS/FCA assembly was propelled with an initial velocity of 157 fps and impacted the plowed ground 750 feet away.

This test indicates that the STS will not be destroyed and will offer protection for the FCA from subsequent environments, such as incident fragments, the fireball pulse, impact, and afterfire.

b. Fragments

Two fragment cases, the centerline explosion and off-center explosion are treated. Both cases yield fragment environments more severe than those expected by command destruct action (yield less than 1%).

Centerline Explosion

The centerline explosion may result in a yield of 4-20%. The source of fragments is the area of the forward dome of the LH_2 tank 8-9 feet below the GLFC. The salient considerations are hit probability, fragment characteristic, fragment velocity, and hit orientation.

The probability of hitting the GLFC is a geometric factor estimated to be 0.4, derived from the ratio of the dome area to the area of fragments in a spherical expansion front as it passes the GLFC. The dome consists of 0.06 inch thick aluminum (85% of area below GLFC) and joints three times as thick (15% of area). Typical fragments are expected to be irregular aluminum sheets of various sizes, with or without joints.

Typical fragment nominal velocities were calculated to be 1000 to 1500 fps. However, upper limit fragment velocities estimated from film tracks could be on the order of 3000 fps for large fragments with low ballistic coefficients.

Since the time interval between shock wave arrival and fragment arrival would be a fraction of a millisecond to a few milliseconds in duration, the moment of inertia of the GLFC would preclude appreciable rotation of the GLFC, and the forward end of the STS/FCA would be facing the fragment flux. The shock tube test indicated that the graphite barrel would be demolished by the incident shock wave of a 30% yield.

The results of fragment impact tests on heated (to pad operating temperature) STS/FCA test specimens using 16 X 18 X 0.06 inch aluminum fragments are summarized below:

Specimen Orientation	Fragment Orientation	Fragment Impact Velocity (fps)	Damage to STS/FCA
End	Edge	1045	STS/FCA integral
End	Flat	1045	STS/FCA integral
End	Edge	1900	Fragment violated STS end cap. FCA penetrated no release
End	Flat	1900	STS/FCA integral
End*	Edge	1830	STS/FCA integral
Side	Edge	975	STS/FCA integral
Side	Flat	1040	STS/FCA integral Beryllium cracked
Side	Edge	2000	STS/FCA integral
End	Flat	3200	STS/FCA integral
End*	Edge	1815	STS/FCA integral
End**	Flat	2800	STS/FCA integral
End**	Edge	2800	FCA end and liner breached

* With graphite and Bendix end cap
** With graphite

The test data indicate that high velocity fragments impacting the front end of the STS/FCA edge-on could defeat the integrity of the STS/FCA. The degree of damage is a function of edge-on fragment velocity. At 1900 fps an edge-on fragment penetrated the FCA, but plugged the aperture. At 2800 fps the STS end cap was cut and the FCA was breached.

Off-Centerline Explosion

The yield range for an off-centerline explosion is taken to be 1-10% TNT equivalent and it occurs at the side of the S-IVB. Fuel release is not expected to result from 1% yields. However, it is postulated that components of the Instrument Unit (IU), a ring located above the S-IVB but below and peripheral to the GLFC, could be placed within the geometric view angle of the GLFC by off-center high yield explosions. The IU is made of aluminum honeycomb sandwich material with cold plates attached to the inner surface. Electronic and electrical components (such as "black boxes," batteries, power distributors, and telemetry assemblies) are mounted on the inner surface of the cold plates.

For a 10% yield, calculated theoretical velocities of massive IU components such as a cold plate and distributor box weighing 62 pounds vary over a wide spectrum depending upon the assumed attitude of shock impingement and other factors. A stationary STS/FCA was destroyed when it was impacted at 680 fps by the above combination mounted on a rocket sled. Evaluation of the test conditions has not been completed and the validity of this test has not been established. Recognition of the STS/FCA failure has been included in deriving the probability of a prompt fuel release due to fragment penetration during high yield abort explosion.

c. Fireball and Afterfire

The fireball model, discussed in Appendix A, was used to evaluate the thermal response of the STS/FCA. The model was considered by most of the Panel to be conservative.

It is expected that for explosive yields of greater than $3\frac{1}{2}$% TNT equivalent, the graphite of the GLFC would be damaged. For yields from $3\frac{1}{2}$ to 30%, shock overpressure would remove the graphite but would not be expected to

violate the integrity of the STS prior to fireball arrival. However, it is recognized that high yield fragment impact conditions could severely violate the STS/FCA and expose the FCA to the fireball. The probability of a catastrophic fuel release of this type has been discussed previously in Part 2.b. of this Section.

In the heat transfer analyses by GE and Sandia, the STS/FCA is exposed uniformly to the heat flux of the fireball for its full duration. This is a conservative assumption for cases where the STS/FCA is propelled from the fireball in a downward or lateral direction. Heat transfer analyses conducted by GE and verified by Sandia indicate that the FCA when protected by the STS would survive the full duration of the fireball with the conservative assumption that the STS/FCA is somehow levitated in the fireball as it rises. The bare FCA when exposed uniformly to the peak heat flux of the fireball is calculated to melt in 4 seconds.

The possibility of ignition and burning of the titanium and beryllium components of the STS was examined. Laboratory tests at Sandia on titanium specimens similar to the STS end cap indicated that ignition of molten titanium (MP 3100°F) could occur in an oxygen-rich gas mixture; however, it was not a violent reaction, and it was not self-sustaining. The STS beryllium barrel is coated and about 0.5 inches thick. Should the coating be disrupted or the barrel cracked, the fireball environment is not expected to sustain beryllium combustion. An adherent BeO coating (MP 4650°F) is formed on Be (MP 2330°F) which arrests combustion via oxygen starvation.

Section IV treats the vaporization of the PuO_2 fuel in the fireball, if it is released.

Following lift-off of the fireball stem, the STS/FCA could fall into a residual fire in the launch area. The fire burns at an average temperature of 1850°F and could persist for 30 minutes or more. GE and Sandia calculations assumed that the STS was not present and showed that the bare FCA will not melt in the afterfire. The FCA contains an internal helium pressure relief mechanism and is designed to fail at the mid-plane without releasing fuel in the event of gradually applied internal pressures.

d. Impact

The prelaunch and launch phase covers an altitude from 280 feet (installed height above pad) to 2000 feet. Following an abort, the GLFC, STS/FCA, or FCA could impact the pad area depending upon the severity of the explosion. The following impact velocities are given for the various SNAP 27 configurations when separated from the vehicle.

	Impact Velocity (fps)*		
	Release Altitude		
Item	280 feet	2000 feet	Terminal
GLFC	126	256	288
STS/FCA	130	290	373
FCA	125	243	264

* Sea level conditions for free fall

Impact could be on various media including sand, concrete, or pad structures. Three types of test data were available to the Panel. These included FCA impact tests, a GLFC impact test, and the shock tube test described earlier.

Seventeen FCA impact tests were conducted wherein heated FCA assemblies with internal pressures of 2.5 to 3 atmospheres were impacted at various velocities and angles on granite. Impact velocities varied from 140 to 264 fps. The results of all FCA impact tests indicated that no fuel would be released.

A GLFC was heated to reentry temperatures and was impacted at 1900°F and 300 fps on dense, moderately cemented clay silt having properties similar to low grade cement. The FCA cracked at the mid-plane weld as designed and no fuel simulant was released.

The test data support the contention that an integral FCA, when either unprotected or protected by the STS or GLFC, is expected to contain the fuel under ground impact velocities in excess of those anticipated in a launch abort. The Panel examined the possibility that the FCA could impact other vehicle components prior to ground impact. The only applicable test data for this case is the 157 fps velocity imparted to the STS/FCA by overpressure and the expected ability of the STS/FCA to survive impact with aluminum skin fragments at velocities up to 2500 fps. It

was also postulated that a piece of beryllium from the STS could puncture the FCA as a result of impact. This failure mode has not been observed in any of the impact and fragmentation tests conducted to date wherein the impact velocities were well in excess of those anticipated for GLFC or STS/FCA assemblies in the launch abort environment.

3. Likelihood and Severity of Prelaunch and Launch Accidents

In Table I the NASA probability for vehicle failure during the prelaunch and launch phase is given as 6×10^{-3} with 10^{-1} of such vehicle failures resulting in fire and explosion. The Panel was unable to quantify the mitigating factors associated with command destruct action during this phase, except to indicate that resultant yields from command destruct would be 1% or less and minimizes the environments for overpressure and fragments.

The Marshall Space Flight Center (MSFC) has not been able to identify any reasonable failure mode of the Saturn V which would result in ground impact of the intact S-IVB stage fully loaded with propellants prior to engine ignition. Nor have such failures been observed in any other vehicles prior to engine ignition. Subsequent to engine ignition and prior to lift-off, Kennedy Space Center (KSC) has indicated that premature holddown release due to single failure points could occur with a 2×10^{-7} probability. However, results of the Manned Spacecraft Center and MSFC investigations indicate that the vehicle would lift-off (or fail to lift-off and shut down safely) without tipover. After lift-off, the only significant failure mode identified which could result in S-IVB intact ground impact prior to command destruct or primary vehicle failure is the saturated control signal mode. MSFC indicates that the critical period for this mode does not continue beyond 20 seconds after lift-off. Although this would cause anomalous flight of the vehicle, the majority of these cases would result in command destruct, structural breakup, or tower collisions prior to striking the ground. Thus, the Panel could not reasonably postulate yield conditions of the S-IVB greater than 20% TNT equivalent, and this condition served as an upper limit.

The Panel considered fragment impact on the STS/FCA in its expected orientation, as a result of centerline and off-centerline explosions of the S-IVB. It is estimated that given an explosion the probability of breaching the capsule

is 6×10^{-3}. The following approach was taken to determine the probability of fuel release from fragments:

(6×10^{-3})	(1.1×10^{-1})	(6×10^{-3})	=	4×10^{-6}
(P abort)	(P explosion)	(P fragment damage)	=	P nominal fragment fuel release

This case is postulated as the nominal case for the prompt release of PuO_2 microspheres as a result of fragment penetration of the FCA from a low yield explosion. The fuel release rate is considered to be up to 4% per second from one half-capsule.

For a high yield explosion (centerline or off center) it is postulated that the PuO_2 microspheres from one half-capsule of the FCA (22,250 curies) could enter the fireball in a minimum time of two seconds. The prompt release of the microspheres to the fireball is considered as the upper limit case in Part IV and it is expected that the probability of occurrence is a factor of 10 less than the nominal case-low yield (i.e., 4×10^{-7}).

The above is exclusive of consideration of destruct action (yield 1%).

The fireball environment on a damaged STS/FCA could result in FCA breachment by melting and is assigned the following probability:

(6×10^{-3})	(1.1×10^{-1})	(10^{-2})	=	7×10^{-6}
(P abort)	(P explosion)	(P capsule melt)	=	P delayed fuel release

The release into the fireball would be delayed for more than 4 seconds, because of the time required for the inner liners to melt.

The release of fuel as a result of FCA impact failure is assigned the following probability:

(6×10^{-3})	(2×10^{-4})	=	10^{-6}
(P abort)	(P FCA impact failure)	=	P fuel release

In summary, the estimated probability of fuel release ranges from 7×10^{-6} to 10^{-6}. The upper limit, in terms of quantity of fuel released to the fireball at its peak thermal flux, is postulated to result from high velocity large fragment

impact. The puncture of the FCA by smaller fragments leading to a reduced release rate and the delayed release as a result of FCA meltdown are treated as nominal cases. The release of fuel as a result of ground impact has not been observed in testing of the GLFC/STS/FCA hardware. However, failure is assumed and source terms are assigned in Section IV.

B. Early Ascent Phase

1. Phase Description

The early ascent phase is defined as the time interval between T + 20 seconds (altitude 2000 feet) to T + 159 seconds. This represents most of the S-IC Boost, and at T + 159 seconds (S-IC cutoff) the altitude is 180,000 feet, the velocity is 8300 fps, with a range of 48 miles and an instantaneous impact point (IIP) less than 100 miles downrange. On a nominal trajectory the locus of vehicle IIP's clears the coastline at T + 32 to T + 36 seconds depending on the launch azimuth (72 or 108°). If thrust from the Number 3 engine is lost at T + 2 seconds and the remaining engines function, the IIP will clear the coast in 81 seconds. Therefore, the IIP during the early part of this phase is over concrete or sandy soil, but the majority is over the ocean downrange.

In the event of an abort with an IIP over land during this phase, destruct is the most likely action and S-IVB energy yields would be 1% or less depending upon the altitude of PDS initiation by the Range Safety Officer. After the IIP has moved over the ocean, flight termination action would be manual engine cutoff or crew initiated abort, the PDS function could be sent, if necessary, only after confirmation of satisfactory LES operation.

2. Accidents Postulated and SNAP 27 Response

It was postulated that the S-IVB stage of the Saturn V/Apollo could spontaneously explode, without benefit of command destruct action between 2000 and 180,000 feet altitude. The shock overpressure, impulse, and fragment environments would decrease in severity, compared to the launch abort, as altitude increases and lower ambient pressure conditions prevail. For altitudes between 2000 and 50,000 feet a firestream model was used to evaluate the thermal response of the GLFC. The firestream is created by propellants being expelled along the trajectory of the Saturn V. Because of the difficulty of maintaining the GLFC in the firestream, the

thermal pulse on the GLFC, STS, or FCA is much less severe than in the launch abort below 2000 feet; however, it has been analyzed and a fuel release assumed. The vaporization of the fuel released was calculated for 2000 to 10,000 feet altitude and a conservative model was used. Above 50,000 feet the effects of the thermal pulse of the firestream on the GLFC, STS, FCA, and fuel were considered negligible.

Land impact, primarily on sand, could occur as a result of aborts during the first 35 seconds or so after launch; thereafter thru S-IC cut-off, ocean impact downrange would result. Although the FCA would be expected to survive land impact, failure is postulated. Ocean impact failure is not expected.

3. Likelihood and Severity of Early Ascent Accidents

a. Fuel Release in Firestream

The early ascent abort is assigned a probability of 2.4×10^{-3} in Table I. Fuel release to the firestream would require a spontaneous explosion which is assigned a probability of 1.7×10^{-1}. The probability and mitigating effects of altitude and destruct action vis à vis SNAP 27 are not considered, although they will significantly reduce the release probability and respirable source term.

The probability of a prompt release of fuel into the firestream is given as follows:

(2.4×10^{-3}) (P abort)	(1.7×10^{-1}) (P explosion)	(7×10^{-4}) (P fragment penetration)	=	3×10^{-6} = P fuel release

b. Impact

The probability of impact failure of the FCA is given, as follows:

(2.4×10^{-3}) (P abort)	(2×10^{-4}) (P impact failure)	=	5×10^{-6} = P fuel release

This applies to impact failure on land. The S-IC flight time for this phase (minus the 20 seconds to reach 2000 feet) is 140 seconds. On a nominal trajectory the vehicle is over land for 15 seconds of the 140 seconds or about 10% of the Early Ascent Phase. This rationale is also generally applicable to the location of microsphere "footprints" created by fuel releases on ascent.

c. Marine Releases

The consequences of potential releases at sea or in fresh water as a result of microsphere "footprints" or FCA impact are treated in Appendix D, where the Oceanographic Subpanel concluded that such releases did not constitute a health hazard.

There is a remote probability that microsphere "footprints" could fall on ships at sea. However, this is not deemed to be a significant concern from a radiological viewpoint.

C. Suborbital Phase

1. Phase Description

This phase includes the S-II Boost and the S-IVB First Burn to orbital insertion.

The S-II Boost has a duration of 374 seconds, and its IIP as a result of any abort remains over the Atlantic Ocean. S-II Boost starts at T + 162 seconds (50 miles range, 220,000 feet altitude, 8100 fps velocity) and S-II cutoff occurs at T + 536 seconds (855 miles downrange, 605,000 feet altitude, 22,200 fps velocity).

The S-IVB First Burn inserts the S-IVB, LM, SM, and CM configuration into a 100 mile parking orbit. S-IVB ignition is at T + 536 seconds at the conditions of S-II Boost cutoff and the S-IVB cuts off at T + 683 seconds (1,340 miles downrange, 25,586 fps velocity) for an operating interval of about 150 seconds. Certain aborts of the S-IVB could result in IIP's on the African Continent during a period of 60 seconds of the 150 seconds S-IVB Burn.

Although command destruct is possible during this phase it is not a primary consideration.

2. Accidents Postulated and SNAP 27 Response

Two accidents are postulated for the Suborbital Phase. The first involves reentry failure of the GLFC and fuel release on reentry. The second involves impact of the GLFC on Africa.

a. Reentry Failure of GLFC

The Reentry Working Group examined the possibility of reentry failures of the GLFC at suborbital reentry velocities (See Appendix B). The failure of the graphite ablator of the GLFC was assigned a probability of 10^{-6}, given an abort without an explosion.

The possibility of a spontaneous S-IVB explosion in flight was also considered. This event was assumed to impair the graphite ablator of the GLFC and result in a fuel release. The failure mode is postulated to be fragment penetration of the GLFC since the effects of fire and overpressure above 50,000 feet are considered negligible.

The reentry conditions at the time of fuel release were such that the fuel could either melt or remain as microspheres. The former case would result in high altitude dispersion and the latter would place "footprints" of microspheres along the ground trace depending upon the point of failure.

b. Impact of GLFC

Impact of the GLFC in the Atlantic or Indian Oceans is the most probable result of suborbital aborts. However, impact on the African land mass was considered and failure of the STS/FCA at impact was postulated.

Sandia conducted three GLFC mass mock-up calibration drop tests and one GLFC drop test. In the calibration tests the models tumbled in free fall and impacted at between 321 and 347 fps. In the full scale GLFC drop test the FCA, containing a fuel simulant, was heated to 1900°F and dropped from 12,116 feet above terrain. The measured impact velocity was 300 fps at the test range altitude (5200 ft above sea level) and the GLFC was observed to tumble end-over-end. The target was a dry lake bed consisting of dense, moderately cemented clay silt. It is estimated that 70% of the earth's land area is less rigid. No fuel simulant was released in this test or in the 17 FCA granite impact tests discussed earlier.

During suborbital reentry it is not expected that significant degradation of the GLFC will occur prior to impact. However, explosions could degrade the GLFC/STS/FCA and a fuel release at impact is postulated and evaluated in Section IV.

3. Likelihood and Severity of Suborbital Accidents

a. Reentry Failure of GLFC

In Table I, the vehicle failure probability during this phase is estimated to be 4×10^{-3}.

For reentry ablator failure the following fuel release probability is derived:

(4×10^{-3})	(10^{-6})	=	4×10^{-8}
(P vehicle failure)	(P ablator failure)	=	P fuel release

For a reentry fuel release due to spontaneous explosions the following probability is derived:

(4×10^{-3})	(8×10^{-3})	(8×10^{-2})	=	10^{-4}
(P vehicle failure)	(P explosion)	(P ablator failure)	=	P fuel release

In the above fuel releases it is postulated that 50% would result in melting the fuel on reentry and dispersion of aerosols in the upper atmosphere and 50% would yield "footprints" of microspheres somewhere along the ground trace. Assuming the ratio of an African overflight interval of 60 seconds to the complete flight interval of the S-II Boost/S-IVB First Burn Phase of 524 seconds, it is estimated that 10% of such "footprints" would be on Africa, given a reentry fuel release. If one considers the increased density of vehicle abort probability at stage ignition, the "footprint" probability on Africa would be further reduced.

Footprints in the ocean or in fresh water were not considered significant by the Oceanographic Subpanel (Appendix D).

b. Impact Failure of GLFC

The critical path to impact failure is an in-flight explosion. The probability of fuel release at impact following an explosion is given as follows:

(4×10^{-3})	(8×10^{-3})	(2×10^{-1})	(5×10^{-3})	=	3×10^{-6}
(P abort)	(P explosion)	(P reentry survival)	(P land impact failure)	=	P fuel release

The 3×10^{-5} value applies to fuel release at land impact assuming that 10^{-1} will impact Africa and that 50% will fail on impact. About 90% will impact in the Atlantic or Indian Oceans, and the consequences are not significant. Mitigating aspects of fuel release such as cratering or burial in soft soils are not considered in estimating the fuel release probability or quantity. Burial on impact would not produce a significant aerosol release to the atmosphere based upon a burial test of the FCA.

D. Orbital Phase

1. Phase Description

This phase includes coast of the S-IVB, LM, SM, and CM configuration in a 100 mile parking orbit. It occurs after S-IVB First Burn cutoff and before S-IVB Second Burn. During this period ullage engines are operated for a short time and attitude maneuvers are conducted. On a nominal mission, S-IVB restart will occur during the first orbit after one hour and 24 minutes of coast.

2. Accidents Postulated and GLFC Response

Should the mission terminate in orbit for any reason, the configuration including the GLFC could reenter at random after orbital decay in a band between 35° N to 35° S Latitude after several weeks.

a. Reentry Failure of GLFC

The Reentry Working Group examined the possibility of GLFC reentry failures at orbital reentry velocities (Appendix B). The failure of the graphite ablator of the GLFC on reentry was assigned a probability of 10^{-6}, given an abort without an explosion.

b. Explosion

The possibility of a spontaneous S-IVB explosion in orbit was also considered. The GLFC failure mode postulated was fragment penetration which would impair the graphite ablator prior to reentry. The result would be fuel melting during reentry with dispersion in the upper atmosphere or "footprints" of microspheres in a band between 35° N to 35° S Latitude depending on the fuel release altitude.

c. Impact of GLFC

The impact response of the GLFC/STS/FCA was discussed earlier, and fuel release at impact is postulated and evaluated in Section IV.

3. Likelihood and Severity of Orbital Accidents

a. Reentry Failure of GLFC

In Table I minor fuel releases on reentry as a result of FCA pressure failure were not considered because of their relative inseverity. A 100% release of fuel at high altitude is assumed in the evaluation in Section IV.

The following fuel release probability for reentry ablator failure is derived:

(2×10^{-2})	(10^{-6})	=	2×10^{-8}
(P orbital abort)	(P ablator failure)	=	P fuel release

Almost all GLFC reentry failures will result in fuel melting and dispersion as aerosols in the upper atmosphere.

b. Explosion

The following fuel release probability for explosion induced GLFC failure is derived:

(2×10^{-2})	(2×10^{-3})	(3×10^{-1})	$= 10^{-6}$
(P orbital abort)	(P explosion)	(P GLFC failure)	= P fuel release

Orbital explosions can cause ablator failure prior to or during the reentry sequence and survival of the STS/FCA during reentry is doubtful. In the explosion case, it is assumed that 50% of the releases will result in fuel melt and dispersion and 50% will result in random "footprints" of microspheres.

c. Impact Failure of GLFC

Table I gives fuel release probabilities for land impact. Ocean impact is expected 75% of the time and is not considered to be significant.

The probability of fuel release at impact as a result of orbital aborts is given as follows:

(2×10^{-3})	(2×10^{-3})	=	4×10^{-4}
(P abort)	(P FCA land impact failure)	=	P fuel release land

The 2×10^{-3} factor accounts for the degradation of the GLFC/STS/FCA during reentry and the ratio of land to water.

E. Superorbital Phase

1. Phase Description

This phase includes a period of about 62 hours from translunar injection until a lunar orbit is achieved.

This phase includes the following subphases:

Translunar Injection consists of the S-IVB Second Burn (5 minutes and 42 seconds) to accelerate the configuration from the parking orbit to translunar velocity of 35,600 fps. The nominal injection provides a "free return" trajectory to earth if deboost into lunar orbit is not initiated.

Translunar Coast is the period following S-IVB Second Burn and prior to the SM burn for lunar orbit insertion. During this period the CSM is separated from the S-IVB, transposed and docked to the LM, then the LM is withdrawn from the S-IVB. Midcourse corrections are made if required.

Lunar Orbit Insertion requires the SM to deboost the spacecraft into a circular lunar orbit. The LM will land on the moon after a lunar orbit coast period and SNAP 27 will be deployed on the lunar surface.

After the lunar orbit is accomplished, it was assumed that the GLFC would not return to earth, although it is recognized that in the very remote event of SM engine failures occurring prior to the lunar landing, the LM Descent Stage (with the GLFC attached) would provide propulsion for an earth return trajectory. However, in this case the LM is targeted for ocean impact.

2. Accidents Postulated and GLFC Response

Some failures will not result in earth impact; however, since no definitive information is available all failures are assumed to return the GLFC to earth. The three types of accidents postulated for this phase are GLFC ablator failure, explosions, and GLFC impact.

a. GLFC Ablator Failure

Two types of reentry conditions are postulated to cause GLFC ablator failure: "skip" reentries and high angle superorbital reentry. Such reentry conditions could result from aborts occurring in Translunar Injection, Translunar Coast, Lunar Orbit Insertion, and as a result of using the LM propulsion to return to earth if the SM fails to start-up. These are discussed in Appendix B.

The "skip" reentry situation results from aborts occurring between Translunar Injection and Lunar Orbit Insertion. The resultant trajectory would be highly elliptical causing the GLFC to graze the earth's atmosphere at a shallow angle ($<4\frac{1}{2}^{\circ}$) at superorbital velocities in multiple orbits with decreasing periods and apogees. Each pass could cause the incremental removal of graphite by ablation as it grazes the atmosphere until the graphite thickness is insufficient to survive the final orbital reentry.

In contrast to the shallow grazing reentries, the GLFC could be placed into a steep angle superorbital trajectory that would result in abnormally high heating rates and thermal stresses on the GLFC on reentry. The graphite of the GLFC has been tested at the highest pressures, but not with simultaneous high heating rates that it could encounter. The combined conditions cannot be simulated in ground tests. The result of ablator failure could be a release of fuel on reentry with fuel aerosols dispersed in the upper atmosphere or "footprints" of microspheres at random on the earth's surface.

b. Explosion

The possibility of a spontaneous S-IVB explosion causing GLFC failure and fuel release on reentry during this phase was also examined. The expected result would be fuel melting during reentry with aerosol dispersion in the upper atmosphere.

c. Impact of GLFC

Impact of the GLFC could occur at locations biased to between 35° N - 35° S Latitude. The impact response of the GLFC/STS/FCA is postulated and evaluated in Section IV.

3. Likelihood and Severity of Superorbital Accidents

a. Reentry Failure of GLFC

The following fuel release probability for reentry ablator failure is derived:

(1.5×10^{-1})	(2×10^{-2})	=	10^{-3}
(P superorbital abort)	(P ablator failure)	=	P fuel release

Reentry failures are expected to result in fuel melting 50% of the time and random microsphere "footprints" 50% of the time. A 100% fuel release is postulated.

b. Explosion

The following fuel release probability for explosion-induced GLFC failure is derived:

(1.5×10^{-1})	(6×10^{-2})	(3×10^{-1})	=	3×10^{-3}
(P superorbital abort)	(P explosion)	(P ablator failure	=	P fuel release

GLFC reentry failures because of explosions are expected to result in fuel melting ten times more often than random microsphere "footprints" because of the severe heating environments expected at fuel release. A 100% fuel release is postulated.

c. Impact Failure of GLFC

Table I gives fuel release probabilities for random land impact only, because water impact is not of significant concern.

The probability of fuel release at impact as a result of superorbital aborts is given as follows:

(1.5×10^{-1})	(2×10^{-2})	=	3×10^{-3}
(P abort)	(P FCA land impact failure)	=	P fuel release

The fuel release probability for impact accounts for the ratio of land to water impacts.

IV. EVALUATION OF POTENTIAL ACCIDENTS

In the previous section, potential accidents which could lead to fuel release were defined and their occurrence probabilities were estimated and summarized in Table I. This section presents the Panel's evaluation of these accidents with respect to postulated radiological source terms (amounts and particle sizes of $_{238}PuO_2$ released) and the resulting isopleth areas (areas in which a lung burden or ground concentration equals or exceeds a given amount) for lung burdens of PuO_2 aerosols and ground concentrations of microspheres.

Source terms for all accidents leading to fuel release were estimated by the Panel. Isopleth areas were derived by the Meteorological Working Group (MWG) and are discussed in detail in Appendix C. Upper limit and nominal releases were estimated by the Panel for the particular release mode considered.

Upper limit releases were defined as being the most adverse that can reasonably be expected to occur. Nominal releases were defined as those that are more likely to occur in the event of an abort. Releases less than nominal were not evaluated due to their reduced severity.

The evaluation is summarized in Table II where the source terms are identified by the amount of PuO_2 released and the particle size released in order to determine meteorological dispersion, lung burdens and ground deposition. Particle sizes of PuO_2 with diameters three microns or less were considered for pulmonary deposition. Particles of PuO_2 greater than three microns in diameter were considered non-respirable and were treated in the ground concentrations. That portion of fuel vaporized in the fireball and firestream was considered PuO_2 vapor, but it was recognized that the PuO_2 vapor will agglomerate on inert airborne particles, propellants, water vapor, dust and other inert ingredients in the fireball.

In Table II, the downwind lung burdens were defined in terms of the areas where datum lung burdens of 0.016 and 0.0005 microcuries (μci)* of $_{238}PuO_2$ would be exceeded. Lung retention values were computed from the product of time-integrated air concentrations, given in Appendix C, and the constant $4 \times 10^{-5} m^3/sec$. This constant is based on an inspired air intake of $2 \times 10^{-4} m^3/sec$ and a pulmonary retention factor of 0.2.

Dispersion and deposition patterns resulting from fuel release were determined by the assumed height of the fireball or firestream and the postulated meteorological stability conditions existing at the time of release. Meteorological Condition 1 represents the nominal stability condition at Cape Kennedy while Condition 2 represents a more conservative condition within the diurnal and seasonal range. Condition 2 does

*1 microcurie (μci) = 10^{-6} curies (ci). See Appendix E for discussion of Biomedical considerations.

not give the highest possible values for the isopleths. The MWG concluded that more severe conditions would not occur more than 10% of the time. Aborts where conditions would be of primary consideration are impact releases from a point source and at ground level.

For ground level releases, the more stable atmosphere and lower wind speeds result in higher downwind concentrations. The low wind speeds and stable conditions are confined primarily to the nighttime and early morning hours, and thus there is a limit to the distance an instantaneous source can travel under these conditions. After 12 hours or less the stable condition would generally change to neutral or unstable conditions and dilution would become more rapid.

The limiting meteorological condition assumed for the evaluation of the point source impact release was a very stable atmosphere and a wind speed of 2.5 m/sec. It is possible that higher doses could exist 10% of the time, primarily because of lower wind speeds which are inversely proportional to the dose. The lower wind speed would limit the downwind extent and the area of a particular isopleth. Using lower wind speeds increases the areas listed in Table II by a factor of two. The parameters used in Table II to describe these conditions are listed below:

Assumed Meteorological Conditions

Abort Zone	Release Mechanism	Type of Particle	Meteorological Condition	Release Height meters(m)	Wind Speed (m/sec)	Stability Condition
LAUNCH SITE	Prompt	Vapor	1	2000	10	Neutral
			2	1000	20	Unstable
		>3	1	2000	10	Neutral
			2	4000	20	Unstable
	Delayed	Vapor	1	2000	10	Neutral
			2	1000	20	Unstable
		>3	1	2000	10	Neutral
			2	4000	20	Unstable
	Impact	<3	1	0	5	Neutral
			2	0	2.5	Very Stable
		>3	1	0	5	Neutral
			2	0	2.5	Very Stable

	To Fire-stream	Vapor	1	4000	10	Neutral
			2	4000	1	Unstable
FLIGHT TRAJ. (EARLY ASCENT)		>3	1	4000	10	Neutral
			2	4000	1	Unstable
	Impact	(Equivalent to Launch Site Impact Releases, except for Location.)				
FLIGHT TRAJ. (REENTRY)	Melt Zone (Burn Up)	45 Km Altitude Release, Atmospheric Dispersion Confined to 1 Hemisphere				
	Outside Melt Zone	Atmospheric Fallout from a Line Source Along Reentry Trajectory				
	Impact	(Equivalent to Launch Site Impact Releases, except for Location.)				

Ground concentration isopleths presented in Table II were defined by datum levels of 62 $\mu ci/m^2$ and 6 $\mu ci/m^2$. Maximum values for both lung burden and ground concentration represent, theoretically, a single point on the ground. However, for purposes of evaluation, the area enclosed by an isopleth line equal to one-half the maximum value is also shown.

The source terms and isopleths for datum lung burdens and ground concentrations are presented in Table II, and their sensitivity to other meteorological conditions are discussed for each postulated accident.

A. Prelaunch and Launch Phase

It was postulated in the previous section that PuO_2 microspheres could be released during this phase of the mission, if the following conditions occur:

1. Launch vehicle explosion resulting in fragments puncturing the FCA (prompt release).

2. Damage to the GLFC and STS exposing the FCA to the fireball (delayed release).

3. Impact failure of the FCA outside of the fire (point source release).

The source terms in Table II are based on judgements of the Panel. For the prompt fuel release condition an upper limit of 50% of the total inventory was assumed. A 2% per second microsphere release rate was assumed for the nominal release situation and for vaporization of the microspheres in the fireball. For the delayed release, a five-second period was assumed before FCA melt released 16% of the total fuel inventory into the fireball with less vaporization than the prompt case. Source terms for impact were considered a function of fuel break-up due to the impact environment and the damage to the FCA.

1. Prompt Release

a. Source Term

It has been postulated that fragments caused by a pad explosion could damage the GLFC/STS/FCA and release microspheres to the fireball. Some of the fuel might vaporize and both vaporized fuel and microspheres could be carried downwind. This section presents the Panel's evaluation of this accident.

The Panel evaluated calculations of vaporization rates of PuO_2 microspheres in the fireball. Attachment 1 of Appendix A shows the fireball temperature as a function of time. Figure 7 shows fuel vaporization as a function of this decaying temperature and the time exposed assuming the fuel remains levitated in the fireball. In the model used for evaluation, ~50% of the fuel released immediately (at the time of fireball initiation) could be vaporized. For microspheres released after five seconds in the fireball approximately 5% of the fuel could be vaporized. For an upper limit fuel release evaluation all of the fuel from a half-capsule of the FCA ($\sim 2 \times 10^4$ ci) was considered to be released immediately to the fireball (Time 0). This condition could result in $\sim 10^4$ ci of PuO_2 vaporized. An evaluation of this release is given in Table II. The remaining fuel from the half-capsule ($\sim 10^4$ ci) was considered as microspheres and evaluated in terms of being carried downwind and deposited on the ground.

A nominal release from a damaged FCA (small particle penetrations) was also considered in the evaluation. For this condition, a microsphere leak rate up to 4 percent of a half-capsule per second was assumed by the Panel. Source terms evaluated for this release consisted of 2×10^3 ci of vapor and 10^4 ci of microspheres. The dispersion of these source terms in a launch pad situation is shown in Table II.

b. Areal Extent of Lung Burdens and Ground Concentrations

Lung burdens depend upon the meteorological conditions existing at the time of and following release. For the two conditions evaluated the maximum lung burden could vary between 8×10^{-4} to 2×10^{-2} µci. The larger value is based on an unstable condition which allows the aerosol to rapidly reach the ground. If the meteorological condition is stable, the cloud will remain at altitude longer and the maximum lung burden when the activity reaches the ground could be less than that indicated for the neutral case. An area of 2 Km^2 in which an 0.016 µci burden could be exceeded begins at 5 Km and extends to 9 Km downwind from Complex 39.

The maximum ground concentration is 500 µci/m^2 and a ground concentration of 62 µci/m^2 is exceeded over an area of 30 Km^2 starting at 2 Km and extends to 15 Km from Complex 39. Lower wind speeds and more stable conditions would result in higher ground concentrations of non-respirable particles in the launch area.

The nominal prompt release could result in a maximum lung burden of 0.004 µci and the same ground concentration as the upper limit case.

2. Delayed Release

a. Source Term

If the FCA is not damaged by fragments but is exposed unprotected in the fireball, it could melt. It was calculated that the capsule could melt in 4 seconds as it falls unprotected through the fireball. In this event, 16% of the total fuel inventory was considered to be released (6750 ci) and 9% of that material was considered to be vaporized, resulting in 600 ci of vapor. It was pointed out in Appendix A that if part of the damaged STS remained with the FCA, capsule melt could be delayed several seconds. Since the amount of fuel vaporized is a function of time of exposure to the fireball, a delay in capsule melt would lower the source term. For example, an 8 second delay in melting the FCA could result in a vapor source term of 20 ci.

The microsphere source term for ground deposition evaluation was assumed to be 50% of the total inventory or 2×10^4 ci.

b. Areal Extent of Lung Burdens and Ground Concentrations

The delayed release of 600 ci of vapor and 2×10^4 ci of particles greater than 3 microns could produce a maximum lung burden of 1.2×10^{-3} µci at 6 Km from Complex 39 (Condition 2) and a maximum ground concentration of 1000 µci/m^2. A ground concentration in excess of 62 µci/m^2 could cover an area of 40 Km^2 starting 2 Km and extending 17 Km from Complex 39.

3. Point Source Release (Impact)

a. Source Term

It was assumed that in some circumstances fuel could be released if the FCA is breached on impact. To determine a source term for this mode of failure, the Panel evaluated data from microsphere fuel impact tests. The test assemblies contained 5.5 grams of microspheres, and they were heated to approximately 1000°F, then impacted into several materials at various velocities. The test assemblies were opened, the fuel was characterized in various size ranges and the corresponding percentage of the total fuel in a SNAP 27 FCA was assumed. The results of this work are summarized below:

Fuel Impact Tests

Impact Velocity (ft/sec)	Impact Medium	Weight % <10µ	Weight % <3µ*	Wt. % Not Accounted For
102	Granite	0.06	0.04	-0.01
106	Granite	0.025	0.025	-1.19
106	Granite	0.08	---	-1.45
116	Concrete	0.30	0.03	+3.92
No Impact	---	0	0	-0.7
103	Sand	0	---	-1.7
104	Granite	0.5	0.37	-3.5
103	Granite	0.65	0.65	-4.35
317	Granite	4.8	---	-13.4
442	Granite	6.4	---	-8.6
456	Concrete & Graphite	12.72	6.3	0

*---Sample not analyzed for particles less than 3 microns.

The Panel considered that the fuel tests, conducted in rigid capsules, could have augmented degradation of the microspheres. If the fuel was in a capsule which

yielded on impact, the production of respirable particles might be less than that indicated in the fuel tests; however, no data is available using less rigid capsules.

With regard to the FCA integrity when exposed to impact forces, 17 impact tests were performed against granite at velocities between 140 to 264 fps with heated capsules containing fuel simulant. The results of all FCA impact tests indicated that no fuel simulant was released.

For the nominal release, an upper limit quantity of fines (10%) and a release of 1% were assumed (50 ci).

b. Areal Extent of Lung Burdens and Ground Concentrations

In the upper limit impact case, 100 ci of aerosols and 500 ci of particles greater than 3 microns are assumed to be released.

Lung burdens greater than 0.016 μci could occur in a 20 Km^2 area as far as 80 Km downwind during very stable meteorological conditions and in an area of 1.3 Km^2 as far as 7.3 Km downwind during neutral meteorological conditions.

The 62 $\mu ci/m^2$ ground concentration isopleth has an area of 0.2 Km^2 and extends 3 Km downwind from the impact point and is within the controlled area around Complex 39.

For the nominal impact case lung burdens in excess of 0.016 μci could occur in an area 11 Km^2 extending as far as 50 Km downwind from the impact point during stable conditions.

B. Early Ascent Phase

1. Source Term

The assumed nominal release disperses microsphere fuel into a firestream for eight seconds (aborts between 2000 to 10,000 feet) as discussed in Appendix A. Using the vaporization model already described, 6% of the fuel could be vaporized. This produces approximately 3000 ci of vapor and 2×10^4 ci of microspheres. Above 10,000 feet altitude the amount of fuel vaporized would be lower and above 50,000 feet vaporization would not be expected. If the FCA is breached and is freed from the structure, the vapor source term would be lower; however, the ground deposition source term or "footprint" could be essentially the same.

FCA failure due to impact on land could produce the same source terms as pad aborts. Ocean impact would occur greater than 90% of the time for aborts during this flight phase and would produce no aerosols.

2. Areal Extent of Lung Burdens and Ground Concentrations

The maximum lung burden expected from the release of 3000 ci of vapor in the firestream during early ascent could vary between 6×10^{-5} and 8×10^{-4} µci depending on the stability condition. These values are for a release at 4000 meters altitude. If the accident occurs at higher altitudes, the lung burdens would be lower, approaching the level for complete hemispherical dispersion.

Ground concentrations resulting from release during this phase of operation would be dependent on the wind speed at the time of release. For very low wind speeds (1 meter/second) the concentration on the ground would be high with a maximum value of 25,000 $\mu ci/m^2$. However, the isopleth area for ground deposition greater than 62 $\mu ci/m^2$ is small (4 Km^2 with a length of 5 Km). For higher speeds the maximum value could be 250 $\mu ci/m^2$. The area with concentrations greater than 62 $\mu ci/m^2$ could be 90 Km^2 with a length of 20 Km.

Point source fuel release conditions resulting from impact failures during this phase of operation would be essentially the same as those described for the launch pad case.

C. Reentry Phase

1. Source Term

If the vehicle aborts during the suborbital, orbital, or superorbital flight phases, the GLFC will be exposed to reentry mechanical and thermal forces. During these phases, PuO_2 microsphere fuel could be released along the reentry trajectory or at the point of impact if the FCA fails due to impact loads.

Reentry

Should the GLFC fail during reentry, the Panel concluded that the source term would be dependent upon the reentry effect on the fuel at the time of release from the FCA. If the PuO_2 microspheres are released within the melt region they will lose a major fraction of their mass with the resulting debris assumed to be dispersed over one hemisphere. Fuel debris ranges in size from a few microns to less than 0.1 microns.

If released outside the melt region, the fuel source term would be in the form of microspheres and be released as a line source along the trajectory resulting in a line deposition of microspheres on the earth.

The zone defined by conditions of release velocities and altitudes in which the microsphere fuel reaches its melting point (2256 ± 34°C) on reentry has been reasonably well determined analytically and verified experimentally by Sandia Laboratories in 25 hyperthermal arc tests simulating the reentry response of the fuel. The source term evaluated for fuel release in the melt zone was a 100 percent release, 44,500 ci. The source term evaluated for fuel release outside of the melt zone was 44,000 ci of microspheres and 500 ci of aerosols less than 3 microns.

Impact

The Panel had difficulty with post-impact source terms for point source ground releases, because the integrity of the GLFC/STS/FCA combination at the time of impact could not be adequately determined for the infinite number of degradation modes which might exist. However, certain observations were considered.

Impact velocity of the structure could vary from 264 to 373 fps depending on what part of the assembly survives reentry (Section III). Impact degradation of the fuel could vary depending on what medium is impacted and the yielding mode of the degraded structure. If the structure is non-yielding the amount of aerosols created by impact could be at a maximum depending on the impact medium. Considering the above impact velocity range, these aerosols could be in the order of 10%, assuming an integral FCA impacting on a rigid medium. Impact of a degraded GLFC/STS/FCA may or may not produce the same amount of aerosols. Thus the source term could be the same (50 ci). An upper limit source term of 100 curies was evaluated. There is some uncertainty in predicting the exact source term for a spectrum of GLFC/STS/FCA configurations and conditions after reentry. Under impact conditions, increased fuel release could be considered. However, the mitigating circumstances of degraded GLFC/STS/FCA configurations impacting on various media could reduce the amount of fines produced. and the amount of aerosols released directly to the atmosphere.

2. Areal Extent of Lung Burdens and Ground Concentrations

The maximum lung burden computed for fuel release during reentry was 2×10^{-6} μci. This assumed that all of the fuel was released on reentry in the melt zone and that the inhalable particles deposited in one hemisphere.

If the fuel was released outside of the melt zone, an upper limit of 44,000 ci of microspheres would be deposited on the earth's surface in a random "footprint" biased between 35° N - 35° S latitude. Ground concentrations in this "footprint" would reach a maximum of 130 $\mu ci/m^2$ and an area of 100 Km^2 within the "footprint" would exceed a level of 62 $\mu ci/m^2$.

Lung burdens and ground concentrations at the impact point where the FCA fails upon impact after reentry would be essentially the same as those described for the Prelaunch, Launch, and Early Ascent impact failure cases. The consequences of the release will be dependent upon the geography of the area in which the system impacts (impact medium, population density, burial, etc.).

V. SUMMARY EVALUATION OF RISK

A. Risk Criteria

1. Radiation Criteria

There are no official guidelines established which specify emergency exposure levels for individuals exposed to $_{238}PuO_2$ in transient, low probability situations such as accidental fuel releases from Saturn V/Apollo aborts involving SNAP 27. The datum lung burden of 0.016 μci of $_{238}PuO_2$ would deliver a uniform radiation dose to the lung of less than 15 rem during the first year after exposure. Appendix E discusses this subject in detail.

The 62 $\mu ci/m^2$ datum for ground concentrations was selected as the reference value based on the limits used by DoD. The 62 $\mu ci/m^2$ for $_{238}PuO_2$ is equivalent to the 1000 $\mu gm/m^2$ established by DoD for $_{239}Pu$. Populated or agricultural areas with concentrations of or above this level will probably require cleanup. A populated area with concentrations less than 62 $\mu ci/m^2$ might require some cleanup depending upon an evaluation of the potential radiological exposure of the people in the area.

2. Meteorological Conditions

The meteorological conditions used in this report are discussed in Appendix C and are considered representative of stability conditions to be expected at Cape Kennedy.

3. Probabilistics

In estimating the likelihood of aborts, the Panel used calculated NASA probability values on Saturn V/Apollo vehicle failures of all kinds and specifically those failures resulting in vehicle explosions and fires. These values are characteristic of those used for non-nuclear risk assessments by the aerospace community.

It is emphasized that the fuel release probabilities used are order-of-magnitude estimates and are useful in determining relative, not absolute, probabilities for accidents.

4. Contingency Plans

This report does not include contingency plans; however, appropriate operations groups are preparing these plans for review and approval prior to launch.

B. Accident Evaluation

1. Potential Accidents

Table I presents a compilation of the potential accidents that SNAP 27 may be subjected to as a result of Saturn V/ Apollo mission aborts. It also gives estimates of their probability of occurrence and the estimated probability of $_{238}PuO_2$ fuel release during the various mission phases. The probabilities of fuel release are summarized below:

Abort Zone	Phase	Release Probability
Launch Site	Prelaunch & Launch	10^{-6} to 7×10^{-6}
	Early Ascent	3×10^{-6} to 5×10^{-6}
Reentry	Suborbital	4×10^{-8} to 2×10^{-4}
	Orbital	2×10^{-8} to 4×10^{-4}
	Superorbital	10^{-3} to 3×10^{-3}

2. Population-at-Risk

Table II presents the estimated radiological source terms, meteorological dispersion, lung burdens, and ground deposition for various fuel releases. While impact releases of aerosols could be worldwide, the mission trajectory biases random impact events to a band between 35° N and 35° S latitude. The following table summarizes the risk to the population:

Event	No. of People (LB* >0.016 μci)	Probability of** No. People (LB >0.016 μci)	Probability of Release	Probability of No. of People (LB >0.016 μci)
Launch Site				
Fireball	0-400	10^{-3}	4×10^{-6}	4×10^{-9}
Impact	0-2000	10^{-3}	10^{-6}	10^{-9}
Worldwide Impact (Population Density)				
1-25	0-2	10^{-1}	3×10^{-3}	3×10^{-4}
25-100	0-20	10^{-1}	3×10^{-3}	3×10^{-4}
100-500	0-90	3×10^{-2}	3×10^{-3}	9×10^{-5}
500-1000	0-200	5×10^{-3}	3×10^{-3}	2×10^{-5}
1000-5000	0-900	2×10^{-3}	3×10^{-3}	6×10^{-6}

* LB - Lung Burden
** Includes meteorologic and geographic variations

The maximum number of people exposed for the upper limit release cases are identified above. The probability of a given number of individuals being in the 0.016 μci isopleth is a function of weather conditions (wind direction, stability) and the population density distribution of the launch site or the impact zone (35°N - 35°S Latitude band).

Areas of ground concentrations above 62 $\mu ci/m^2$ could result from impact failure of the GLFC/STS/FCA on MILA or at random locations biased to between 35°N - 35°S Latitude. Random microsphere "footprints" could exceed the above ground concentration datum as a result of some types of reentry releases. Impacts or "footprints" at sea are not considered significant.

CONFIDENTIAL

TABLE I
Probability Estimates for Fuel Release
SNAP 27/Apollo Mission

Potential Accident Abort Zone	Flight Interval	Fuel Release Mechanism	Probability Estimates: Vehicle* Failure (NASA Input)	Vehicle Explosion With Fire (NASA Input)	FCA Failure (Working Group Input)	Fuel Release Total Probability
Launch Site	Prelaunch and Launch	Prompt/Fragment Penetration Delayed/Loss of STS, FCA Melt Point Source/FCA Impact Failure	6×10^{-3}	1.1×10^{-1} --- ---	6×10^{-3} 10^{-2} 2×10^{-4}	4×10^{-6} 7×10^{-6} 10^{-6}
Launch Site or Ocean	Early Ascent	Prompt/Fragment Penetration Point Source/FCA Impact Failure	2.4×10^{-2}	1.7×10^{-1} ---	7×10^{-4} 2×10^{-4}	3×10^{-6} 5×10^{-6}
Reentry	Suborbital	Explosion Release A. Melt Zone B. Outside Melt Zone GLFC Reentry Failure Release A. Melt Zone B. Outside Melt Zone Land Impact Failure/FCA Melt or Impact Failure	4×10^{-2}	8×10^{-2} --- --- --- 8×10^{-2}	(8×10^{-2}) 4×10^{-2} 4×10^{-2} (10^{-6}) 5×10^{-7} 5×10^{-7} 10^{-2}	(2×10^{-4}) 10^{-4} 10^{-4} (4×10^{-8}) 2×10^{-8} 2×10^{-8} 3×10^{-5}
	Orbital	Explosion Release A. Melt Zone B. Outside Melt Zone GLFC Reentry Failure Release A. Melt Zone B. Outside Melt Zone Land Impact Failure/FCA Melt or Impact Failure	2×10^{-2}	2×10^{-3} --- ---	(3×10^{-1}) 1.5×10^{-1} 1.5×10^{-1} (10^{-6})** 10^{-6} Negligible 2×10^{-2}	(10^{-5}) 6×10^{-6} 6×10^{-6} (2×10^{-8})** 2×10^{-8} Negligible 4×10^{-4}
	Superorbital	Explosion Release A. Melt Zone B. Outside Melt Zone GLFC Reentry Failure Release A. Melt Zone B. Outside Melt Zone Land Impact Failure/FCA Melt or Impact Failure	1.5×10^{-1}	6×10^{-2} --- --- --- ---	(3×10^{-1}) 3×10^{-1} 3×10^{-2} (10^{-2})** 5×10^{-3} 5×10^{-3} 2×10^{-2}	(3×10^{-3}) 3×10^{-3} 3×10^{-4} (10^{-3})** 8×10^{-4} 8×10^{-4} 3×10^{-3}

*Values do not include human errors or ground support equipment failures.
**Represents 100% release; lesser amounts could be released with higher probabilities.

CONFIDENTIAL

TABLE II
EVALUATION OF POTENTIAL ACCIDENTS

Potential Accident Abort Zone	Release Mechanism and Value Disposition	Type of Particle Released	Source Term (Curies)	Meteorological Condition	LUNG RETENTION (μ ci) Maximum Value: Value	Maximum Value: Isopleth Area (Km^2)** Max.Val./2	Maximum Value: Downwind Touchdown Distance (Km)**	Maximum Value: Downwind Length (Km)	0.016: Isopleth Area (Km^2)	0.016: Downwind Touchdown Distance (Km)	0.016: Downwind Length (Km)	0.0005: Isopleth Area (Km^2)	0.0005: Downwind Touchdown Distance (Km)	0.0005: Downwind Length (Km)
LAUNCH SITE (PRELAUNCH AND LAUNCH)	Prompt Upper Limit	Vapor	10^4 10^4	1 N 2 U	0.0008 0.02	1600 8	150 3	450 9	0 2	0 5	0 4	600 600	150 2	350 58
	Nominal	Vapor	2×10^3 2×10^3	1 N 2 U	0.0002 0.004	1600 8	150 3	450 9	0 0	0 0	0 0	0 100	0 2	0 28
	Delayed Nominal	Vapor	6×10^2 6×10^2	1 N 2 U	0.00005 0.0012	1600 8	150 3	450 9	0 0	0 0	0 0	0 15	0 3	0 12
	Impact Upper Limit	<3μ	10^2 10^2	1 N 2 S	0.2 0.2	0.14 5	0 0	2.3 30	1.3 20	0 0	7.3 80	50 130	0 0	60 100
	Nominal	<3μ	50 50	1 N 2 S	0.2 0.2	0.08 1.7	0 0	1.5 17	0.7 11	0 0	4.8 50	20 110	0 0	40 100
FLIGHT TRAJECTORY (EARLY ASCENT)	To Firestream Nominal	Vapor	3×10^3 3×10^3	1 N 2 U	0.00006 0.0008		- -		0 0	0 0	0 0	0 0	0 0	0 0
	Impact (Similar to Launch Site Impact Releases)													
FLIGHT TRAJECTORY (REENTRY)	Melt Zone (Burn-up)	<3μ	4.5×10^4	Long Settling Time	2×10^{-6} Hemisphere		-	-	0	0	0	0	0	0
	Outside Melt Zone (Fragment Impact)	<3μ	5×10^3		2×10^{-6} Hemisphere		-	-	0	0	0	0	0	0
	Impact (Similar to Launch Site Impact Releases)													

* Isopleth area described within the brackets represents an area where the lung retention would be greater than 0.1 μci. This value is not the maximum for a point source release. Maximum value would occur at the point of impact.

** Multiply Km by 0.621 to obtain miles. Multiply Km^2 by 0.386 to obtain square miles.

APOLLO LUNAR SURFACE EXPERIMENT PACKAGE
WITH SNAP-27 RADIOISOTOPE ELECTRIC GENERATOR

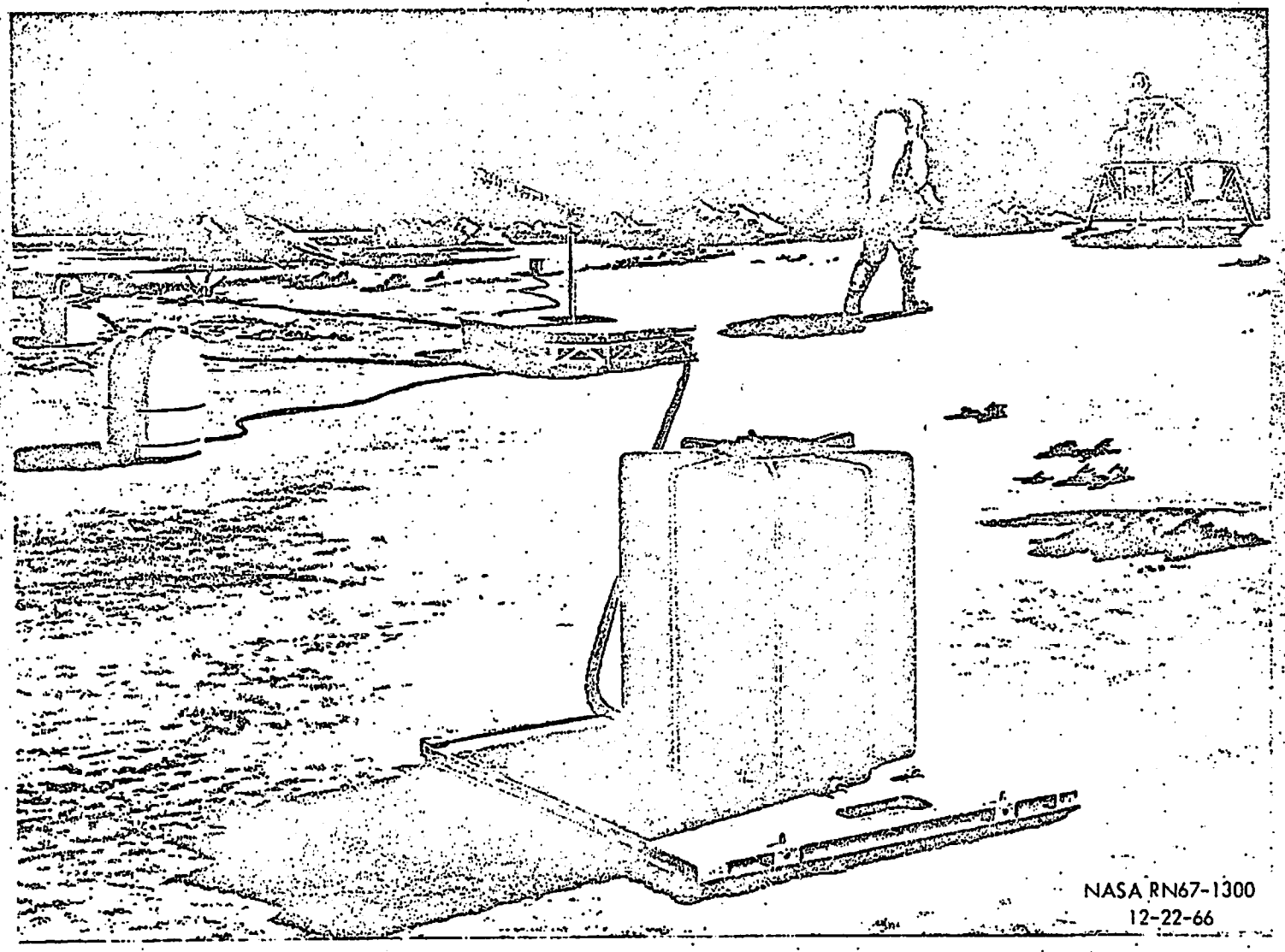

FIGURE 1

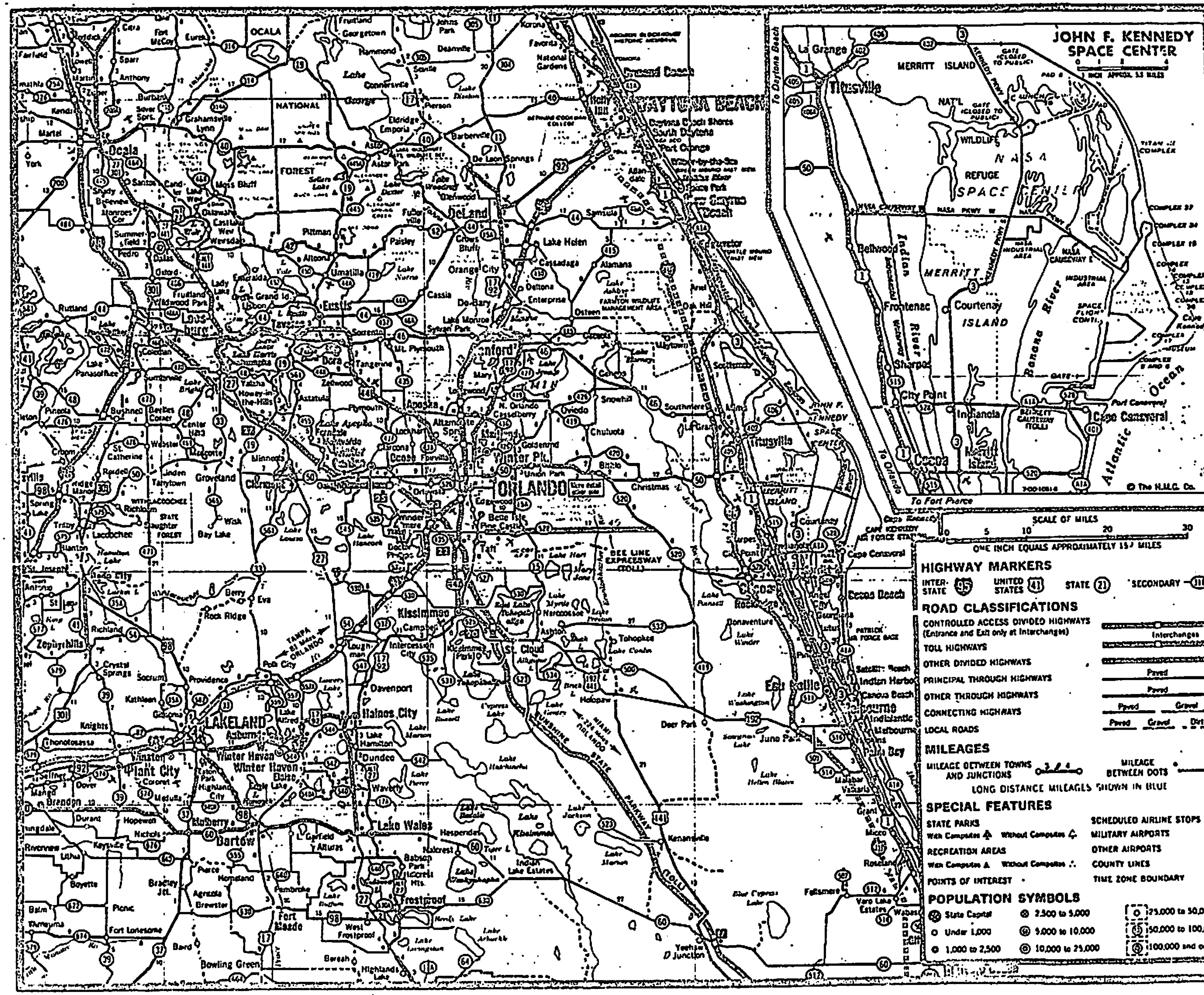
JOHN F. KENNEDY SPACE CENTER
MERRITT ISLAND
NAT'L WILDLIFE REFUGE
NASA SPACE CENTER
Titusville
La Grange
Bellwood
Frontenac
Sharpes
City Point
Courtenay
Indianola
Cocoa
Indian River
Banana River
Atlantic Ocean
Cape Canaveral
To Daytona Beach
To Orlando
To Fort Pierce
© The H.M.G. Co.
SCALE OF MILES
ONE INCH EQUALS APPROXIMATELY 15.7 MILES
HIGHWAY MARKERS
INTER-STATE
UNITED STATES
STATE
SECONDARY
ROAD CLASSIFICATIONS
CONTROLLED ACCESS DIVIDED HIGHWAYS (Entrance and Exit only at Interchanges)
TOLL HIGHWAYS
OTHER DIVIDED HIGHWAYS
PRINCIPAL THROUGH HIGHWAYS
OTHER THROUGH HIGHWAYS
CONNECTING HIGHWAYS
LOCAL ROADS
Interchanges
Paved
Gravel
Dirt
MILEAGES
MILEAGE BETWEEN TOWNS AND JUNCTIONS
MILEAGE BETWEEN DOTS
LONG DISTANCE MILEAGES SHOWN IN BLUE
SPECIAL FEATURES
STATE PARKS
RECREATION AREAS
POINTS OF INTEREST
SCHEDULED AIRLINE STOPS
MILITARY AIRPORTS
OTHER AIRPORTS
COUNTY LINES
TIME ZONE BOUNDARY
POPULATION SYMBOLS
State Capital
Under 1,000
1,000 to 2,500
2,500 to 5,000
5,000 to 10,000
10,000 to 25,000
25,000 to 50,000
50,000 to 100,000
100,000 and over
ORLANDO
DAYTONA BEACH
LAKELAND
Ocala
DeLand
Sanford
Kissimmee
St. Cloud
Winter Park
Winter Haven
Haines City
Lake Wales
Bartow
Plant City
Eustis
Leesburg
Apopka
Titusville
Eau Gallie
Melbourne
Cocoa Beach
OCALA NATIONAL FOREST
Lake George
BEE LINE EXPRESSWAY (TOLL)
SUNSHINE STATE PARKWAY
MIAMI 224 Miles ORLANDO
TAMPA 80 Miles ORLANDO

FIGURE 2

FIGURE 3

CAPE KENNEDY & MERRITT ISLAND LAUNCH AREA

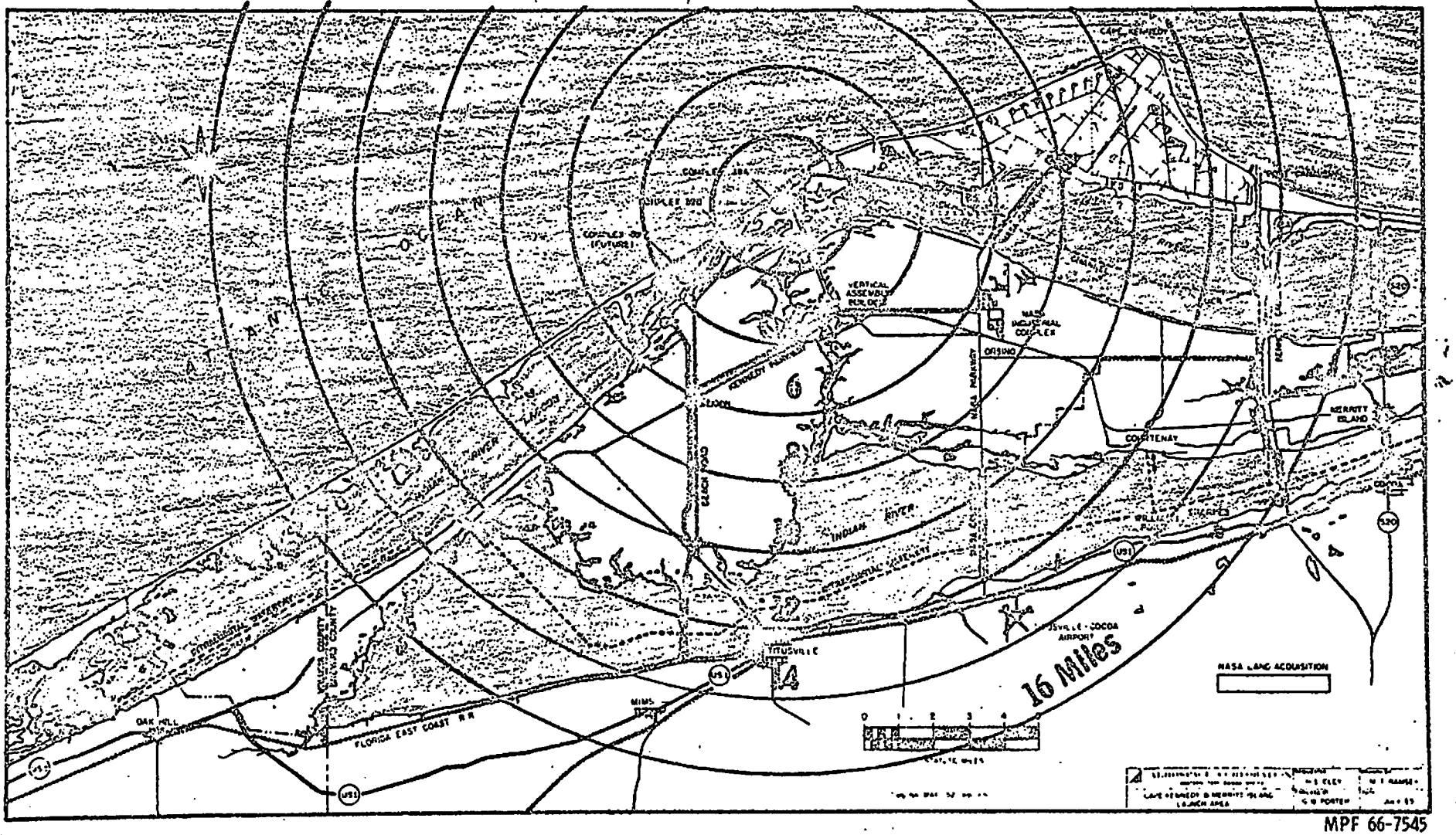

MPF 66-7545

FIGURE 4

SATURN V/APOLLO CONFIGURATION

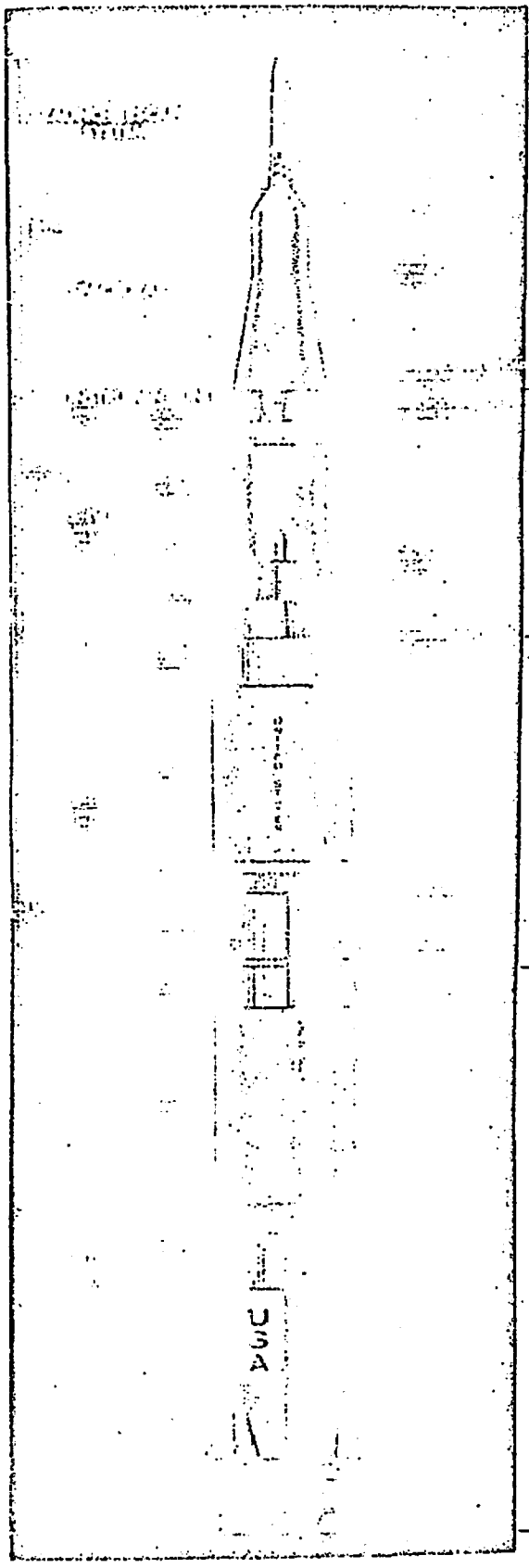

Spacecraft (LM & Service Module)

Fuel:	N_2H_4/UDMH & N_2O_4 ; 61,000 lbs
Velocity:	Coast to lunar orbit injection
Time:	Approximately 62 hours

S-IVB Stage

Fuel:	LOX & LH_2 ; 230,000 lbs.
First Burn:	(Earth orbit injection)
Velocity:	22,000 to 25,600 fps
Altitude:	105 n. miles
Range:	855 n. miles to 1,290 n. miles
Time:	536 sec. to 658 sec.
	coast orbit; 658 sec. to 2 hr. 40 min.
Second Burn:	(Translunar Injection)
Velocity:	25,600 fps to 35,600 fps
Altitude:	105 n. miles to 160 n. miles
Range:	Orbit over Houston, Texas, at ignition
Time:	2 hr. 40 min. to 2 hr. 45 min.

S-II Stage

Fuel:	LOX & LH_2 ; 935,000 lbs.
Velocity:	8,300 fps to 22,000 fps
Altitude:	33 n. miles to 105 n. miles
Range:	50 n. miles to 855 n. miles
IIP:	Remains over the Atlantic Ocean
Time:	159 sec. to 535 sec.

S-IC Booster

Fuel:	LOX & RP-1; 4,723,000 lbs.
Velocity:	0-8,300 fps
Altitude:	0-33 n. miles
Range:	48 n. miles
IIP:	<100 n. miles
Time:	0 - 159 sec.

NOTE: All times are from lift-off.

Figure 6

FUEL CAPSULE ASSEMBLY (FCA)

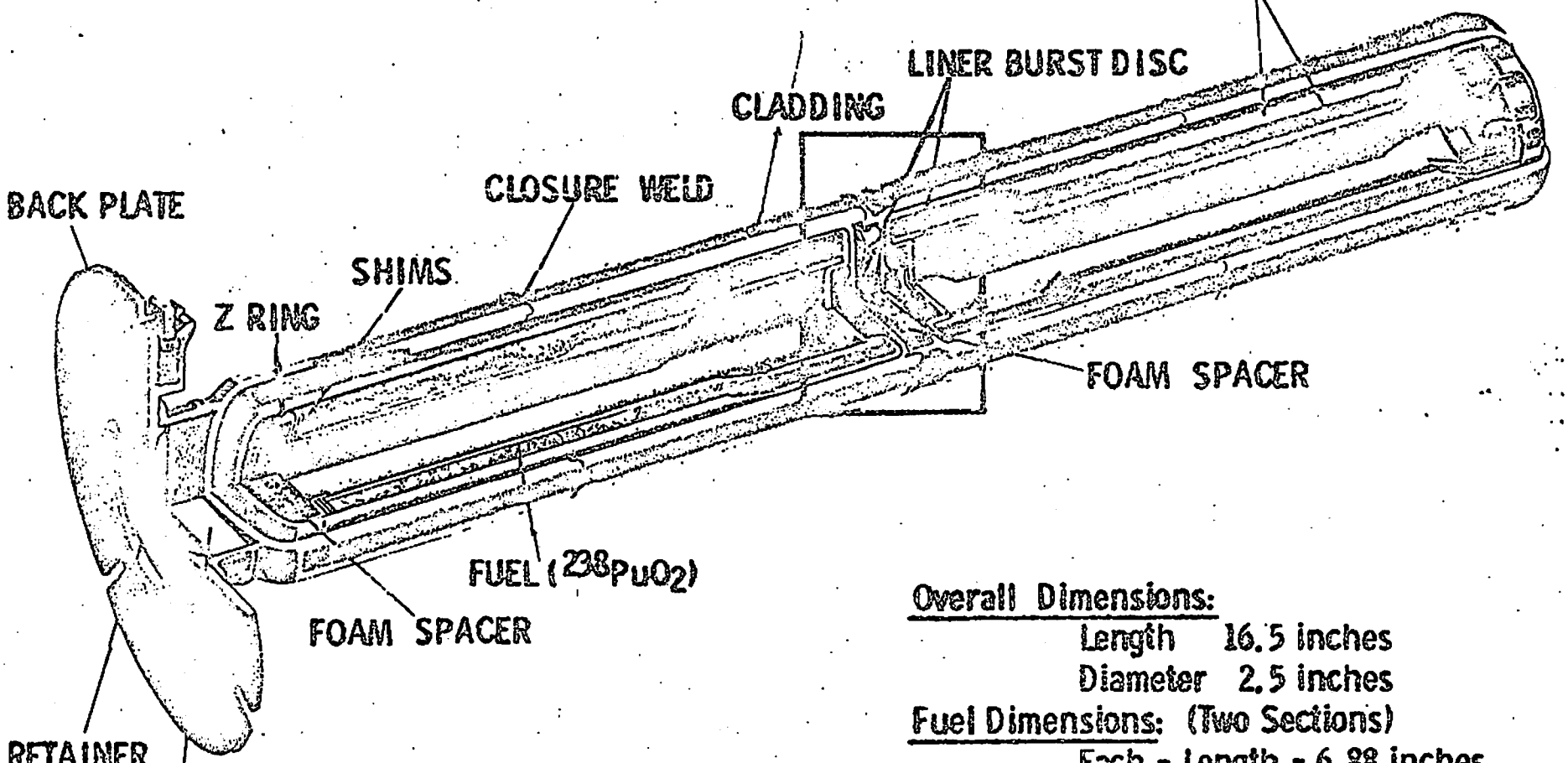

Overall Dimensions:

Length 16.5 inches
Diameter 2.5 inches

Fuel Dimensions: (Two Sections)

Each - Length - 6.88 inches
Width (thickness) - 0.407 - 0.475 ins.

Weights:

Total - 15.46 lbs.
Fuel - 8.36 lbs. (nominal)

Note: All specified components are Haynes 25 except where noted.

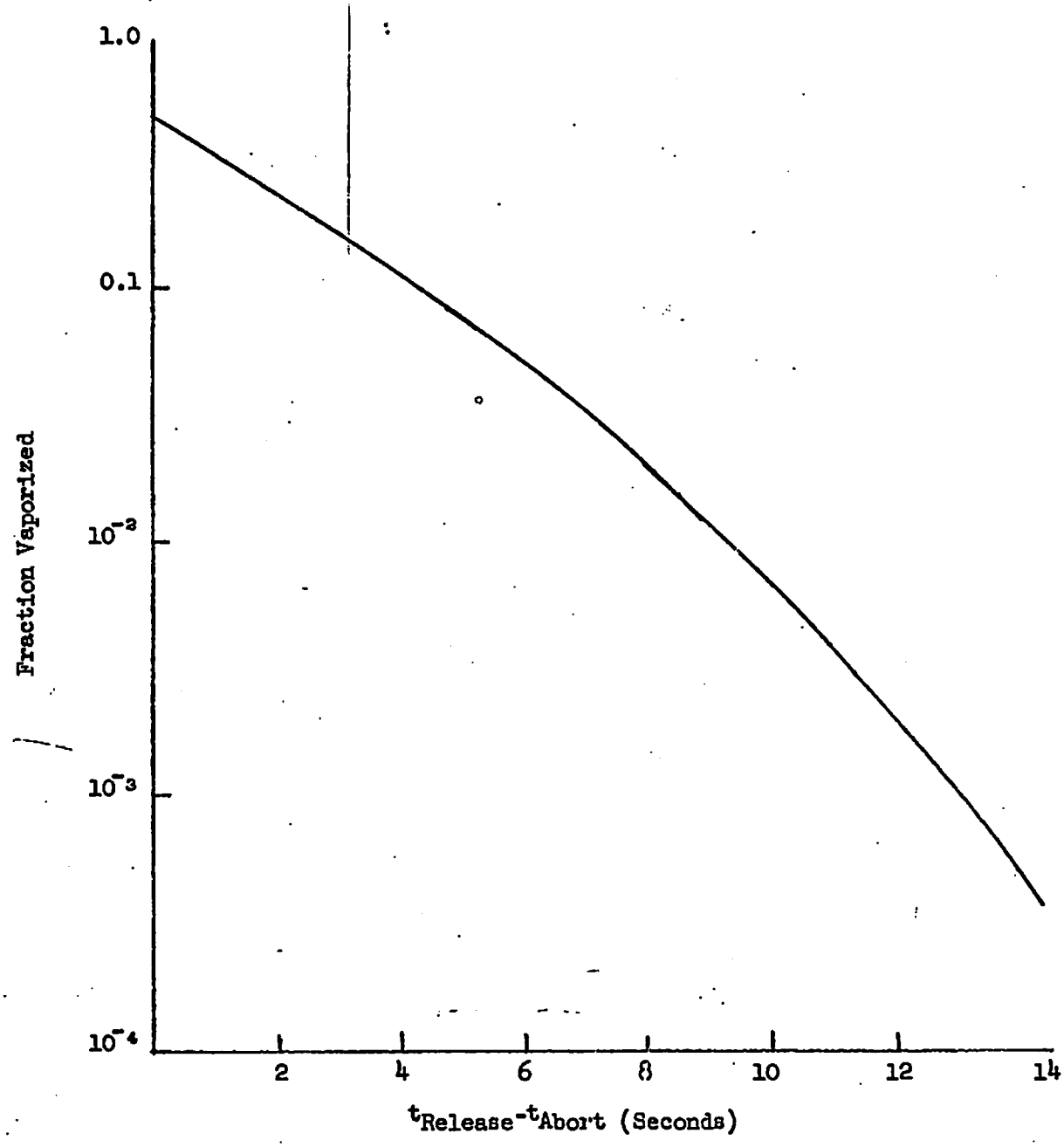

Fraction of SNAP 27 Fuel Vaporized as a Function of the Time Interval Between Fireball Initiation and Release to the Saturn V Fireball.

FIGURE 7

APPENDIX A

REPORT

of

SNAP 27/ALSEP RANGE SAFETY WORKING GROUP

for

SNAP 27 INTERAGENCY SAFETY REVIEW PANEL

REPORT

of

SNAP 27/ALSEP RANGE SAFETY WORKING GROUP

for

SNAP 27 INTERAGENCY SAFETY REVIEW PANEL

I. INTRODUCTION

The SNAP 27/ALSEP Range Safety Working Group was organized to evaluate the nuclear range safety aspects of the SNAP 27. This evaluation includes an assessment of the probability of the potential nuclear fuel releases during range operations and missile abort situations during prelaunch and ascent flight. The assessment includes determination of the physical state and location of the fuel capsule and fuel to establish potential source terms.

The evaluation task was broken up into three specific areas. These were defined as follows:

A. Ground Handling, Storage, and Transportation. This area includes transportation on and off Merritt Island Launch Area and Cape Kennedy Air Force Station, storage and handling operations at Cape Kennedy Air Force Station, and the installation of the GLFC and FCA on the LM during prelaunch checkout.

B. Launch Abort. This area includes all prelaunch checkout operations with the GLFC and FCA installed on the missile, engine ignition and lift-off to an altitude of 600 ft. (The

600 ft altitude was selected as the minimum altitude that range destruct action could be taken during an abort.

C. Ascent Abort. This area includes post-launch flight from approximately 600 ft to between 275,000 and 300,000 ft altitude. The upper altitude was selected so that the fuel particles, if released during an ascent abort, remain outside the predicted fuel melt zone during reentry.

II. REFERENCE DOCUMENTS

A. SNAP 27 Safety Report (Vols I, II, and III).

B. Supplement No. 1 to SNAP 27 Safety Report, Vol II.

C. Preliminary SNAP 27 Source Term Estimates (U) GE STE-68.

III. MEETINGS.

A. 11-12 Sept 1968, Air Force Eastern Test Range, Fla.

B. 24-25 Sept 1968, Subcommittee, Air Force Eastern Test Range, Fla.

C. 22-24 Oct 68, Kirtland AFB, New Mexico.

IV. CONCLUSIONS. The assessment of the nuclear range safety aspects of the SNAP 27/ALSEP mission is summarized in the following subparagraphs:

A. Ground Handling, Storage, and Transportation.

(1) It is highly improbable that a fuel release will occur during transportation, storage, and handling, including

insertion of the FCA into the GLFC. The following accident or abnormal situations were identified and evaluated:

(a) Fire - highway, storage or pad

(b) Lightning

(c) Missile impact - fire or impact

(d) Highway accident - impact or submergence

(e) Loss of coolant in GSC

(f) Internal pressurization of FCA

(g) Hurricane - wind, lightning, impact or submergence

(h) Drop - storage, highway or gantry

(i) Handling tool malfunction

It is noted that the storage location is within the missile impact limit lines for adjoining launch pads and in the event of a pad abort has an impact hit probability associated with this location.

(2) Transportation, storage, and handling of the SNAP 27 FCA will be accomplished within the radiation safety guidelines provided by AEC to NASA. These activities will be performed in accordance with "Handling Procedures" and "SNAP 27 Radiological Control Plan" which will be reviewed by AEC/NASA/DOD authorities. Consequently, personnel exposures should not exceed appropriate radiation exposure criteria. These two documents were not available for review; however, it is anticipated that the operating procedures and plans, when developed and approved, will verify this conclusion.

B. NASA Reliability Numbers. A review was made of the probability numbers assigned to the Prelaunch, SIC, SII Boost Phases specific to the success, abort, explosion and fire, and other effects events. For these phases and events, a cross correlation was made of the data presented in Preliminary SNAP 27 Source Term Estimates (U), DIN: STE-68, Sept 15, 1968, Figures 1, 2, 3 and 4, in Attachment A, and the document, Saturn V Probability of No Ignition and Probability of Explosion by Marshall Space Flight Center dated July 1, 1968. A determination was made that the probability numbers as presented up to and including explosion and fire are still valid and consistent with the current vehicle probability data maintained by the Marshall Space Flight Center. It is recognized that these numbers do not include spacecraft, GSE, or human error estimates. Any attempt to include a probability number for human error would be highly speculative and it would probably not greatly affect the final probability numbers. It was further noted that for SIC and SII Boost Phases, the Range Safety Destruct event was considered to be a conservative one; however, it whould be recognized that in the event that Range Safety Destruct occurs, the explosion and fire results in a low order yield.

C. Prelaunch and Launch Pad Abort Environment.

A comprehensive hazard analysis indicates that the characteristics of a shock wave resulting from an explosion

of the Saturn V vehicle and reaching the GLFC will be less than 600 psi overpressure and 2200 psi milliseconds impulse in over 90% of the incidents. This condition can occur only during the time from propellant loading of the S-IVB stage up to 600 ft altitude on ascent.

This is a conservative estimate based upon a structural failure mode analysis, project PYRO, and estimates of "close-in" liquid propellant explosions. It is expected that the following factors would tend to reduce this level and/or increase the 90% probability factor:

(1) The distance from the GLFC to the center of the explosion was assumed to be a minimum value of 37 feet, i.e., the closest known LH_2/LOX interface. Structural failure analysis indicates explosion may center at greater distances, which would result in lower shock overpressures to the GLFC under similar conditions.

(2) Most of the mixing of the propellants probably will occur outside the SIVB rather than within the tankage, thereby reducing the shock wave overpressure because of less confined mixing and greater distance.

(3) With the propellant quantities in this vehicle it is probable that ignition will occur prior to that delay time required to obtain propellant mixing which would produce the 600 psig overpressure shock wave to the GLFC.

At an altitude of over 600 feet, range safety destruct action would be the most probable abort mode; however, it is not possible to preclude accidental explosions above 600 ft. The range safety destruct action is expected to produce a shock wave of less than 65 psi overpressure to the GLFC.

There have been only four explosions involving over 25,000 lbs of LH_2 and LOX; i.e.,

(a) An intentional failure of an S-IV stage (100,000 lbs).

(b) An accidental failure of an S-IV stage (100,000 lbs).

(c) An accidntal failure for an S-IVB stage (240,000 lbs).

(d) An accidental Atlas Centaur (45,000 lbs LH_2/LOX).

The TNT equivalent yields of the four listed explosions are estimated to range from 1% to 13%.

Calculations based on data from these incidents indicate shock overpressures of 110 to 420 psi at the GLFC at a 37-foot minimum distance.

After detailed consideration of the data available, the committee considers 600 psi as a conservative upper limit of overpressure at the GLFC. The committee recognizes that conditions can be postulated which would yield higher pressures; however, the probability of achieving these conditions seems remote.

The subcommittee which examined the pad abort thermal environment concluded that the GE and Sandia models were acceptable with reservations. An estimate of the thermal environment which the GLFC may encounter from the propellant burning is shown by Attachment 1.

Increased heat fluxes to the GLFC due to specific metal-oxidant reactions were not considered in the fireball thermal analysis. A review of available data will be performed to evaluate the effects of such reactions. The following comments were furnished by Oak Ridge National Laboratory by letter dated 6 Nov 68:

"Based on the GE SNAP 27 Safety Report, Vol II, Accident Model Document, the beryllium SHS is not expected to melt. However, due to blast and shrapnel, the beryllium might be at least cracked, exposing fresh metal surfaces. At the relatively low temperature of beryllium (less than 2000°F) an adherent oxide should be produced which would tend to be self-extinguishing.

"For the titanium hat components, the GE safety analysis predicts 88% melting as a result of the fireball. From the DMIC (Defense Metals Information Center Report 224) Report, it would appear that ignition and burning of these components should be expected. Since this reaction is exothermic, it seems reasonable to expect complete melting or burning of the titanium parts or both. At the least, this would be a source of additional heat to the capsule clad."

It was the opinion of the working group that the fragmentation phenomena associated with the vehicle abort does not lend itself to precise analysis. Capsule rupture from a fragment impact will provide the most critical condition of fuel release to the thermal environment.

The working group agreed with the Sandia "best estimate" calculation method of the most probable fragment size in the case of a center line explosion. However, the Sandia fragmentation model considered only skin fragments characteristic of the material in the S-IVB top dome and did not take into account larger size fragments such as pieces from instruments and equipment and also did not consider explosions originating from other locations than the center line of the S-IVB stage. Therefore, the following areas should be resolved:

(a) The Sandia fragmentation model should be applied to an explosion ignition point at the LO_2/LH_2 interface directly below the GLFC (i.e., junction of common bulkhead and side wall of the S-IVB stage).

(b) Authentication of the fuel release rate and condition of the fuel from a capsule that has been perforated by a fragment should be accomplished.

(c) Evaluation of the integrity of the GLFC and/or FCA from sequential exposure to the shock wave and (1) impact of the GLFC (as a projectile) into vehicle structure or equipment (2) in conjunction with the thermal input.

D. Potential Source Terms. The committee has considered the GE and Sandia Corp estimates of the source terms and as a result developed Table 1 to summarize the estimates. In this table the upper value of each individual range and the assumptions used to develop these values are considered to be conservative by this committee.

Prelaunch

Independent calculations by GE and Sandia indicate that, if microsphere fuel is injected into the abort fireball at the time of abort initiation, approximately 50% of the fuel injected will be vaporized. However, both GE and Sandia agree that instantaneous release of the total fuel inventory is not credible.

Total instantaneous release would require total destruction of both halves of the FCA. The only mechanism available for instantaneous failure of the FCA is fragment penetration, which could affect only one half-capsule.

Because the fireball cools rather rapidly, the amount of vaporization depends strongly upon the interval between fireball initiation and microsphere release. For example, if fuel is released 5 seconds after fireball initiation, both GE and Sandia have estimated that between 5% and 10% of the release fuel will be vaporized.

On the basis of fragment penetration test data, GE and Sandia agree that it is likely that only a portion of the

fuel could be released from the damaged half-capsule, and that this could be released over a period of several seconds.

For the typical case in which the FCA is penetrated, the following assumptions and estimates of the quantity of fuel vaporized made by GE and Sandia were accepted by the committee as a conservative estimate for a range of values for the inhalation source term for an immediate release.

GE estimate of Vapor Source Term for immediate release:

2% of fuel released in fireball/sec

5 sec release gives 0.1 fraction released (4500 curies)

30% of fuel released is vaporized

Fuel vaporized - 1350 curies

Sandia Corp Vapor Source Term for immediate release:

FCA ruptured by explosion and fragmentation

50% of fuel in one capsule released in 12 seconds (11,250 curies)

8% of this fuel is vaporized

Fuel vaporized is 900 curies

Even if the FCA survives the explosion intact but the SHS is damaged, the heat of the fireball could melt the FCA and release fuel. Release will then be delayed by the time required to melt the capsule.

For the typical case in which delayed release occurs, the following assumptions and estimates of fuel vaporized made by GE and Sandia were accepted by the committee as a conservative

estimate for a range of values for the inhalation source term for a delayed release:

GE Estimate of Vapor Source Term:

Capsule melts in 5 seconds

15% of fuel released to fireball after 5 sec (6750 curies)

9% of fuel released is vaporized

Fuel vaporized is 600 curies

Sandia Corp Vapor Source Term delayed release:

SH damaged by explosion and fragmentation

FCA melted in fireball after 8 seconds

16% of fuel in one capsule released during next 4 sec (3600 curies)

0.5% of fuel released is vaporized

Fuel vaporized is 20 curies

GE and Sandia values were obtained independently using different assumptions and approaches to the definition of the source term. The numbers used in the assumptions to define the source term are sensitive to the time of release as noted previously. This committee finds that there are uncertainties associated with the source values; indeed, on the basis of information and data available for immediate release, the differences between the GE and Sandia values is no greater than these uncertainties.

For the delayed case, the difference between the GE and Sandia values is a result of the different assumption used

by GE and Sandia. For release of fuel Sandia assumed that the SHS was still in place but damaged at the point of impact, and that release of fuel resulted from melting of the capsule at one end. GE assumed in their model for delayed release of fuel that the SHS was no longer in place and release of fuel resulted from melting the capsule on the longitudinal axis.

These results are summarized in Table 1. In the GE model, the release given for the case in which the FCA is penetrated is the sum of the "immediate release" and "delayed release" just discussed. If FCA penetration occurs, SHS damage will also occur; hence, there could also be capsule melt and delayed release.

Ascent

Once the vehicle is off the pad and airborne the abort situations can be caused by spontaneous explosions due to a propulsion malfunction or a controlled destruct condition. In the latter situation the abort environment is minimized and would in most cases result in an intact GLFC impacting on either the land mass near the pad or the ocean. For the spontaneous explosion abort situation the integrity of the FCA can be compromised by fragment impact and/or the thermal effects of the ensuing fireball or firestream. As with the launch pad conditions, the quantity of respirable material will be dependent upon the time and the rate at which the fuel is released into the thermal environment. In the GE analyses a

fireball model was used for altitudes up to 2000 feet and a firestream model above 2000 feet. The effects of the firestream were considered to be negligible above 50,000 feet. The committee concurred in this conclusion. For the firestream maximum release condition GE considered the following:

The fuel capsule was assumed to be breached, to remain attached to the vehicle and to spill fuel into the firestream for eight seconds duration and subsequently spill fuel to the atmosphere such that only 60 percent of the total fuel load remains in the FCA at ground impact. As a result, the fraction of fuel released as a vapor was calculated to be six percent or 2700 Ci for aborts between 2000 and 10,000 feet, vaporization is less for aborts at higher altitudes. In the GE model it was assumed that the firestream maintains its peak temperature for eight seconds and the microspheres that are released to the firestream are exposed to this peak temperature for two seconds without cooling. If there is any error in these assumptions it is probably in the direction of overestimating the thermal environment. The uncertainties of the thermal environment for microspheres released to the firestream are greater than they were for the pad abort fireball.

Table 1 summarized the various source terms for condition of the system following booster explosion.

Impact. The source term for fuel on the ground (land or water) can result from fallout of released fuel at some altitude or from a breached capsule at the time of impact. The quantity of material for the various system failure modes are presented in Table 1. Respirable particles can be formed at impacts. The committee considered data for rigid fueled capsule impacted to 450 feet per second on granite targets as a source of information to evaluate this condition and disregarded the GE evaluation. The committee elected to consider, for the terminal velocity of the system based on drop data, that the amount of fuel degraded to respirable size particles would be approximately 10% of the total inventory, or 4500 curies. If the capsule ruptured at impact, it was considered that one percent of the inhalable particles become airborne, or 45 curies. The remainder of the fuel is assumed to remain at the point of impact. The above conclusion is based on producing minor cracks on impact.

E. Abort Probabilities

The probabilities from the Abort Sequence Trees developed by General Electric (updated verbally 23 Oct 68) were reviewed. The GE study was then compared to an internally developed Sandia Corp study of the critical event paths leading to fuel vaporization. The working group found the two independent studies to be in general agreement with respect to methodology

and the numerical results within an order of magnitude or less. In these cases, the group has expressed the probability of event occurrence in terms of a probability range and submits that the probability lies between the upper and lower limits of the range. No attempt was made, nor was it considered essential to extend the Sandia Corp study to include all fuel release probability cases. The group submits that since the two studies agree so closely in the critical event area (fuel vaporization) and that since this area represents the "worst case" and thus the controlling or decision making events, that further validation of the GE probabilities for all fuel release areas is not warranted.

The probabilities expressed for each study represent a summation of the probabilities that certain events have occurred leading up to the final event. For example, the probability of a delayed fuel release given an explosion and fire in a prelaunch abort situation consists of the following elements:

(GLFC Destroyed SHS Damaged FCA Intact)	x	(FCA Melts in Fireball)		
2.24×10^{-3}	x	.75	=	1.68×10^{-3}
(GLFC Destroyed SHS/FCA Breached	x	(FCA Melts in Fireball)		
7.41×10^{-4}	x	.75	=	5.56×10^{-4}
	SUMMATION --------			2.24×10^{-3}

The summation (2.24×10^{-3}) represents the total probability of a delayed fuel release to the fireball, given an explosion and fire in the prelaunch.

In arriving at the basic event probabilities, the two studies (GE and Sandia) separately considered available experimental data, primarily in the areas of FCA impact tests, fragmentation impact effects on the GLFC, airdrop tests, and thermal radiant heating tests. Recognizing that limited test data were available, theoretical data, augmented by judgment, was a primary source in developing both studies. The group submits that the agreement between these two independent studies lends credence to the probabilities developed, even though much of both studies is based on theoretical data.

Shock tube explosive tests scheduled to be conducted by Sandia Corp will provide new experimental data that could alter the probabilities. Additionally, any change to the pressure, thermal, and fragmentation models could similarly effect the probabilities expressed in the attached table.

The probabilities expressed in the attached table are the best possible estimates based on available information.

Attachment 1

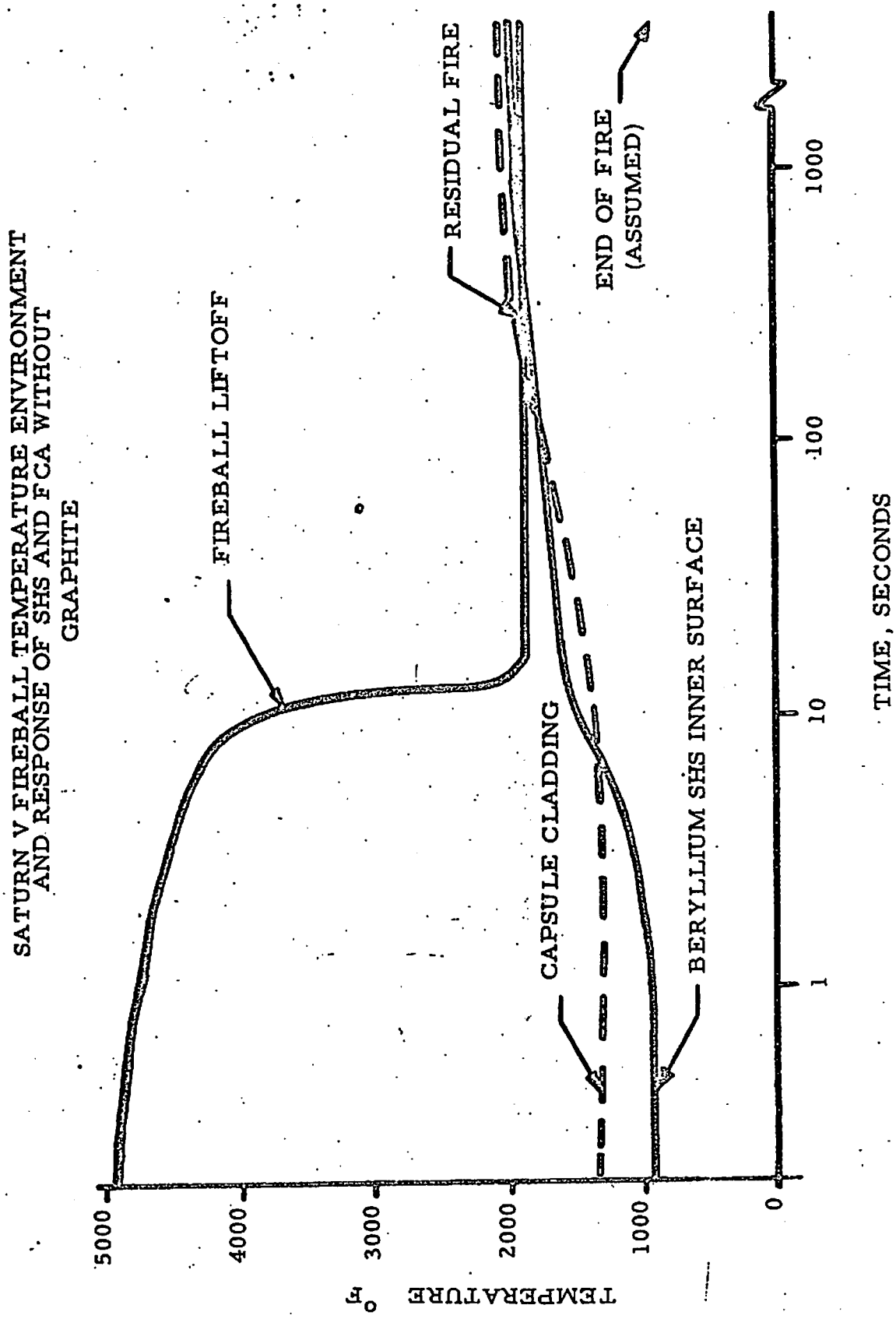

APPENDIX B

REPORT OF SNAP-27 REENTRY WORKING GROUP

FOR SNAP-27 INTERAGENCY SAFETY REVIEW PANEL

REPORT OF SNAP-27 REENTRY WORKING GROUP FOR SNAP-27 INTERAGENCY SAFETY REVIEW PANEL

SUMMARY

The SNAP-27 Reentry Working Group has reviewed the safety of the SNAP-27 for abort reentries. Aborts at superorbital, orbital and suborbital speeds were studied; effects of explosions were examined separately. For the relatively mild environment of aborts at suborbital and orbital speeds, the probability of release of fuel into the atmosphere is less than 10^{-6}. For aborts at superorbital speed, possible failures, from excessive removal of heat-shield material at shallow reentry angles and from excessive thermoelastic stresses at steep reentry angles, result in a probability of fuel release into the atmosphere on the order of 10^{-3}. Explosions result in a probability of fuel release into the atmosphere on the order of 10^{-4}.

INTRODUCTION

The SNAP-27 Reentry Working Group was convened to evaluate and document the safety analysis of SNAP-27 for abort reentries (as stated in the charter, attachment 2 of reference 1). The first meeting of the Working Group took place at the General Electric Company, King of Prussia Park, Pennsylvania, September 5 and 6, 1968. During the first meeting, General Electric personnel presented to the Working Group a safety review (reference 2) which concentrated on the critical reentry cases not covered in their three-volume Safety Report (reference 3). A critique by the Working Group of the presentations and the Safety Report raised questions about the safety of SNAP-27 for abort reentries; these questions are documented

in the minutes of the first meeting (reference 4). The second meeting, at General Electric, October 29-31, 1968, (agenda and attendance list attached) was planned to answer the questions raised, and on the basis of the answers, to tabulate probabilities for fuel release from abort reentries. This report summarizes the findings of the Working Group.

REVIEW OF REENTRY ANALYSIS

Questions raised about the safety of SNAP-27 for abort reentries and the work done to answer the questions are summarized in this section of the report; details are given in Appendices.

Effect of New Weights and Drag Coefficients on Reentry Analysis.- A study conducted by Sandia of the effect of new, and presumably more accurate, weights and drag coefficients on heating rates to the SNAP-27 fuel cask (GLFC) is presented in Appendix A. From this study, it is concluded that the new data don't make significant changes in the reentry analysis; the existing trajectory, drag and heating calculations are adequate for the cases considered.

Are Considered Entry Conditions the Most Severe that Might be Encountered?- Appendix B presents a Sandia trajectory analysis for grazing superorbital reentries. This analysis, and a similar analysis by the Mission Analysis Divison at the Ames Research Center (Appendix B1) indicates that numerous orbits can occur before final reentry. Multiple orbits can impose heat loads greater than those for the trajeoctories considered in the Safety Report (reference 2).

Perturbation effects of the gravitational fields of the moon, sun and major planets on the grazing trajectories have been studied at the Ames Research Center. As indicated in Appendix B1, the perturbation effects can be very large; they can either increase or decrease the number of orbits.

In contrast to the shallow, grazing reentries, superorbital reentries can also occur at initial flight-path angles larger than the 38° considered in the Safety Report (reference 2). These steep reentry angles can result in maximum stagnation pressures, for example, of about 10 atmospheres and maximum heating rates of about 3,300 Btu/ft^2-sec, as compared with 4 atmospheres and 1800 Btu/ft^2-sec for reentry angles of 38°.

Consequences of More Severe Reentry Conditions than those Considered.- Appendix C describes a Sandia analysis of the ablation and thermal response of the GLFC for multiple-orbit reentries. The analysis indicates that complete graphite removal will occur in the stagnation region if the GLFC passes through the atmosphere more than about 20 times (with stable orientation) before final reentry.

For the very steep trajectories (flight-path angles greater than 38°), the graphitic heat-shield material has now been tested at the highest pressures, but not the simultaneous high heating rates that the GLFC can encounter. The tests were conducted in arc-jet facilities at the Ames (Appendix D) and Langley Research Centers (Appendix E). The models ablated smoothly in both tests, rather than by spallation. The ablation mode is not known for the simultaneous high pressures and high heating rates.

Comparison of Ablation Analyses and Experiments.-

Appendix F presents a comparison of measured and predicted ablation rates. The data are for two sets of test conditions: (1) the maximum heating rate and total heat load approximately correspond to those for abort from earth orbit; the stagnation pressure is an order of magnitude lower than the flight maximum, but the effects of pressure on ablation in this pressure range is well understood; and (2) heating rate approximately the maximum for 38° reentry but again stagnation pressures almost an order of magnitude less than the flight maximum. However, for the relatively high pressures corresponding to steep reentries, the effects of pressure on ablation are not as well understood as in the lower pressure range. Agreement between the predicted and measured recession is excellent for the earth-orbit condition. For the steep superorbital reentry, however, the predicted recession is about 50 percent below that measured; the predicted surface temperature is 650°R below that measured. Because of the small amount of material ablated in steep reentries these discrepancies are not of too much concern from the ablation standpoint. Nevertheless, inability to predict surface recession and surface temperature might be an indication of uncertainties in material properties.

Uncertainty in Structure Safety Margin.-

A comparison of stresses calculated by G. E. and by Sandia is shown in Appendix G. The same trajectory information and material properties were used in both sets of calculations, but different computer programs were used. Relatively good agreement between the results for the two methods is indicated.

Available data on the structural properties of the GLFC were studied in detail by Messrs. Biffle, Sauer and Vosteen of the Reentry Working Group prior to the second meeting. The use of average properties, rather than the most conservative data points, was thought to constitute unconservative design procedure.

A study of the density distribution through the thickness of the graphitic material indicated much flatter variations of density, Appendix H, than those given in figure P4-36 of Supplement No. 1 to the SNAP-27 Safety Report (reference 2). G. E. personnel agreed that tag-end samples of the flight hardware also indicated flatter density variations than originally specified.

The Working Group discussed possible variations in material thermal properties but no conclusions were reached as to the magnitude of reasonable variations to expect.

Effects of variations of material thermal properties on GLFC and capsule temperatures are shown in Appendix I (a Sandia study). Arbitrary variations of density, specific heat, thermal conductivity and emissivity were chosen. They were pessimistically all varied in a direction to increase internal temperatures. For the case examined, the property variations resulted in a 90°F increase in the temperature of the beryllium secondary heat shield and a 70°F increase in the capsule clad temperature.

Effects of variations of material structural properties on GLFC stresses are presented in Appendix J (a Langley Research Center study). Using a density variation of 91#/ft^3 at the outer edge, 85#/ft^3 at the center and 87.5#/ft^3 at the inner edge of the graphitic heat shield, instead of the steeper density gradients shown in figure P4-36 of reference 2, a negative safety margin of 16 percent was calculated.

Arguments were presented, supported by stress calculations made by G. E., that thermal stress failures would not propagate because the graphite cylinder was held together by aerodynamic loading. Aerospace performed an elastic isotropic cylinder analysis (Appendix J1) which demonstrates that the aerodynamic loads reduce the already suspect margins. An analysis done at the Langley Research Center confirms this (Appendix J2); negative stress margins are predicted for -20° as well as -38° super-orbital reentries.

Mode of Failure of Fuel Capsule.-

Radiant heat tests were conducted at Sandia on two capsules loaded with simulated fuel (Appendix K). The capsules were pressurized to simulate the helium pressure existing after one of the capsules was tested to destruction. On this test, the outer shell cracked open and the inner shell expanded as an inner tube in a tire. If during reentry the capsule failed in the same manner as in the test, fuel release would be unlikely. However, the mode of failure of the capsule is not well understood. Therefore, it is felt that this type of failure should not be counted upon. To decrease helium pressure and therefore chances of capsule burst and release of fuel, it is recommended that the capsule should be vented as soon before launch as is practicable.

Earth Impact.-

Analytic and experimental studies have been conducted of the terminal velocity and response to earth impact of the intact GLFC (Appendix L). The analytic studies indicated terminal velocities between 285 and 450 feet per second, depending on the attitude (side on stable, planar tumble, or random tumble) of the GLFC and whether the analysis was by G. E. or Sandia.

Three drop experiments indicated terminal velocities of 300,330 and 360 feet per second. In one drop experiment, a simulated GLFC was preheated to 1900°F; the internal pressure was 4 atmospheres. The GLFC impacted on hard soil. Both end caps flew off, intact; the cylinder showed delamination but no cracks. The beryllium secondary heat shield and the capsule cracked but there would have been no fuel release.

Consideration has been given to the condition of the GLFC fuel-capsule assembly after reentry, just prior to impact. It is possible that the graphite and secondary heat shields could be removed during reentry with the fuel capsule undamaged or partially damaged (ablated) such that little fuel would be released in the atmosphere. The fuel might then be released on impact, as the capsule is further damaged on impact. It should be noted, however, that impact tests of bare fuel capsules undamaged before impact indicated satisfactory containment of fuel.

Appendix L1 presents an analysis by Baldwin and Allen of the Ames Research Center which describes the distance single particles with a given initial velocity will travel in still air. The analysis indicates, for example, that single plutonium dioxide microspheres which rebound from the earth at speeds of .1 km/sec or less, and are 1 micron or less in diameter, will travel less than 5 cm in still air. It is not known how much farther one microsphere will travel in the wake of a larger microsphere; nor were effects of wind conditions considered.

What Happens to Microspheres if they are Released?

A Sandia analysis of microsphere reentry is described in Appendix M. This analysis, and a less detailed analysis conducted at the Ames Research

Center, essentially confirms the melt zone shown in figure N-2 of volume 2 of the SNAP-27 Safety Report (reference 3). A conclusion of Appendix M is that plutonium dioxide microspheres released within the melt region will lose a major fraction of their mass and the resulting debris will range in size from a few microns to less than 0.01 microns.

GLFC Attitude During Reentry.-

Studies of the attitude time history of the GLFC during reentry have been made. In addition to the single six-degree-of-freedom run by G. E. described in Section P2.2.1 of reference 2, about 20 cases have recently been run at the Ames Research Center (Appendix N). As expected, the attitude-time history of the GLFC was found to depend upon initial spin and tumble rates, initial entry angle and how rapidly the dynamic pressure was increasing or decreasing. In general, it was found that the motion arrested, or oscillated in a small angle range about the side-on-stable mode of entry, in the important region of reentry heating. Effects of ablation which decrease the range of oscillations (reference 5) were not included in the analysis. In none of the cases was the reentry in the bombing (hemispherical end forward) mode. The bombing mode is not expected because the center-of-pressure in this attitude is forward of the center of gravity; thus, the GLFC is statically unstable in this attitude. Expected spin rates are not high enough to provide sufficient gyroscopic stability in this mode to overcome static instability.

Flight Tests.-

The Reentry Working Group discussed the possibility and desirability of flight tests of the GLFC. Flight tests for aborts from earth orbit

were not thought to be necessary. It was agreed that flight tests of grazing, superorbital reentries were impractical. Flight tests to check thermoelastic stresses would be very difficult and costly, even if possible. A meaningful experiment would require: (1) propulsion to drive the GLFC into the atmosphere to get the proper external temperature (higher than can be obtained naturally from earth orbit), (2) some means of internal heating to simulate that provided by the plutonium dioxide heat source, (3) thorough instrumentation and (4) recovery. In short, flight tests were thought to be impractical in this application.

PROBABILITY OF FUEL RELEASE IN MELT ZONE

The above information together with abort and explosion probabilities furnished to the Working Group was used to generate a table of probabilities for fuel release in the melt zone (Table 1). Abort and explosion probabilities were obtained from reference 6. How the probabilities for the various reentry angles was arrived at is described in Appendix O. The other probability numbers are the best judgment of the Reentry Working Group based on the Review of the Reentry Analysis above.

CONCLUSIONS

1. The probability of fuel release into the melt zone from failures during aborts at suborbital or orbital speeds is less than 10^{-6}.
2. The probability of fuel release into the melt zone from failures during aborts at superorbital speeds is about 10^{-3}.
3. The probability of fuel release into the melt zone from explosions is about 10^{-4}.

TABLE I

PROBABILITY OF FUEL RELEASE IN MELT ZONE

SUPERORBITAL REENTRY

Event Probability	Angle (degrees)	Possible Failure Mode	Failure Probability: Any Kind	Fuel Release	Fuel Fraction	Fuel Melt	Total**
.0075	$0 < \gamma < 3.9$ (like orbital decay)	High Temp (a)	.6	10^{-3}	10^{-3}	1	4.5×10^{-6}
		High Temp (b)	.2	5×10^{-3}	2×10^{-3}	1	7.5×10^{-6}
		High Temp (c)	.13	10^{-2}	5×10^{-3}	1	1.0×10^{-5}
		Ablation or thermal stress	.067	.5	.5	.5	1.25×10^{-4}
.0004	$3.9 < \gamma < 4.1$	Total ablation prior to final reentry	.75	1	1	.2	6×10^{-5}
.0015	$4.1 < \gamma < 4.35$	Partial ablation prior to reentry, total ablation during reentry	.5	1	1	1	7.5×10^{-4}
.0024	$4.35 < \gamma < 5.1$ (Some graphite remains)	High Temp	.5*	.1	10^{-3}	1	1.2×10^{-4}
		Ablation	.3*	.1	1	1	7.2×10^{-5}
.0378	$5.1 < \gamma < 6.25$	High Temp.	.2	10^{-2}	10^{-3}	1	7.6×10^{-5}
.0378	$6.25 < \gamma < 6.75$	High Temp. Thermal Stress	.2	10^{-2}	10^{-3}	1	7.6×10^{-5}
.015	$6.75 < \gamma < 20$	Thermal Stress	.15	.5	1	.5	5.5×10^{-4}
.0076	$20 < \gamma < 90$	Spallation	.05*	.8*	1	.5*	1.5×10^{-4}
		Thermal Stress	.4	.5	.5	.5	7.6×10^{-4}

TABLE 1 - Continued

Event Probability	Angle (degrees)	Possible Failure Mode	Failure Probability: Any Kind	Fuel: Release	Fuel: Fraction	Fuel: Melt	Fuel: Total
ORBITAL DECAY							
.03		(a) Capsule Burst	.8	10^{-3}	10^{-3}	1	2.4×10^{-5}
		(b) (a) + SHS Melt	.2	5×10^{-3}	2×10^{-3}	1	3×10^{-5}
		(c) (a) + (b) + Clad Melt	.1	10^{-2}	5×10^{-3}	1	3×10^{-5}
		(d) Ablation	10^{-6}	1	1	1	3×10^{-8}
SUBORBITAL							
.07		(a)					
		(b)					
		(c)					
		(d) Ablation	10^{-6}	1	1	.5	3.5×10^{-8}

TABLE I - Concluded

EXPLOSIONS

Event Probability		Possible Failure Mode	Failure Probability: Any Kind	Fuel: Release	Fuel: Fraction	Fuel: Melt	Fuel: Total
.0012 (1)	12,000'/sec < V < 26,000'/sec	GLFC shatters	.3	.25	1	.5	4.5×10^{-5}
		Capsule Shatters	.001	1	.75	.5	6×10^{-7}
or .0084 (2)		GLFC Shatters	.3	.25	1	.5	3.1×10^{-4}
		Capsule Shatters	.001	1	.75	.5	4×10^{-6}
.0006 (1)	26,000'/sec < V < 36,000'/sec	GLFC shatters	.3	1	1	.9	1.6×10^{-4}
		Capsule Shatters	.001	1	1	.5	3×10^{-7}
or .0086 (2)		GLFC shatters	.3	1	1	.9	2.3×10^{-3}
		Capsule Shatters	.001	1	1	.5	4.3×10^{-6}

*Insufficient information
(a) Capsule Burst
(b) Burst + SHS Melt
(c) Burst + SHS Melt + Clad Melt

(1) NASA Estimate
(2) Sandia Estimate (includes explosions during LM breakup)

REFERENCES

1. Letter from Associate Administrator for Advanced Research and Technology, NASA; subject: Aerospace Nuclear Safety Evaluation Panel and Working Group, dated August 29, 1968.

2. Supplement No. 1 to SNAP-27 Safety Report, General Electric Missile and Space Division, September 16, 1968.

3. SANP-27 Safety Report

   General Electric Missile and Space Division, July 24, 1968.

   Vol. 1: Reference Design Document, DIN: 6300-325

   Vol. 2: Accident Model Document, DIN: 6300-300

   Vol. 3: Safety Analysis Report, DIN: 6300-299

4. Minutes of first meeting of SNAP-27 Reentry Working Group, General Electric Missile and Space Division, King of Prussia Park, Pennsylvania, Sept. 5, 6, 1968.

5. Tobak, Murray and Peterson, Victor L.: Theory of Tumbling Bodies Entering Planetary Atmospheres with Application to Probe Vehicles and the Australian Tektites. NASA TR R-203, July, 1964.

6. Estimates of Apollo Manned Lunar Landing Mission Reliability, furnished by NASA for use in the SNAP-27 Safety Report.

LIST OF APPENDICES

A. Drag Comparison Study (Sandia)

B. Trajectories and Heating Environment for Multiple Orbit Reentries (Sandia)

B.1. Multiple-Orbit Reentries (Ames)

C. Ablation for Multiple-Orbit Reentries (Sandia)

D. High Pressure Ablation Tests (Ames)

E. High Pressure Ablation Tests (Langley)

F. Comparison of Ablation Analyses and Experiments (Sandia)

G. Comparison of Stresses Calculated by G. E. and by Sandia

H. Density Distribution Through Thickness of Heat Shield (Ames)

I. Effects of Variations of Material Thermal Properties on GLFC and Capsule Temperatures (Sandia)

J. Effects of Variations of Material Structural Properties on GLFC Stresses (Langley)

J.1. GLFC Stresses Resulting from Aerodynamic Loading (Aerospace)

J.2. GLFC Stresses Resulting from Aerodynamic Loading (Langley)

K. Radiant Heat Tests of Fuel Capsule (Sandia - G. E.)

L. GLFC Terminal Velocity (Sandia - G. E.)

L.1. Maximum Altitude and Range of Particles in Still Air (Ames)

M. Microsphere Reentry Studies (Sandia)

N. Attitude-Time History of GLFC During Reentry (Ames)

O. Reentry-Angle Probabilities (Marshall)

APPENDIX C

REPORT OF THE METEOROLOGICAL WORKING GROUP

SNAP-27 SAFETY REVIEW PANEL

REPORT OF THE METEOROLOGICAL WORKING GROUP
SNAP-27 SAFETY REVIEW PANEL

JANUARY 17, 1969

Meteorological Working Group Members
J. Holland, DBM, Chairman
C. Anderson, AFWL
R. Baker, DRL
H. Church, Sandia
J. Fuquay, PNL
J. Kaufman, MSFC
R. Klecker, REG
P. Krey, HASL
E. Stiegall, PHS
J. Miller, DBM
I. Van der Hoven, ESSA

REPORT OF THE METEOROLOGICAL WORKING GROUP
SNAP-27 SAFETY REVIEW PANEL

	Page
Summary	
1. Introduction	1
2. Abort Sequences Leading to Release of Fuel to the Atmosphere	2
2.1 Prelaunch and Liftoff	2
2.1.1 FCA Thrown Clear of Fireball	2
2.1.1.1 Ground Release of Fine Particles	3
2.1.1.2 Resuspension	4
2.1.2 FCA Exposed to Fireball	4
2.1.2.1 Release of Fine Particles Resulting from Vaporization	5
2.1.2.2 Release of Microspheres to Fireball	6
2.2 Lift-Off to LET Jettison	7
2.2.1 Ground Impact of Fuel Capsule	7
2.2.2 High Altitude Fine Particle Release	7
2.2.3 High Altitude Microsphere Release	9
2.3 Sub-Orbital Boost and Earth Orbit	9
2.3.1 Random Earth Impact Between 35°N and 35°S	10
2.3.2 FCA Rupture Due to Aerodynamic Heating	10
2.3.2.1 Release of Unmelted Microspheres	11
2.3.2.2 Fine Particle Release Resulting from Melting of Fuel	11
2.4 Translunar Injection to Lunar Orbit Insertion	11
2.4.1 Random Earth Impact	12

Page

2.4.2 Re-Entry Melting of FCA 12

2.4.2.1 High Altitude Microsphere Release 12

2.4.2.2 High Altitude Fine Particle Release 12

3. Parametric Description of Concentration, Deposition and Exposure 12

3.1 Cold, Ground-Level Release 13

3.1.1 Exposure 14

3.1.2 Deposition and Resuspension 17

3.2 Hot Cloud Release 23

3.2.1 Cloud Rise 23

3.2.2 Deposition of Microspheres 24

3.2.3 Fine Particle Release in the Fireball 31

3.3 High Altitude Release 38

3.3.1 Ascent to Earth Orbit 38

3.3.2 Random Re-Entry 40

3.3.3 High Altitude Fine Particle Release 41

REPORT OF THE METEOROLOGICAL WORKING GROUP
SNAP-27 SAFETY REVIEW PANEL

SUMMARY

1. INTRODUCTION

The Meteorological Working Group, a sub-committee of the SNAP-27 Safety Review Panel, has as its purpose the analysis of potential atmospheric and ground concentrations of radioactive material should the SNAP-27 fuel containment equipment fail to fully contain the $^{238}PuO_2$ fuel. This includes a review of relevant parts of the General Electric Missile and Space Division's SNAP-27 Safety Report (which will be referred to as "G.E.").

The Meteorological Working Group has held two meetings, the first August 22-23, 1968, at AEC Headquarters, Germantown, Maryland, and the second September 11-13, 1968, at Patrick Air Force Base, Florida.

SNAP 27 fuel is in the form of high-fired $^{238}PuO_2$ microspheres ranging in size from 50-250 microns diameter. Total fuel load is 44,500 curies of which about .001% consists of fines of less than 3μm diameter that exist in the as-built fuel. Containment of the fuel is in the form of 1) the fuel capsule assembly (FCA) which provides double encapsulation with an inner liner and outer clad of high strength alloy; 2) a graphite LM (Lunar Module) fuel cask (GLFC) which consists of a graphite outer shell and inner metallic secondary heat shield (SHS).

The FCA is designed to contain the fuel and the helium generated through alpha decay for a period of time longer than the planned mission life. It consists of two "capsule halves" vented to a central section. The GLFC is designed to provide protection against thermal environments resulting from

fireballs caused by booster explosions or re-entry from earth orbit or super-orbital velocities. The SHS is designed to withstand blast overpressure from booster explosions. It will also protect the FCA from melting if the graphite outer shell is removed by heat, blast or shattering due to impact.

2. ABORT SEQUENCES LEADING TO RELEASE OF FUEL TO THE ATMOSPHERE

The following described abort sequences are deemed to be those most likely to result in release of the fuel capsule and/or its contents ($^{238}PuO_2$) to the environment.

2.1 Prelaunch and Liftoff

The prelaunch phase begins with the installation of the fuel capsule on the LM and ends with the liftoff of the Saturn V vehicle. The accident most likely to release fuel during this phase of the mission would be explosion of a Saturn V booster stage and the resulting fire. The critical elements of this type of accident are the pressure wave (blast), shrapnel and thermal environment. This kind of accident could occur either during prelaunch or immediately after S-IC ignition but before the vehicle clears the immediate launch pad area. This type of abort could result in the following fuel release conditions.

2.1.1 FCA Thrown Clear of Fireball - (Cold Ground Release)

In this situation the FCA would impact on the ground outside the fireball. Analyses indicates that the pressure pulse may fracture the outer shell of the GLFC, but the SHS is designed to withstand the blast pressure effects and also protect the FCA against melting. In the unlikely event that the fuel capsule were ruptured on ground impact or by shrapnel, some $^{238}PuO_2$ fuel could be released as comminuted particles and fines ($<3\mu m$ diameter) and microspheres

(50-250μm diameter). This would constitute a ground level release. While the comminuted particles (including fines) would be subject to downwind dispersal and resuspension by surface winds (if capsule is not buried) the microspheres, if any were released, would remain on the ground within a few hundred meters of the point of impact due to their larger mass. While only these two particle size categories will be analyzed in most cases, it should be borne in mind that a major or minor part of the released material could have a size spectrum in the intermediate range.

2.1.1.1 Ground Release of Fine Particles

Design features inherent in the GLFC and SHS are intended to provide a high degree of assurance that the FCA will be contained in the GLFC to the point of impact on the earth. Also, the bare fuel capsule has demonstrated its ability to contain simulated fuel when impacted at 250 ft/sec on granite. However, the probability that the GLFC and SHS will be destroyed or damaged and the bare fuel capsule exposed and ruptured must be considered. The temperature of the FCA inside the GLFC is approximately 1800°F. This would be a contributing factor to its possible rupture and spillage of PuO_2 fuel at the surface of the earth.

If capsule impact is on soft earth burial is possible. In this event, any fuel released would be retained underground. However, erosion and weathering could result in exposure and suspension in the atmosphere of the released fuel.

Impact and breaking of the capsule on the land surface will result in some release but not necessarily all of the fuel to the atmosphere. The release would consist of fines and comminuted particles (< 3μ diameter) and microspheres.

Fines and comminuted particles released will be subject to dispersion by the prevailing winds at the time of impact. Possible fuel transport and

dispersion has been calculated by G.E. and the Meteorological Working Group for various atmospheric conditions. A release of fine particles with a mass median diameter of 1μm has been assumed. Calculations have been made showing areas bounded by isopleths of constant ratio of lung dose (D_L) to fuel release fraction (F_f). The calculations were made assuming no depletion of the PuO_2 content of the cloud due to ground deposition.

2.1.1.2 Resuspension

Fine particles deposited on the surface of the earth are subject to resuspension and transport by wind action. Such particles on a surface are difficult to resuspend by wind action if the entire surface consists of similar fine particles. However, due to a process known as saltation, whereby larger airborne particles impinge on the smaller particles, the small particles or "fines" can be resuspended into the atmosphere. Also, movement of vehicles, people or animals over the surface of the earth may further disturb and resuspend the particles. The long half-life of Pu^{238} would permit the possibility of resuspension to exist over a long period of time.

The quantity of fines available for resuspension will vary with time, due to loss to the winds and also due to the action of rain and surface water and to being covered by dust.

G.E. and the Meteorological Working Group have presented mathematical expressions which permit a reasonable approximation of the fraction of fines available which become airborne due to action of the wind. From this the rate of resuspension and air concentration can be approximated.

2.1.2 FCA Exposed to Fireball

A Saturn V fireball temperature environment may approach 5000° F at the time of ignition. The temperature at ground level will drop to about 4000° F within ten seconds after ignition and by about 12 seconds decline to the residual fire temperature of 2000° F (below the melting point of capsule and microspheres). The temperature inside the rising fireball will remain high for a longer time. The residual fire on the ground, or launch pad, may last as long as 60 minutes. Fireball lift-off will occur within 8-12 seconds after ignition. In order to inject fuel directly into the fireball the GLFC, secondary heat shield and fuel capsule must be breached. Analysis indicate the bare capsule will melt at 2400° F in 3.8 seconds if exposed at time of ignition of the fireball and could conceivably rupture earlier due to internal pressure buildup. Fuel exposure at this time due to rupture or melting of the FCA will result in microsphere release followed by vaporization of a portion of the microspheres. Vaporization and microsphere release are discussed in the following two sections, 2.1.2.1 and 2.1.2.2.

2.1.2.1 Release of Fine Particles Resulting from Vaporization (Hot Cloud Fine Particle Release)

Any fuel released due to a fuel capsule rupture during the first ten seconds of a fireball could be partially vaporized into inhalable size (condensing to an estimated .01μ diameter), G.E. analysis indicates that up to 62% of the fuel (microspheres 50-250μ diameter) spilled into a fireball at its ignition could be vaporized under stagnant conditions and approaching 90% if the particles and gases have large relative velocity. If spilled at five seconds after ignition the amount vaporized would be 10% and at 10 seconds 0.2%. Vaporized fuel and fines would be carried aloft by the fireball cloud rise. Some disagreement exists as to the maximum height to which the cloud and vaporized fuel would rise.

G.E. postulates an average cloud rise of 550 meters. However, others, including members of the Meteorological Working Group estimate cloud rises of up to 4000 meters. Also, G.E. estimates particle sizes (vapor) to be .01μ diameter.

2.1.2.2 Release of Microspheres to Fireball (Hot Cloud Microsphere Release)

Large fuel particles released to a rising fireball will be carried some distance above ground by the drag effects of the rising hot gases, after which they will fall to earth due to gravity through a nearly normal atmosphere to produce a fallout pattern on the ground downwind from the point of release.

As indicated above, not all microspheres released to the fireball are vaporized to sub-micron size. In fact, many particles are only partially vaporized if there is a delay of a few seconds in exposing them.

G.E. data show that if the fuel is released at ignition time t=0 (air flow = 25m/sec) 7% of the total fuel mass released will remain as particles ranging in size from 65-193μ diameter. If fuel release is at t=4.8 seconds, (air flow = 25m/sec) 76% of the total fuel mass will remain as particles ranging from 41 to 240μ diameter. Thus, it is obvious that a large range of uncertainty is inherent in the fraction of the fuel which will remain as microspheres.

After determining the expected terminal velocities of the large particles and estimating updraft velocities in the rising fireball, the Meteorological Working Group concludes that all particle sizes could be lifted to cloud stabilization altitude. This agrees with G.E. estimates for the 550 m cloud rise but is also true for other cloud heights assumed.

2.2 Lift-Off to LET Jettison

This phase of the launch lasts from lift-off at zero altitude to LET (Launch Escape Tower) jettison. During this period the fuel capsule would impact on the ground near the launch pad site if abort occurs during the first 40 seconds of flight. After 40 seconds (roughly 25,000 feet), and extending through the termination of the S-IC Boost phase and until LET jettison at the end of S-II Boost Phase 1 (at 3 min., 14 sec. and 275,000 ft) all impacts or fuel releases will be over the ocean.

Abort situations to consider during lift-off to LET are of three types; 1) ground impact of fuel capsule, 2) high altitude release of fuel (due to rupture of the capsule by pressure wave or fragments) in which no melting occurs, 3) fuel melting in firestream (high altitude fine particle release). These are discussed briefly below:

2.2.1 Ground Impact of Fuel Capsule (Cold Ground Release)

The results of this type of release are the same as for the release discussed in Section 2.1.1 of this report, except insofar as higher impact velocity may change the conditions of release.

2.2.2 High Altitude Fine Particle Release - (Fuel Melting in Firestream)

During the lift-off to LET jettison phase of the mission consideration is given to the possibility of an explosive abort in which the capsule and/or fuel particles are released into the firestream. Again, any protection provided by the GLFC and SHS are disregarded. It is assumed that the fuel capsule is ruptured either by the pressure wave resulting from the explosion or by shrapnel and that the fuel, consisting of microspheres (50-250μ diameter) and comminuted fines

(< 3μ diameter) is released into the firestream. Some portion of the microspheres will be vaporized into submicron size (~.01μ diameter) while the remaining microspheres will be either partially vaporized or not at all.

Analyses of fuel vaporization in a firestream are performed parametrically. G.E. analysis assumed the firestream temperature to be 4500° F and the percentage of fuel vaporized in the firestream was for three periods of exposure, 0.5, 1.0 and 2.0 seconds at abort altitudes from 10,000 to 50,000 feet. The analysis consists of determining the mass transfer from single microspheres (50-250μ diameter range) at fireball temperatures. The results of the G.E. calculations were as follows:

Table 2.2.2 Fraction of Fuel Vaporized in a Firestream (Stagnant Case)

Altitude 10^3 ft.	Initial Temperature °F	Fuel Exposure Time - Seconds 0.5	1.0	2.0
PAD	4900	0.190	0.33	0.49
10	4560	0.057	0.114	0.228
20	4240	0.016	0.032	0.064
30	3900	0.0025	0.007	0.014
40	3580	0.00057	0.00114	0.00228
50	3270	0.00007	0.00015	0.00030

These data indicate that if an abort occurred at altitudes of 50,000 feet or above essentially no fuel would be vaporized due to firestream exposure. It is unlikely any particle will remain in the firestream longer than two seconds.

Vaporized particles (fine particles) released at ground level or near the surface of the earth are discussed in Section 2.1.1.1 of this report. Vaporized

particles (fine particle release) released into the upper atmosphere will be dispersed by atmospheric motion with little effect due to gravity because of the small free-fall terminal velocities of the particles. While the fine particulate material from high altitude release will be very widely spread over the surface of the earth, the large particles (microspheres) will settle rapidly to earth over a relatively limited area.

2.2.3 High Altitude Microsphere Release - (No Melting - Outside Melt Zone)

From lift-off to LET jettison at 275,000 ft. microsphere release can result from 1) rupture of a capsule which has been thrown clear of the firestream or 2) from residual large particles which have not been completely vaporized after firestream exposure. The quantity of fuel released in the first case could conceivably range up to full release (44,500 Ci). In the second case, the amount of total microsphere fuel release could range from approximately 50% from a release at 10,000 ft. (3 km) up to 99.9% of total fuel load at 50,000 ft. (15 km). Above 60,000 ft. (18 km) vaporization would be negligible due to the extremely short time the fuel could be exposed to the firestream and also due to the relatively low temperature of the firestream.

2.3 Sub-Orbital Boost and Earth Orbit

This part of the mission extends through the following phases:

LET Jettison	3 min. 14 sec.	275,000 ft.
S-II Engine C.O.	8 min. 56 sec.	605,000 ft.
S-IVB Booster Full Thrust	8 min. 51 sec.	605,000 ft.
S-IVB Engine C.O.	11 min. 23 sec. (earth orbit)	607,600 ft.
S-IVB Ignition	1 hr. 35 min. .08 sec. (begin translunar phase)	

The GLFC will impact in the ocean if abort occurs during the first 78 seconds of the S-IVB burn. After that impact will be in Africa until near the end of S-IVB first burn. Starting with the end of S-IVB first burn following the ascent phase and ending with S-IVB re-ignition (beginning of translunar injection phase) impact can be anywhere on the earth's surface between 35°N and 35°S.

An explosion from LET jettison (S-II boost through translunar injection phase) should not be expected to damage the GLFC. However unlikely, the possible release of a bare capsule resulting from pressure damage to GLFC and SHS or rupture of the capsule by shrapnel must be considered. A bare capsule, released at that altitude would be subject to aerodynamic heating and release and ablation of the $^{238}PuO_2$ fuel particles. Peak heating occurs at 220,000 ft in the case of earth orbit decay.

If, on the other hand, the intact GLFC impacts at random on the earth's surface, the graphite shell will be destroyed in most cases. Burial of the SHS and fuel capsule could occur at the moment of impact. The capsule might rupture when it impacts the earth due to the high temperature (approximately 1800° F) of the cladding at impact. Some of the fuel (fines and comminuted microspheres) could then be released to the atmosphere (cold ground release) if the capsule ruptured on the earth's surface. Fuel impacting the ocean would in time be dispersed and dissolved in the water.

2.3.1 Random Earth Impact Between 35°N and 35°S - (FCA Rupture and Release of Comminuted Fuel)

This type of release is described in Section 2.1.1 of this report.

2.3.2 FCA Rupture Due to Aerodynamic Heating

2.3.2.1 Release of Unmelted Microspheres

Fuel spilled inside the "melt zone" would be expected to break up (ablate) into smaller particles. Any microsphere size particles which survived reentry heating would eventually settle to earth with no further change in form during the fall. This type of release (high altitude microsphere release - no melting) is discussed in Section 2.2.3 of this report. The only difference being that the fallout pattern resulting from upper mesospheric releases would be larger by several orders of magnitude than those occurring in the lower mesosphere or stratosphere. Since the particles would be spread over a larger area (footprint) the ground concentration would be correspondingly less.

2.3.2.2 Fine Particle Release Resulting from Melting of Fuel - (High Altitude Fine Particle Release in Melt-Zone)

Parametric determinations of tropospheric concentrations and deposition on the ground are the same for the present case of aerodynamic heating as for the firestream vaporization case discussed in Section 2.2.2.

2.4 Translunar Injection to Lunar Orbit Insertion

There are four phases to this part of the mission. They are as follows:

		hr	min	sec
I. Translunar Injection	S-IVB re-ignition	1	35	08
II Initial Translunar Coast Phase	S-IVB Engine C.O.	1	40	50
	Initiate SCM/LM Separ.	1	57	05
	Docking Complete	2	20	00
	S-IVB Jettison Complete	2	41	40
S-IVB Jettison to Lunar Orbit Insertion Phase	S-IVB Jettison Complete	2	41	40
	SM Ignition	4	43	56
	(sub-phase) SM III C.O.	62	17	02
Lunar Orbit Insertion Phase	SM Ignition	63	16	39

The Translunar Injection Phase begins with S-IVB re-ignition at the end of Earth Orbit and ends with withdrawal of the LM from the SLA on the S-IVB. Some aborts could result in the GLFC and fuel capsule impacting the moon or entering into solar orbit. Effects of an explosion at this phase would be less severe than explosion during earth orbit. After the withdrawal of the LM from the S-IVB during the Translunar Coast Phase explosion is much less likely to be a problem. Aborts then would most likely result in release of the intact GLFC.

Fuel releases during any of the above four phases would include any of the following:

2.4.1 Random Earth Impact - Cold Ground Release (fine particle and comminuted fines released at earth surface)

2.4.2 Re-entry Melting of FCA

2.4.2.1 High Altitude Microsphere Release (release of unmelted fuel)

2.4.2.2 High Altitude Fine Particle Release (fuel ablation to fine particles)

All of the above types of releases are discussed in previous sections of this report.

3. PARAMETRIC DESCRIPTION OF CONCENTRATION, DEPOSITION AND EXPOSURE

In this section the methods of calculation used by G.E. and the MWG will be discussed and compared. In all the equations used, the concentration, deposition and exposure are directly proportional to the source strength. Accordingly, the results will be presented in units of air concentration per unit source strength, deposition per unit source strength and exposure per unit source strength. On the other hand, distances or areas over which specific values ("criteria") of concentration, deposition and exposure are exceeded

are not, in general, linear functions of source strength. Consequently it is impossible to base any judgment of hazard on the parametric results alone. In the panel report such evaluations will be made by introducing specific source terms and "criteria" into the parametric results.

3.1 Cold, ground-level release

This problem arises in the case of rupture of the FCA on ground impact in the absence of fireball heating, melting, vaporization or entrainment into a buoyant cloud. The fine component of the pre-existing particle size distribution, and fines resulting from comminution of microspheres on impact, could become airborne, drift with the surface wind existing at the time, and be dispersed and deposited by the ambient turbulence.

Formulas for this case predict monotonically decreasing air concentrations in the downwind direction. The rate of decrease and the associated rates of vertical, lateral, and longitudinal spread of the cloud depend on the intensities of the three vector components of the turbulence, on the interactions of the components, on the spectral (scale) distribution of turbulent energy and on the interactions of the various spectral components.

Only semi-empirical formulations with empirically determined parameters are available. That of O. G. Sutton, on which a body of test data has been obtained at a variety of sites, is the one used by G.E. in the SNAP-27 Safety Report, Vol. III. Dr. I. Van der Hoven of the MWG used a widely accepted method developed more recently by F. Pasquill. J. Fuquay of the MWG applied an empirical method based on a series of tracer tests conducted at Cape Kennedy in Project Ocean Breeze. These experiments covered a distance range of only a few km so

that considerable extrapolation is required for present purposes.

3.1.1 Exposure

In these calculations it is assumed that the particles have negligible settling velocity. This is approximately true for particles of diameter less than 3μm (settling velocity < .003 m/sec or about 10 m/hr). This size range is roughly equivalent to that thought to be "respirable" and to that likely to be carried away from the impact point by the wind.

It is also assumed that the particles are released in a short time so that the exposure of any individual to the cloud of particles is limited to a period of the order of minutes during which he can be assumed to remain in the same location and to breathe at a constant rate. Then the number of particles inhaled depends only on the time integral of concentration at his location and on the air volume inspired per unit time. The time history of concentration during the passage of the cloud or the exact value of the concentration at any particular time or place are considered immaterial.

Therefore, only the parametric "exposure" is evaluated for this case. The exposure E of an individual at location (x,y) is defined as:

$$E(x,y) = \int_{t_1}^{t_2} X(x,y,t)\, dt$$

where X(x,y,t) is ground level air concentration, Ci/m^3, t is time, sec, and x,y are coordinates, m. For mathematical convenience t_1 and t_2 are usually taken as 0 and infinity.

If the quantity released is Q (Ci), the parametric exposure E/Q has the units sec/m^3. When multiplied by a source term Q (Ci) and by a respired volume

rate (m^3/sec) this will give the number of curies inhaled. Multiplication again by a retention factor gives the resulting lung burden.

Table 3.1.1.1 gives estimates of E/Q at three distances for typical clear or partly cloudy daytime conditions (unstable temperature lapse rate) obtained by G.E. and Van der Hoven (Pasquill type B, $\overline{u}$ = 5 m/sec).

Table 3.1.1.1 E/Q Unstable Conditions (sec/m^3)

Distance	G.E.	Van der Hoven
1 km	$5x10^{-6}$	$4x10^{-6}$
10 km	$8x10^{-8}$	$4x10^{-8}$
100 km	$< 10^{-8}$	$4x10^{-10}$

The neutral case can be considered either (very loosely) as an approximation of the average over many trials made under a representative distribution of weather conditions, or (more precisely) as the expected results under overcast conditions with moderate wind speed or during transition periods between typical nighttime and typical daytime conditions. For this case the G.E. and Van der Hoven (Pasquill type D, $\overline{u}$ = 5 m/sec), results are given in Table 3.1.1.2.

Table 3.1.1.2 E/Q Neutral Conditions (sec/m^3)

Distance	G.E.	Van der Hoven
1 km	$3x10^{-5}$	$2x10^{-5}$
10 km	$5x10^{-7}$	$9x10^{-7}$
100 km	$1x10^{-8}$	$4x10^{-8}$

In clear nighttime conditions over land, or with a flow of warm air over a cooler surface the air is moderately stable to very stable depending on such variables as wind speed and the rate and duration of surface cooling. The G.E.

results for these two conditions as defined by Sutton, and Fuquay's estimates based on Project Ocean Breeze experiments conducted under stable conditions are shown in Table 3.1.1.3.

Table 3.1.1.3 E/Q Stable Conditions (sec/m^3)

Distance	G.E. (S)	G.E. (VS)	Fuquay
1 km	$3x10^{-4}$	$>10^{-3}$	$8x10^{-4}$
10 km	$6x10^{-6}$	$1x10^{-4}$	$4x10^{-5}$
100 km	$1x10^{-7}$	$3x10^{-6}$	$2x10^{-6}$

In unstable conditions the MWG agrees with G.E. within a factor of 2 to a distance of 10 km and agrees in predicting a very rapid decrease of exposure beyond this distance, the exact rate being uncertain. In neutral conditions the MWG agrees with G.E. within a factor of 2 to 10 km and a factor of 4 to 100 km, the MWG estimate being the higher. This is the only case which is sufficiently well documented, and sufficiently reasonable as an average over the travel time involved to be considered quantitative for distances greater than about 20 km. In stable conditions it is clear that a wide range of uncertainty exists as to the exposures to be expected. The MWG agrees that the levels are likely to fall within the range covered by the G.E. "stable" and "very stable" cases. "Very stable" conditions are unlikely to persist over cloud travel distances greater than about 50 km from a ground level release. On the other hand, it is conceivable that exposures corresponding to this case could occur at distances of the order of 20 km ($4x10^{-5}$ sec/m^3) to 50 km downwind ($1x10^{-5}$ sec/m^3) in the case of an early nighttime release with a

light onshore wind or in the case of a light wind daytime trajectory across a relatively cool water surface. Curves showing cloud passage exposure, deposition density and resuspension exposure per unit source versus distance downwind are shown in Figure 1 using MWG and G.E. calculations.

In the cold ground level release case, the ground surface area within which any given exposure is exceeded can be approximately interpolated or extrapolated from the values given in Table 3.1.1.4. The values are based on the MWG parametric estimates shown in Figure 2 where cloud passage exposure, deposition density and resuspension exposure per unit source versus area are plotted.

Table 3.1.1.4 Area Over Which E/Q is Exceeded

E/Q	Unstable		Neutral		Stable	
(sec/m^3)	(m^2)	(mi^2)	(m^2)	(mi^2)	(m^2)	(mi^2)
10^{-4}	$8x10^3$	.003	$2x10^4$	.01	$3x10^5$	0.1
10^{-5}	$8x10^4$	.03	$3x10^5$	.1	$8x10^6$	3
10^{-6}	$7x10^5$	0.3	$4x10^6$	1.5	$1.5x10^8$	60
10^{-7}	$4x10^6$	1.5	$6x10^7$	20	$3x10^9$	1200

3.1.2 Deposition and Resuspension

Although only a small fraction of fine particles (diameter < 3μm) from the airborne cloud are deposited on the ground within the first 100 km downwind, the persistence and resuspension of the deposited fraction could result in finite exposures over a long period of time.

The deposition density D (Ci/m^2) following passage of the airborne cloud, will be v_g E where v_g is the so-called "deposition velocity" (m/sec) and is not

in general the same as the particle settling velocity. The values of v_g chosen by G.E. range from 1.5×10^{-4} m/sec in very stable conditions to 1.8×10^{-3} m/sec in unstable conditions.

Since particles with diameters up to 3μm are included in the size range we have defined as "fine particles," and the smaller particles will coagulate with natural dust particles, gravitational settling velocities as high as 3×10^{-3} m/sec could occur. This value can be used to estimate the maximum deposition hazard in the absence of firm data on deposition velocities due to other processes (turbulent impaction, vegetation filtration, electrostatic and thermal precipitation).

Deposition by rain is ignored in this analysis on the grounds that this process would place the fine particles in a relatively unavailable distribution. Such "washout" could increase deposition density by 1 to 2 orders of magnitude. Solution and uptake by plants are not considered since it is assumed that the inhalation hazard would be controlling. It should be remembered that these assumptions may not be valid and that either resuspension or ingestion could present problems following washout by rain.

Using the MWG estimates of exposure with $v_g = 3 \times 10^{-3}$ m/sec the values of D/Q in Table 3.1.2.1 are obtained for unstable, neutral and stable meteorological conditions. If the bulk of the mass of the airborne particles is contained in the size range below 1μm diameter the deposition will be an order of magnitude smaller than those given here.

Table 3.1.2.1 Deposition/Source Strength

Distance	Unstable	Neutral	Stable
1 km	$1x10^{-8}$ m^{-2}	$6x10^{-8}$ m^{-2}	$2x10^{-6}$ m^{-2}
10 km	$1x10^{-10}$	$3x10^{-9}$	$1x10^{-7}$
100 km	$1x10^{-12}$	$1x10^{-10}$	$6x10^{-9}$

Opinions differ as to the mechanism of resuspension. In particular it is not clear whether fines will be resuspended at all after being deposited in a bed of coarser particles. If so, it is not clear whether a threshold wind speed is required for resuspension to begin or whether transient local shear in turbulent eddies produce some finite probability of resuspension even in light winds. Experiments by Healy and Fuquay (1958) with fluorescent tracer particles at Hanford and by Olafson and Larson (1963) and Wilson (1960) with plutonium explosively dispersed at the Nevada Test Site suggest ratios of air concentration $X(\mu gm/m^3)$ to deposition concentration $D(\mu gm/m^2)$ given in Table 3.1.2.2.

Table 3.1.2.2 X/D

a. Fresh deposit, tracer particles of density 1.5 gm/cm^3:

Diameter	Wind Speed 5m/sec	Wind Speed 10m/sec
1.5μm	$7x10^{-2}m^{-1}$	0.3 m^{-1}
8μm	$6x10^{-4}$	$2x10^{-3}$
14μm	$8x10^{-5}$	$3x10^{-4}$
78μm	$6x10^{-7}$	$2x10^{-6}$

b. Plutonium particles versus time after initial deposition:

1. Wilson data :

0-16 days	$2x10^{-7}$ m^{-1}	to	$6x10^{-6}$ m^{-1}
128-160 days	$1x10^{-8}$ m^{-1}	to	$2x10^{-7}$ m^{-1}

2. Olafson and Larson data

first 21 days: average $3x10^{-8}$ (0 to $2x10^{-7}$)m^{-1}

The plutonium data, showing ratios less than 10^{-5} m^{-1}, are considered more relevant to the present case, although the possibility of ratios approaching 1 m^{-1} cannot be ruled out if strong winds should occur shortly after cloud passag over a relatively bare, smooth surface.

The plutonium data indicate that the particles become less available to wind pickup at a rate which can be approximated by an exponential with a half time of 35 days. Based on this model, J. Fuquay has estimated the exposure due to re-suspended particles. For resuspension beginning at any time after initial deposition, the exposure increases with exposure time but approaches a finite limit. This limiting exposure is less than 1/100 of the cloud passage exposure even in the extreme case of large deposition velocity (several cm/sec) and extremely strong wind pickup (turbulent eddy velocity = several m/sec) starting immediately after deposition and continuing indefinitely. For more plausible conditions (v_g < 1 cm/sec, eddy velocity < 1 m/sec) the ratio of resuspension exposure to cloud passage exposure is of the order of 10^{-6} for one day and 10^{-4} for indefinite exposure.

Using $2x10^{-7}$ m^{-1} as a conservative (high) estimate of X/D for the first few weeks after deposition, Table 3.1.2.3 shows parametric peak air concentratio

per unit source strength (m^{-3}) for the deposition densities shown in Table 3.1.2.1.

Table 3.1.2.3 Peak Air Concentration of Resuspended Particles X/Q

Distance	Unstable	Neutral	Stable
1 km	$2x10^{-15}$ m^{-3}	$1x10^{-14}$ m^{-3}	$4x10^{-13}$ m^{-3}
10 km	$2x10^{-17}$	$6x10^{-16}$	$2x10^{-14}$
100 km	$2x10^{-19}$	$2x10^{-17}$	$1x10^{-15}$

If $3x10^{-4}$ m/sec is taken as a more plausible estimate of the average deposition velocity for a fine particle population such as that postulated, and $3x10^{-8}$ m^{-1} as a conservative estimate of the average value of X/D during the first few months after deposition, the average air concentrations shown in Table 3.1.2.4 are obtained along the downwind axis of a deposition pattern laid down under the given meteorological conditions.

Table 3.1.2.4 Average Air Concentrations of Resuspended Particles Per Unit Source, X/Q (m^{-3})

Distance	Unstable	Neutral	Stable
1 km	$3x10^{-17}$ m^{-3}	$2x10^{-16}$ m^{-3}	$6x10^{-15}$ m^{-3}
10 km	$3x10^{-19}$	$9x10^{-18}$	$3x10^{-16}$
100 km	$3x10^{-21}$	$3x10^{-19}$	$2x10^{-17}$

Similarly, taking 10^{-4} as a plausible estimate (with large uncertainty) of the ratio of total lifetime resuspension exposure E' to cloud passage exposure E', the resuspension exposures per unit source strength E'/Q (sec/m^3)

along the axis of the deposition patterns produced in unstable, neutral and stable meteorological conditions, based on MWG estimates of E, would be as given in Table 3.1.2.5.

Table 3.1.2.5 Resuspension Exposure Per Unit Source E'/Q (sec/m^3)

Distance	Unstable	Neutral	Stable
1 km	4×10^{-10} sec/m^3	2×10^{-9} sec/m^3	8×10^{-8} sec/m^3
10 km	4×10^{-12}	9×10^{-11}	4×10^{-9}
100 km	4×10^{-14}	4×10^{-12}	2×10^{-10}

These are equivalent to exposures of a few days at the peak air concentrations given in Table 3.1.2.3 or a few months at the average concentrations given in Table 3.1.2.4. Although insignificant compared to cloud passage exposures, these might be dominant in the event that people return after being evacuated from the path of the airborne cloud.

It should be borne in mind that the above resuspension estimates are based on experiments conducted over desert terrain with particles of different character and size distribution from those expected in the case of the postulated accidents. Both the experimental results and the available theoretical models permit a very wide range of estimates even for the given experimental conditions. Factors not taken into account, such as humidity, precipitation, vegetative cover, pavement, vehicular traffic and agricultural treatment will further widen the range of uncertainty. If, for example, the capsule were to impact in a city, the consequences might be vastly different from those pictured here.

Also, it should be noted that the assumptions underlying the use of integrated "exposure" may not be well justified for exposures occurring over long periods of time.

3.2 Hot Cloud Release

If a release of fuel should occur within the fireball produced by an explosion of the Saturn V vehicle, both primary microspheres and secondary particles resulting from melting, vaporization, or comminution would be entrained in the updraft and dispersed from some height above ground.

3.2.1 Cloud Rise

G.E. has assumed a cloud center height of 550 m based on estimates by High and Fletcher (1965). More recently, High (1968) has made new estimates of the fireball dimensions and duration. Since the total weight of propellant is about 3 kilotons, even relatively small fractional energy yields would be in the region for which nuclear explosion cloud height data are available. High's estimate of 1400 feet for the cloud diameter at liftoff would correspond to the maximum diameter of the fireball from a 15 KT (TNT equivalent) nuclear explosion. Data in The Effects of Nuclear Weapons (Glasstone, 1962) would suggest diameters of 800 feet for a 3 KT explosion and 400 feet for a 17% Saturn explosion (0.5 KT). Data on individual cloud heights listed there indicate cloud base and top heights above ground from surface or near-surface explosions given in Table 3.2.1.

Table 3.2.1 Cloud Heights from Reported Nuclear Detonations (km above ground)

Yield (KT)	Cloud Base	Cloud Top
< 0.1	0.5	2
0.1 to 1	1.5	3
~1	2.5	5
2 - 5	3	6

Members of the MWG feel that cloud center heights in the 1-2 km range are most plausible for a Saturn explosion and heights up to 4 km may be possible depending on meteorological conditions. J. Kaufman cited calculations based on the model of Morton, Taylor and Turner, as well as observations on F-1 static engine tests, in support of cloud heights of 1.5 km for one engine (20%) and 2.2 km for all 5 engines of the S-1C. H. Church provided an estimate of 1.4 km for a 20% energy yield.

The effect of increased cloud height is in general to spread the debris over a larger area, reducing the concentrations everywhere at the ground except for effects of particle sedimentation. This may result in a larger or smaller number of people being exposed above any particular level, depending on the ratio of the exposure criterion to the source term.

In addition to the 550 m cloud height assumed by G.E., the effects of cloud heights of 1000, 2000, and 4000 m will be considered.

3.2.2 Deposition of Microspheres

G.E. computed the deposit density for the given microsphere size distributio with a cloud center height of 550 m, uniform crosswind distribution over a conste width of 430 m equal to the cloud diameter, and constant wind speed of 5 m/sec.

H. Church of the MWG provided estimates obtained by Sandia with the DIFOUT code for the same cloud height but using a selection of observed Cape Kennedy wind velocity profiles.

The maximum deposit density $D(Ci/m^2)$ per unit source strength Q(Ci) and the distance of the maximum are given in Table 3.2.2.1 for the G.E. calculation and the six cases evaluated by Sandia.

Table 3.2.2.1 Maximum D/Q and Distance of Maximum

Profile	Mean Wind Speed (m/sec)	Max. D/Q (m^{-2})	Distance of Max. (km)
G.E.	5.0	3.3×10^{-6}	.80
Sandia #12	0.96	4×10^{-5}	.20
Sandia #71	1.7	1.3×10^{-5}	.25
Sandia #50	1.67	1.1×10^{-5}	.3
Sandia #11	4.65	5×10^{-6}	.85
Sandia #67	6.5	2.2×10^{-6}	1.0
Sandia #63	10.5	1.2×10^{-6}	1.75

The distances of nearest and farthest occurrence of D/Q exceeding certain specific values, interpolated from graphs, are shown in Table 3.2.2.2 for the same cases.

Table 3.2.2.2 Distances of nearest and farthest occurrence (km)

D/Q (m^{-2}):	10^{-9}	10^{-8}	10^{-7}	10^{-6}	10^{-5}
G.E.	.4 - 5.3	.4 - 3.6	.5 - 2.4	.5 - 1.6	none
Sandia #12	0 - .9	0 - .8	0 - .7	0 - .5	0 - .4
Sandia #71	0 - 1.8	0 - 1.4	0 - 1.0	0 - .7	.1 - .4
Sandia #50	0 - 1.8	0 - 1.5	0 - 1.2	0 - 1.0	.2 - .5
Sandia #11	.3 - 1.9	.3 - 1.7	.4 - 1.5	.5 - 1.2	none
Sandia #67	.2 - 6.0	.3 - 4.2	.4 - 3.0	.6 - 1.8	none
Sandia #63	.2 - 11.5	.5 - 6.7	.7 - 3.9	1.4 - 2.2	none

The G.E. values for the maximum D/Q, distance of maximum D/Q, and distance range (length) of each D/Q contour along the axis of the fallout pattern fall near or between those obtained by Sandia with observed wind profiles having vector mean speeds of 4.65 and 6.5 m/sec between the surface and a height of 550 m. The Sandia patterns do not increase in length as rapidly with decreasing D/Q as do the G.E. patterns. This is expected since the Sandia model includes lateral spread due to turbulent diffusion and directional shear while the G.E. model does not.

Areas within D/Q contours (isopleths) were computed by G.E. but not by Sandia. However, the lengths of the Sandia D/Q contours can be used to estimate the areas within the contours provided that the G.E. areas are assumed to be approximately correct for a vertically averaged wind of 5 m/sec. Let L be the length from nearest to farthest occurrence of a given value of D/Q, d_o the

initial diameter of the cloud, and A the area within the contour. If the lateral width is assumed to increase in proportion to the increase in length, i.e. as $c(L-d_o)$, where c is constant, but without change in shape, the area would be proportional to $cL^2 + (1-c)\,Ld_o$.

The formula $A = .07L^2 + .7Ld_o$ gives a close fit to the areas obtained by G.E. for D/Q contours from 10^{-9} m^{-2} to 10^{-5} m^{-2} when d_o is taken as 430 m (G.E. cloud diameter) and the value of L for each contour is an average of those obtained by Sandia for the 4.65 m/sec and 6.5 m/sec wind profiles. This formula is essentially that for an ellipse whose short axis grows from the initial diameter 1/11 as fast as its long axis.

Using this formula for the light wind profile (0.96 m/sec at 550 m), the strong wind profile (10.5 m/sec) and the two intermediate cases (4.65 and 6.5 m/sec) the areas shown in Table 3.2.2.3 are obtained. Areas obtained from the G.E. report are also shown for 5.0 m/sec.

Table 3.2.2.3 Area Over Which D/Q is Exceeded (km^2)

550 m wind speed	D/Q (m^{-2}):	10^{-9}	10^{-8}	10^{-7}	10^{-6}	10^{-5}
0.96 m/sec		.32	.28	.24	.17	.13
4.65 m/sec		.66	.56	.41	.24	0
5.0 m/sec (G.E.)		1.9	1.4	.82	.32	0
6.5 m/sec		4.1	2.2	1.3	.46	0
10.5 m/sec		12	4.5	1.7	.28	0

It is seen that D/Q exceeds 10^{-9} m^{-2} over an area 40 times larger with strong winds than with light winds. On the other hand D/Q never exceeds 10^{-5} m^{-2} except in the lightest winds, when all the particles fall in a small area. The largest area with D/Q exceeding 10^{-6} m^{-2} occurs with intermediate winds.

In view of the convincing indications that the cloud might rise to heights as great as 4 km it is necessary to consider the consequences of larger cloud heights. The deposition of microspheres has not been calculated directly for these cases. However, useful order of magnitude estimates can be developed by scaling all dimensions in proportion to the height.

Assume that the particles lying along a given D/Q isopleth labelled D_1/Q containing an area A_1 for a cloud center height h_1 and a mean wind speed u_1 from the surface to h_1 are distributed along a geometrically similar isopleth D_2/Q of area A_2 when the cloud height is changed to h_2 and the wind speed at cloud height is changed to u_2. Assume that the length of the long axis of the isopleth containing the same particles is proportional to both cloud height and mean wind speed from the surface to cloud height.

$$\frac{L_2}{L_1} = \frac{u_2\ h_2}{u_1\ h_1}$$

From the similarity assumption:

$$\frac{A_2}{A_1} = \left(\frac{u_2\ h_2}{u_1\ h_1}\right)^2$$

$$\frac{D_2}{D_1} = \left(\frac{u_1\ h_1}{u_2\ h_2}\right)^2$$

If a reference cloud height h_o and a reference wind speed u_o are chosen the area A of the isopleth D/Q for any other height h or mean wind speed u would be

$$A = A_o \left(\frac{u \; h}{u_o \; h_o} \right)^2$$

where A_o is the area of the D_o/Q isopleth for fallout from a cloud at height h_o with wind speed u_o at height h_o. The non-dimensional area parameter $A^* = A \; u_o^2/u^2h^2$ would be a function only of the non-dimensional deposit density parameter $D^* = D \; u^2h^2/u_o^2Q$.

The value of D* along the downwind axis of the pattern would be a function only of the non-dimensional distance parameter $x^* = xu_o/uh$ or the corresponding non-dimensional length parameter $L^* = Lu_o/uh$.

When the data contained in the preceding three tables are put in non-dimensional form according to this model with u_o = 1 m/sec, the deposition densities and distances fall within a factor of two, and the areas within a factor of four, of the universal pattern described by the parameters given in Table 3.2.2.4. Curves showing non-dimensional microsphere deposition versus non-dimensional distance and area are shown for microsphere releases in Figure 3.

Table 3.2.2.4 Non-dimensional microsphere deposition pattern

D*	10^{-4}	10^{-3}	10^{-2}	10^{-1}	1	10	20 (Max.)
Nearest x*	.03	.04	.06	.08	.10	.15	0.3
Farthest x*	2.5	2.0	1.5	1.2	0.9	0.5	0.3
A*	1.0	.6	.35	.20	.10	.04	0

$D^* = (D/Q)h^2(u/u_o)^2$, or $D = D^*Qu_o^2/u^2h^2$

$X^* = (x/h)\ (u_o/u)$, or $x = x^*hu/u_o$

$A^* = (A/h^2)(u_o/u)^2$, or $A = A^*h^2u^2/u_o^2$

D = deposit density (Ci/m^2)

u = wind speed (m/sec) cloud height

h = cloud height (m)

u_o = reference wind speed = 1 m/sec

Q = source term (Ci)

x = distance downwind (m)

A = area (m^2) within D/Q isopleth

As an example, given $Q = 10^4$ Ci, h = 1000 m (cloud center height) and u = 10 m/sec, then the maximum deposit density is 2 mCi/m^2 at a distance of 3 km. In this case the nearest occurrence of a deposition density of $10\mu Ci/m^2$ (10^{-5} Ci/m^2) ($D^* = 0.1$), for example, would be at $x^* = .08$, or $x = x^*\ u/1\ msec^{-1}$ = .08 km, the farthest occurrence would be at 12 km, and the area within the $10\mu Ci/m^2$ isopleth would be $A = A^*\ h^2u^2/1\ m^2sec^2 = 2x10^7m^2$ or 20 km^2. For a deposit density of $100\mu Ci/m^2$ $D^* = 1$, the nearest and farthest distances are 1 km and 9 km, and the area 10 km^2.

If the cloud height is increased to 4000 m and the wind speed increased to 25 m/sec with the same value of Q, then for $D = 10\mu Ci/m^2$, $D^* = 10$, the nearest distance becomes 15 km, the farthest 50 km, and the area $4x10^8m^2$ or 400 km^2. For $D = 100\mu Ci/m^2$, $D^* = 100$ and this value does not occur anywhere. For these conditions the maximum deposit density is $20\mu Ci/m^2$, which occurs at a distance of 30 km downwind.

For arbitrary assumed conditions, of course, it would be necessary to interpolate between the D* values for which dimensions are tabulated above. For example if a source term Q and a deposition criterion D are given, I* can be computed for assumed cloud heights and wind speeds, x*'s and A* interpolated

for this value of D*, and the corresponding dimensional values of the x's and A computed.

Although weathering and degradation of microspheres after deposition on the ground are expected, the resuspension problem has not been evaluated. If the fines which result from this process are produced at a rate which is small compared to the 1 month half-time with which they become unavailable for resuspension, the airborne concentrations would be many orders of magnitude smaller than those arising from any accident involving direct dispersal of a similar quantity of fines.

3.2.3 Fine Particle Release in the Fireball

G.E. has calculated cloud passage exposure at ground level due to atmospheric transport and diffusion of fines from a cloud height of 550 m, for four conditions of atmospheric stability. The distance of maximum exposure varies from a few km in "unstable" conditions to several hundred km in "very stable" conditions. J. Fuquay has independently evaluated the stable case using diffusion rates based on data obtained at Cape Kennedy during Project Ocean Breeze. He obtains a distance of 4000 km for the maximum ground level exposure (an enormous extrapolation from observed data over a few km). The exposure at this point is only a factor of two lower than that estimated by G.E. at much shorter distances in the neutral and stable cases.

This points out two serious problems with the fireball vaporization case. One is the great uncertainty of atmospheric diffusion calculations for elevated clouds in stable conditions. The second is the fact that travel times to the point of maximum ground exposure are so great (several days) that it becomes

incredible that stability conditions would remain constant throughout the travel. These problems are magnified by the possibility that the cloud height might be considerably greater than 550 m.

The MWG feels that it is inappropriate to assume a rate of diffusion appropriate to stable conditions for more than 12 hours of travel. The G.E. results imply maximum ground level exposures from a 550 m cloud at about 10 to 20 minutes travel in the "unstable" case, 1 hour in the "neutral" case, 10 hours in the "stable" case and 5 days in the "very stable" case. On this basis the predicted pattern for the "very stable" case would not be considered plausible.

Two general modes of transport and diffusion can be visualized for a cloud injected in an elevated stable layer. The first, appropriate at altitudes within the planetary boundary layer and subject to diurnal convective mixing, would be for the bulk transport to remain reasonably steady and horizontal and for the rate of diffusion to increase during daytime to that typical of unstable or neutral conditions. In this case, ground-level distributions similar to those calculated for neutral conditions, though perhaps narrower and longer, might be expected at distances corresponding to travel times slightly longer than the time required for daytime mixing to penetrate to cloud height. The G.E. "stable" case seems to approximate a pattern of this type. This shows a maximum E/Q of the order of 4×10^{-8} sec/m^3 at about 70 km downwind, values exceeding 3×10^{-8} sec/m^3 over an area of the order of 300 km^2 at distances of 50 to 100 km, exceeding 10^{-8} sec/m^3 up to 200 km, and exceeding 10^{-9} sec/m^3 up to 1200 km.

The second mode, appropriate for cloud heights of the order of a km or more, would be for synoptic-scale quasi-isentropic vertical motions to affect significantly the height and stability of the layer in which the cloud is imbedded, and to determine the size and location of the area over which it reaches ground level. For this case an increase of effective horizontal diffusivity with travel time as found by Hage, Heffter and Crawford would seem appropriate.

The G.E. "very stable" pattern with a maximum E/Q of 6×10^{-8} sec/m^3 at 500 km, and Fuquay's stable pattern with a maximum of 1.5×10^{-8} sec/m^3 at 4000 km probably grossly over estimate the distance and areas over which such exposures can reasonably be expected in this case. This is suggested both by the low cloud height assumed, and because the effective diffusivity is not increasing at a sufficiently rapid rate in the models used. Van der Hoven has estimated, for a cloud height of 1000 m in neutral stability, with a 5 m/sec wind, a maximum E/Q of 3.5×10^{-9} sec/m^3 at about 150 km (8 hours travel). It seems unlikely that this value will be exceeded at any greater distance from this or any greater cloud height.

For the unstable case, G.E. estimates for a 550 m cloud rise and Van der Hoven's estimates for 1000, 2000 and 4000 m appear to be mutually consistent and are summarized in the Table 3.2.3.1. The areas for the 1000, 2000 and 4000 m clouds are estimated from the lengths by the relationship $A = .19L^2$ derived from the 550 m results. Curves showing hot cloud fine particle dispersion per unit source versus downwind distance and area are shown in Figures 4 and 5.

Table 3.2.3.1 Hot Cloud Parametric Exposure, Unstable Case

Cloud Height	550 m	1000 m	2000 m	4000 m
Max E/Q (sec/m^3)	1.3×10^{-7}	5×10^{-8}	1.3×10^{-8}	7×10^{-9}
distance of max E/Q	3 km	6.5 km	10 km	15 km
$E/Q \geq 10^{-7}$ sec/m^3				
nearest distance	2.2 km	none	none	none
farthest distance	5 km			
area	1.6 km^2			
$E/Q \geq 10^{-8}$ sec/m^3				
nearest distance	1.3 km	3 km	8 km	none
farthest distance	23 km	20 km	16 km	
area	90 km^2	55 km^2	12 km^2	
$E/Q \geq 10^{-9}$ sec/m^3				
nearest distance	1 km	2.5 km	5 km	9 km
farthest distance	75 km	64 km	62 km	60 km
area	1000 km^2	700 km^2	600 km^2	500 km^2

For the neutral case with a 550 m cloud height the G.E. calculations appear to represent a plausible distribution of exposure. For higher cloud rise, the cloud will travel farther and be elongated more rapidly in a given time because of the increased wind speed and shear. The time required to diffuse to ground level will increase more rapidly than the cloud height because of the decrease of vertical eddy diffusivity with height. The volume of air in which the source will be diluted by the time it reaches ground level will therefore increase more rapidly than the square of the height. The exposure, however will not necessarily decrease as rapidly as will the concentration because the increasing length of the cloud will be compensated to some degree by increasing duration of exposure.

Thus a scaling model based on a variation of maximum ground-level exposure inversely as the square of cloud height would seem to be quite conservative. The distances of maximum exposure must increase more rapidly than the first power of

the height. To be conservative we can assume this distance will increase as the square of height, the longitudinal (downwind) profile of exposure will preserve the same shape, and the width will increase only linearly with cloud height. Then areas will increase as the cube of height for concentration isopleths whose values decrease as the square of height (the inverse relation to area is not required for exposure as it is for surface deposition). Thus if E_o/Q is the value of a given isopleth for a cloud height of 550 m, its length L_o and its area A_o, then for any greater height h, the isopleth $E/Q = \left(\frac{550\ m}{h}\right)^2 E_o/Q$ will have a length $L = (h/550\ m)^2\ L_o$ and an area $A = (h/550\ m)^3\ A_o$. These parameters are summarized in Table 3.2.3.2 and in Figures 4 and 5 for h = 1000, 2000 and 4000 m. Those calculated by Van der Hoven for h = 1000 m are included for comparison.

Table 3.2.3.2 Hot Cloud Parametric Exposure, Neutral Case

Cloud height	550 m	1000 m		2000 m	4000 m
Calc. method	G.E.	V.d.H.	Scaling	Scaling	Scaling
Max E/Q (sec/m^3)	3×10^{-8}	3.5×10^{-9}	9×10^{-9}	2×10^{-9}	5×10^{-10}
distance of max	18 km	140 km	60 km	240 km	1000 km
$E/Q > 10^{-9}$ sec/m^3					
nearest distance (km)	7	50 km	30	150	none
farthest distance (km)	220	600 km	400	600	
area (km^2)	1000		2000	1600	

It is implied that travel times of the order of a day or more are involved in diffusion to the ground from 2000 m or higher under these conditions.

In the stable case it is estimated that the maximum exposure may be of the same order of magnitude as that for the neutral case but that the distance, length and area will increase directly with the duration of persistency of stable

conditions. For cloud heights greater than 550 m, the cloud travel speed will not be expected to be affected by stability. The width can be assumed to be largely determined by the spread during the active mixing period at the end of the inversion. Thus both the longitudinal (downwind) dimensions and the areas affected at each exposure level can be assumed to be approximately proportional to the distance of maximum exposure. Using a wind speed of 5 m/sec for all heights, the distances and areas shown in Table 3.2.3.3 and in Figures 4 and 5 for the stable (12 hour) case are obtained. Since travel times exceeding 1 day or distances exceeding 1000 km would most likely involve either exposure of the cloud to unstable conditions or entrainment in synoptic scale vertical motion fields, it is not considered reasonable to make quantitative estimates for these cases.

Table 3.2.3.3 Hot Cloud Parametric Exposure, Stable Case

Cloud height (m):	550	1000	2000	4000
Max. E/Q (sec/m^3):	3×10^{-8}	9×10^{-9}	2×10^{-9}	5×10^{-10}
Distance of max (km):				
1 hr persistence	36	80	260	1000
6 hr persistence	140	170	350	1100
12 hr persistence	230	280	460	1200
Area for E/Q $\geq 10^{-9}$ sec/m^3 (km^2):				
1 hr persistence	2000	3000	1800	0
6 hr persistence	7000	6000	2400	0
12 hr persistence	13000	10000	3000	0

As a limiting case, it may be noted that a uniform dispersion of the source through a depth of 4000 m would produce a 1-day exposure of 10^{-9} Q sec/m^3 over

an area of about 200,000 km^2. From the above tabulations it would seem that, due to non-uniform distribution, the maximum credible area for this exposure level, regardless of cloud height or atmospheric stability, is perhaps a tenth of this or 20,000 km^2. For the same depth of mixing, the corresponding "uniform dispersion" area for a 1-day exposure of 10^{-10} Q sec/m^3 would be $2x10^6$ km^2, and the maximum credible area might be 200,000 km^2.

The order of magnitude of the density of surface deposit remaining after passage of the cloud of airborne fines in the fireball case can be estimated in the same way as was done for the cold ground-level release. Since the "fines" include particles as large as 3μm in diameter a deposition velocity as large as $3x10^{-3}$ m/sec could apply to at least part of the debris. Multiplying the exposure values by this deposition velocity gives a conservative (high) estimate of the deposition. These estimates are given in the following table.

3.2.3.4 Deposition D/Q, Hot Cloud Case

	Unstable	Neutral	Stable (12 hr)
Cloud height 550 m			
Max D/Q (m^{-2})	$4x10^{-10}$	$1x10^{-10}$	$1x10^{-10}$
Distance of max	3 km	18 km	230 km
Cloud height 1000 m			
Max D/Q (m^{-2})	$1.5x10^{-10}$	$3x10^{-11}$	$3x10^{-11}$
Distance of max	6.5 km	60 km	280 km
Cloud height 2000 m			
Max D/Q (m^{-2})	$4x10^{-11}$	$6x10^{-12}$	$6x10^{-12}$
Distance of max	10 km	240 km	460 km
Cloud height 4000 m			
Max D/Q (m^{-2})	$2x10^{-11}$	$1.5x10^{-13}$	$1.5x10^{-13}$
Distance of max	15 km	1000 km	1200 km

Even the largest of these parametric deposition values would require Q = 1.5×10^5 curies to give a deposit density of $60 \mu Ci/m^2$. This possible pathway of exposure is clearly of lesser significance than some of the others. Curves showing hot cloud fine particle dispersion exposure per unit source strength and deposition density versus area are shown in Figure 5.

3.3 High Altitude Release

An explosion or impact which ruptured the fuel capsule at any point along the trajectory from lift-off to lunar orbit injection could result in fallout of microspheres. While these would not be respirable it is of interest to estimate their deposition density on the ground.

3.3.1 Ascent to Earth Orbit

H. Church has provided the MWG with calculations of the deposit density for the given microsphere size distribution released from 15, 45, 60 and 90 km altitud Deposition density per unit source versus distance downwind for high altitude release of microspheres is plotted in Figure 6. The parametric results are summarized in Table 3.3.1.1. The winds used were observed Cape Kennedy winds for various times of year.

Table 3.3.1.1 D/Q, Parametric Microsphere Deposit (m^{-2})

Release altitude: Distance	15 km	45 km	60 km	90 km
0-25 km	0	0	0	0
25-50 km	$3 \text{to} 7 \times 10^{-9}$	$1 \text{to} 3 \times 10^{-9}$	$0 \text{to} 1 \times 10^{-9}$	$0 \text{to} 1 \times 10^{-9}$
50-100 km	$.3 \text{to} 5 \times 10^{-9}$	$.1 \text{to} 2 \times 10^{-9}$	$.8 \text{to} 1 \times 10^{-9}$	$.5 \text{to} 1 \times 10^{-9}$
100-150 km	$0 \text{to} 4 \times 10^{-10}$	$.7 \text{to} 9 \times 10^{-10}$	$4 \text{to} 8 \times 10^{-10}$	$1 \text{to} 8 \times 10^{-9}$

Table 3.3.1.1 D/Q, Parametric Microsphere Deposit (m^{-2}) (continued)

Release altitude: Distance	15 km	45 km	60 km	90 km
150-200 km	0	$0 to 3x10^{-10}$	$1 to 5x10^{-10}$	$.6 to 5x10^{-10}$
200-250 km	0	$0 to 8x10^{-11}$	$.6 to 2x10^{-10}$	$.4 to 2x10^{-10}$
250-300 km	0	$0 to 4x10^{-11}$	$4 to 8x10^{-11}$	$0 to 1x10^{-10}$
300-400 km	0	0	$0 to 4x10^{-11}$	$0 to 3x10^{-11}$
> 400 km	0	0	0	0

Most of the time these patterns would be laid down in the 180° sector to the east of the release point. In midsummer, however, there is a high probability of the fallout occurring west of the release point.

Although G.E. used the Sandia calculations for each particle size class, they used a different method of superimposing size classes. The results for the 45 km release are shown in Table 3.3.1.2. The curves showing area covered versus deposition density for the G.E. and Sandia calculations are plotted in Figure 7 for comparison. The Sandia distribution is more spread out, with no area receiving a deposit density greater than 10^{-8} Q/m^2. The two calculations agree in giving an area of approximately 200 km^2 for deposit density exceeding 10^{-9} Q/m^2. The Sandia results appear more plausible although G.E. points out the possibility of variation in atmospheric slowing-down distance with particle size counteracting the spreading effect of variations in terminal velocity during fall

Table 3.3.1.2 High Altitude Microsphere Deposition Areas

	G.E.		Sandia	
Area with D/Q exceeding:	km^2	mi^2	km^2	mi^2
$10^{-11} m^{-2}$	500	200	4600	1800
$10^{-10} m^{-2}$	400	150	1600	600
$10^{-9} m^{-2}$	200	80	200	80
$10^{-8} m^{-2}$	80	30	0	0
$10^{-7} m^{-2}$	30	10	0	0
$10^{-6} m^{-2}$	5	2	0	0

3.3.2 Random re-entry

Sandia Model B has been used to compute deposit density and ground level air concentration of both the microsphere particle population and an "ablation debris" particle population with a logarithmic distribution extending from 50μm down to .0005μm.

The microsphere release is assumed to take place at 45 km altitude, 40°N and 105°W with a "mean seasonal fitted" wind field. The microsphere results are included in the deposit density estimates given in the previous table for a 45 km release.

The "ablation debris" release was evaluated for a "mean seasonal fitted" wind field with releases at 45 km altitude at latitudes 17°N, 40°N and 75°N. Deposit densities from 1 to $3 \times 10^{-12} m^{-2}$ cover areas of the order of $10^4 km^2$ at distances of the order of several hundred km for the particles in the neighborhood of 50μm diameter, down to 2 to $9 \times 10^{-16} m^{-2}$ covering areas of the order of

1 to $2x10^8 km^2$ (20 to 40% of the area of the earth) for the particles 2 to 5μm in diameter. The smaller particles (< 2μm) would be distributed worlwide, although the major part might be limited to the hemisphere (northern or southern) in which the release is assumed to occur.

It can be concluded that degradation products in the size range intermediate between the "respirable" range (< 3μm) and the microsphere range can produce deposit densities exceeding given levels from 10^{-15} to $10^{-12} m^{-2}$ over areas indicated in Table 3.3.2 and in Figure 8.

Table 3.3.2 Degraded Microsphere Deposition, Logarithmic Distribution

Deposit density $D/Q(m^{-2})$	$> 10^{-15}$	$> 10^{-14}$	$> 10^{-13}$	$> 10^{-12}$
Length (km)	10^5	10^4	3000	1000
Area (km^2)	$3x10^8$	10^7	10^6	$3x10^4$

3.3.3 High Altitude Fine Particle Release

The fraction of "ablation debris" in the "respirable" size range (< 3μm) can conceivably approach 100% of the source under some re-entry conditions. The worldwide dispersion and deposition of this particle population has been estimated by P. Krey by analogy with the observed behavior of the SNAP-9A debris as well as the high altitude ^{102}Rh and ^{109}Cd tracers released in nuclear weapons tests. As an upper limiting assumption (possibly applicable in the case of re-entry at a high latitude in winter) all the debris was confined to one hemisphere. The resulting total exposure, $4.8x10^{-13} sec/m^3$, is consistent with the parametric value $2.6x10^{-13} sec/m^3$ obtained by G.E. for

dispersion in both hemispheres. The maximum concentration at ground level, $6x10^{-21}m^{-3}$, occurring 3 years after injection of debris into the upper stratosphere, is also consistent with the $3x10^{-21}m^{-3}$ parametric concentration obtained by G.E.

Uniform distribution over the earth, of course, would give a deposit density of $2x10^{-15}m^{-2}$. Confinement to one hemisphere would double this, and latitude banding may introduce another factor of 2 for middle latitudes.

COLD GROUND - LEVEL RELEASE
CLOUD PASSAGE EXPOSURE, DEPOSITION DENSITY AND RESUSPENSION EXPOSURE PER UNIT SOURCE VS. DISTANCE DOWNWIND

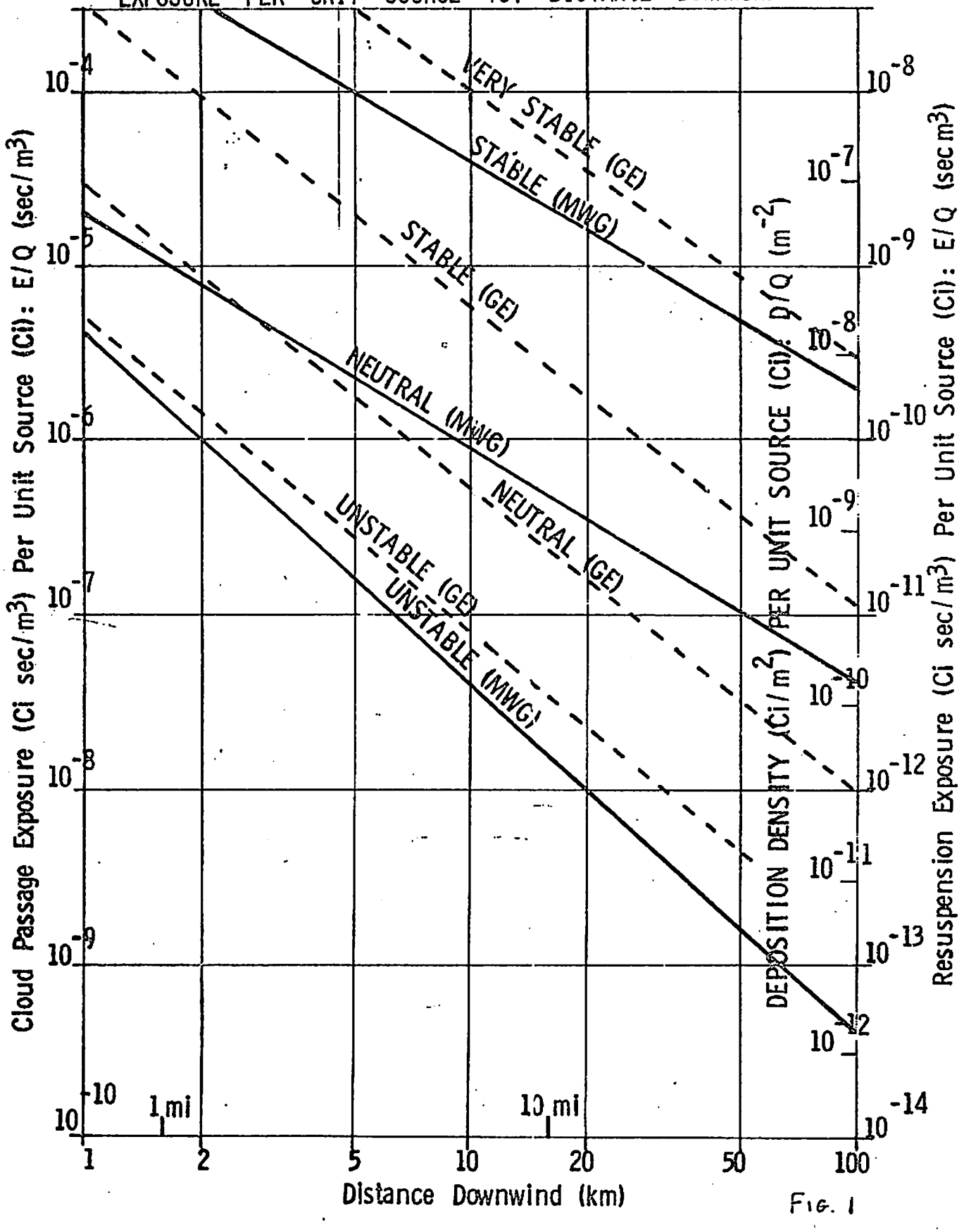

FIG. 1

COLD GROUND-LEVEL RELEASE
CLOUD PASSAGE EXPOSURE, DEPOSITION DENSITY AND RESUSPENSION EXPOSURE
PER UNIT SOURCE VS. AREA COVERED

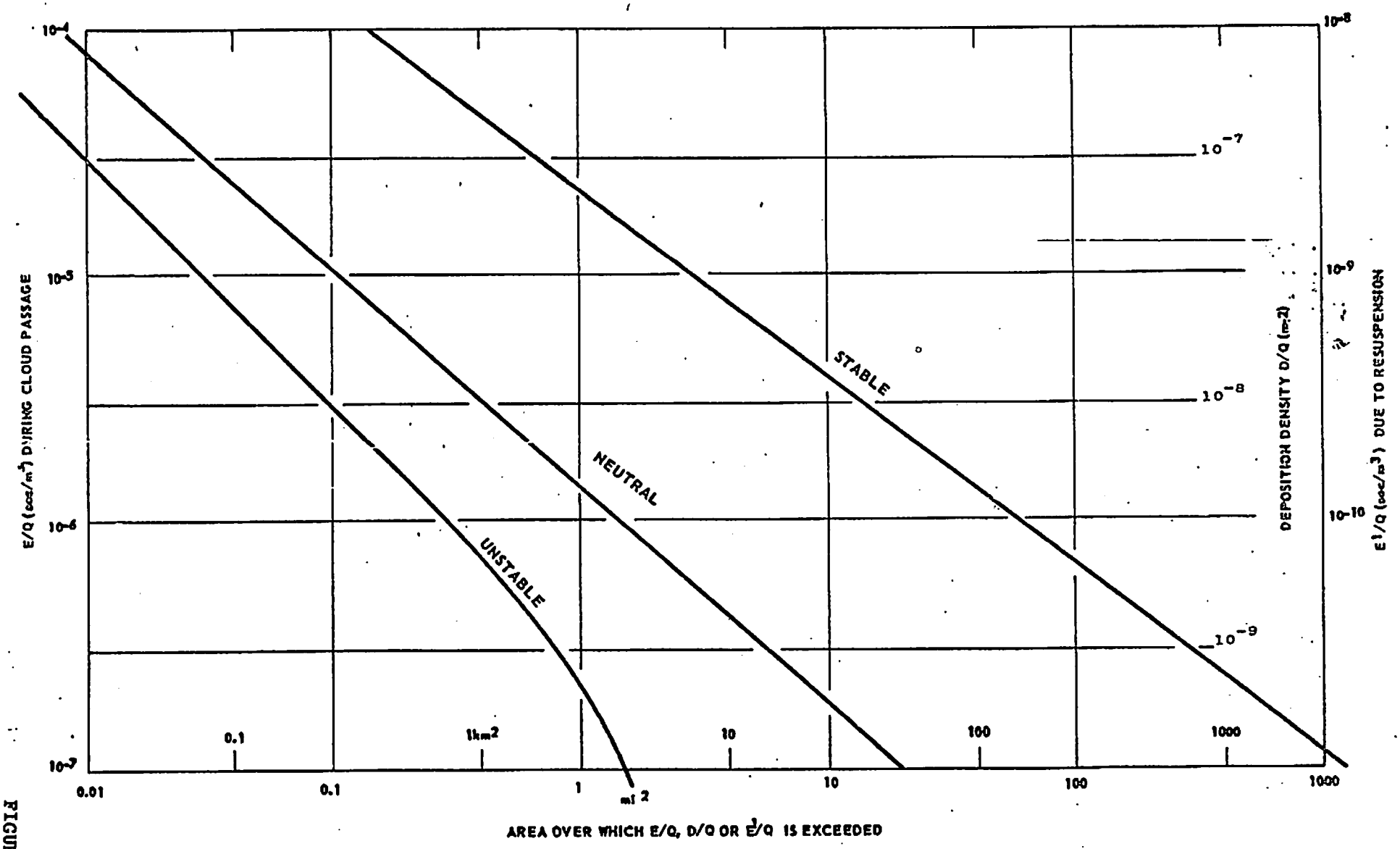

FIGURE 2

FIGURE 3

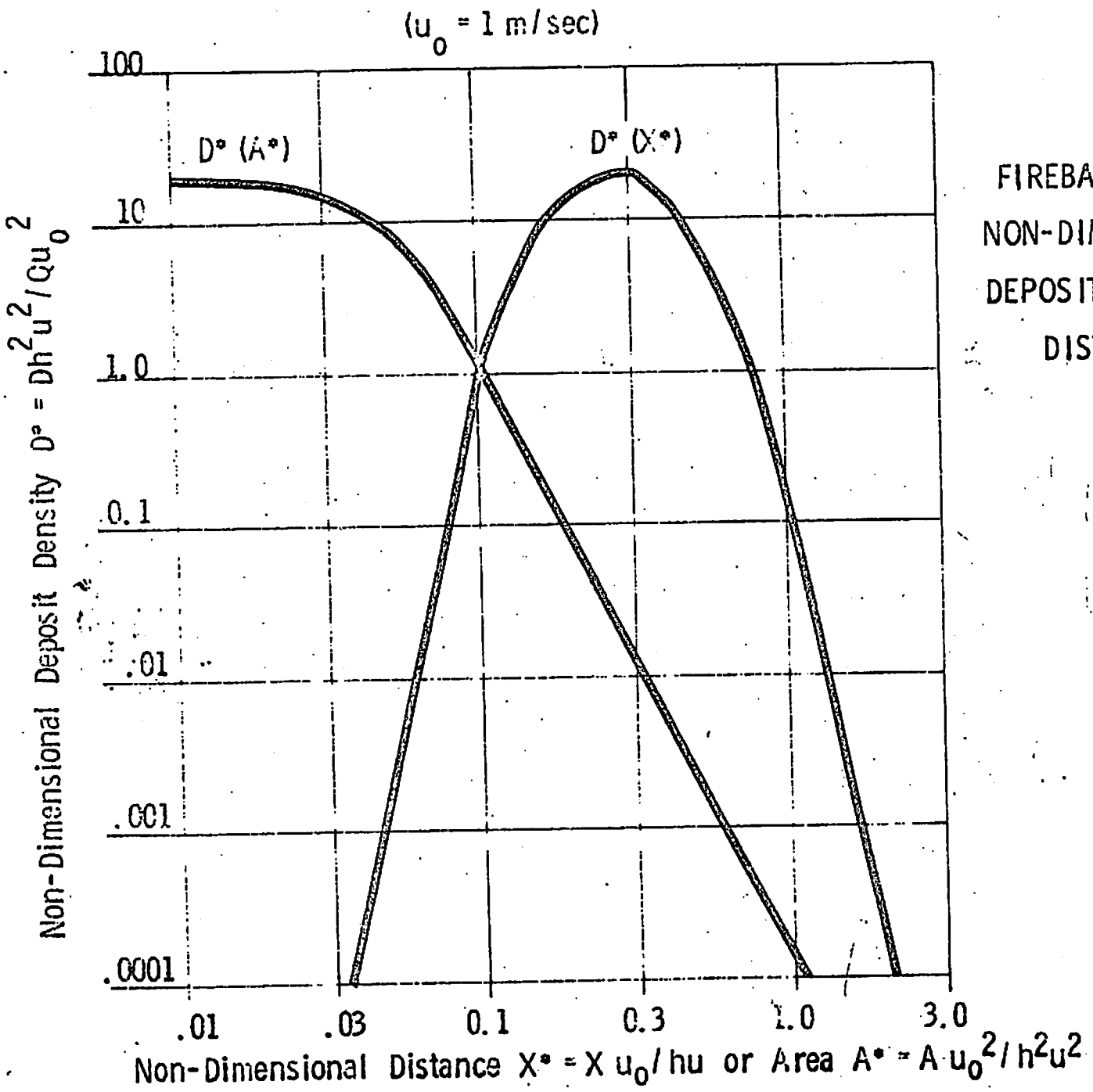

FIREBALL RELEASE - HOT CLOUD
NON-DIMENSIONAL MICROSPHERE
DEPOSITION VS. NON-DIMENSIONAL
DISTANCE AND AREA

128 :-744

FIGURE 1

HOT CLOUD FINE PARTICLE DISPERSION
EXPOSURE PER UNIT SOURCE VS. DISTANCE DOWNWIND

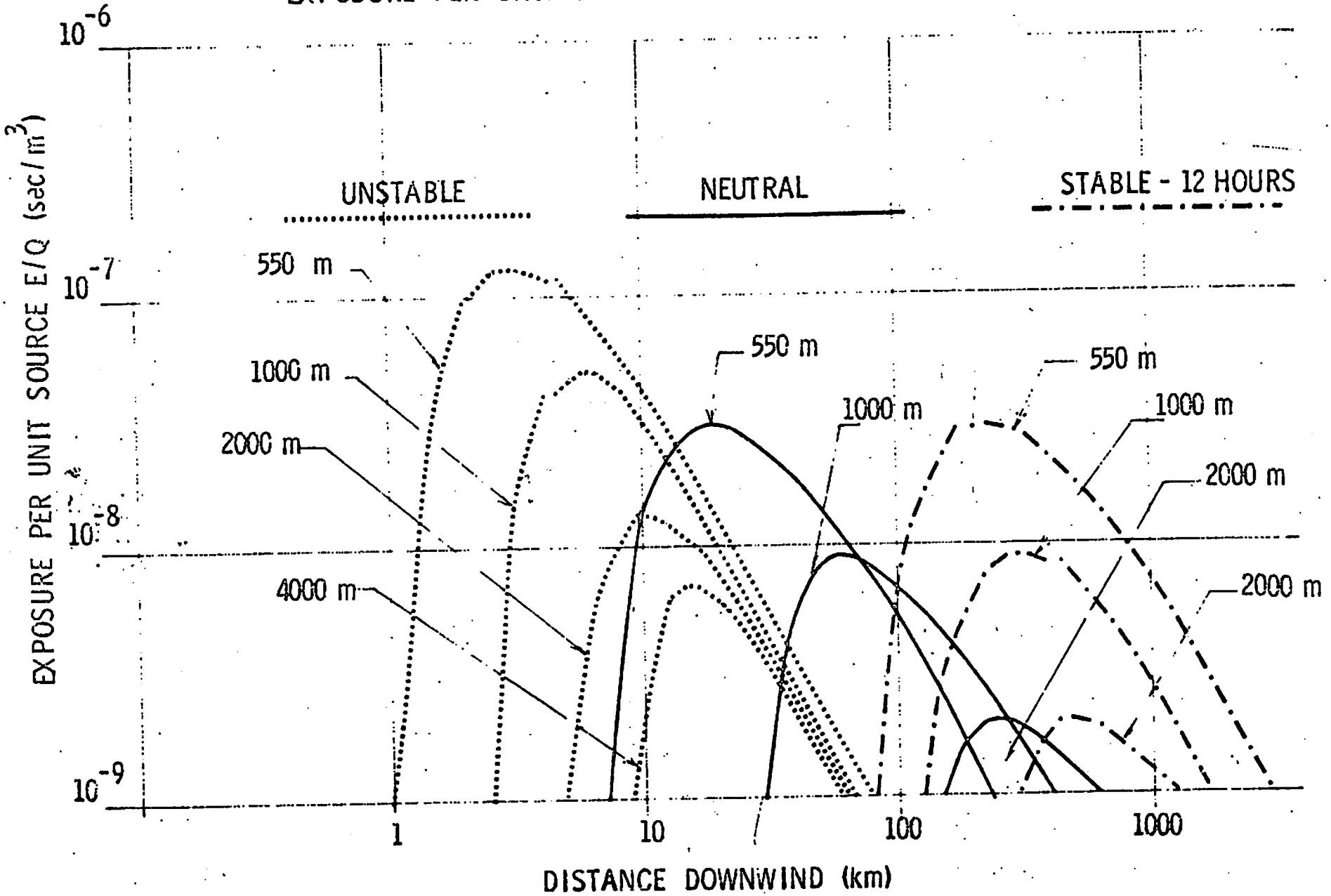

128 S-739

FIGURE 4

HOT CLOUD FINE PARTICLE DISPERSION
EXPOSURE PER UNIT SOURCE VS. AREA COVERED
(ALSO DEPOSITION DENSITY PER UNIT SOURCE
FOR DEPOSITION VELOCITY $V_G = 3 \times 10^{-3}$ m/sec)

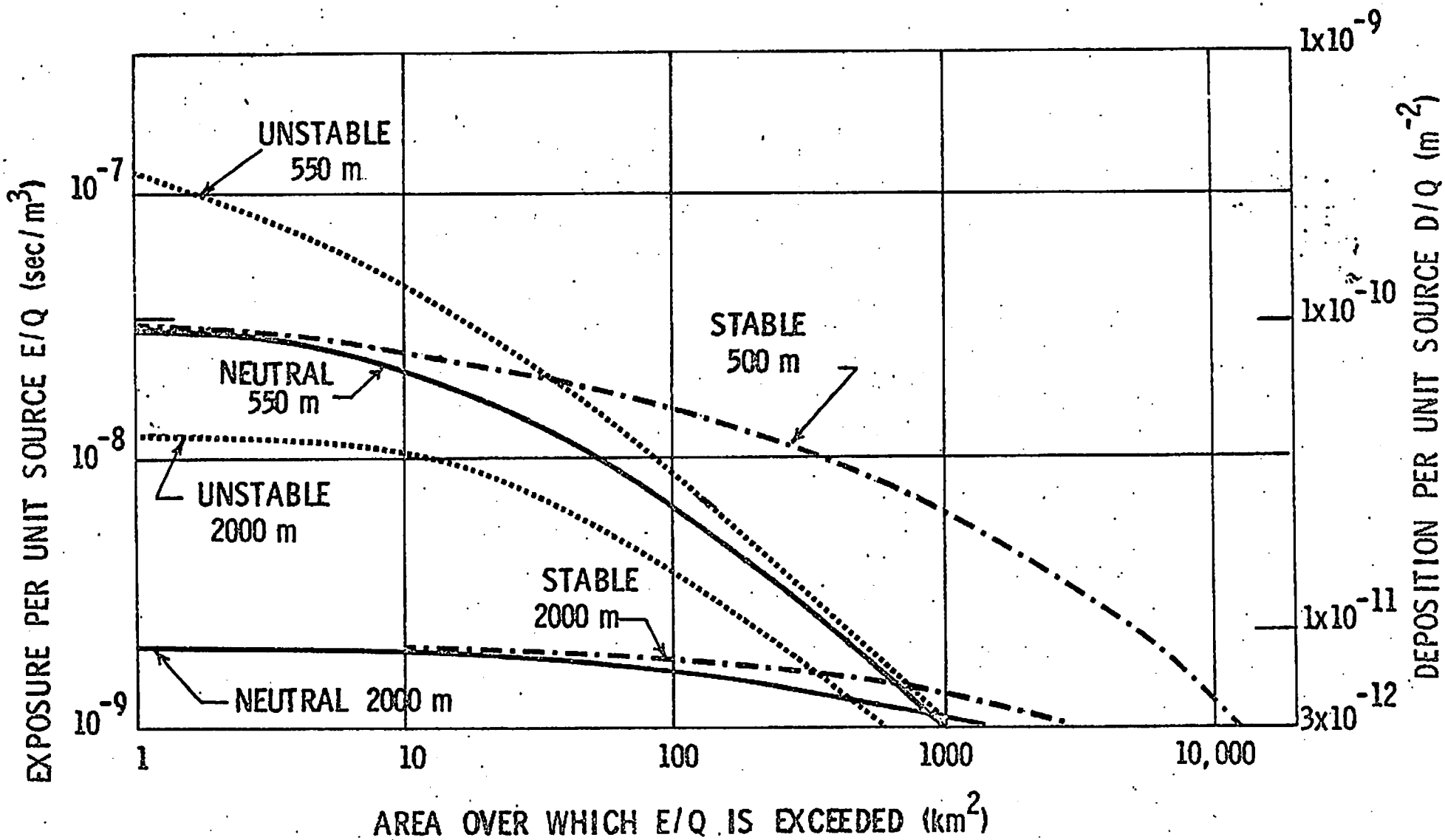

FIGURE 5

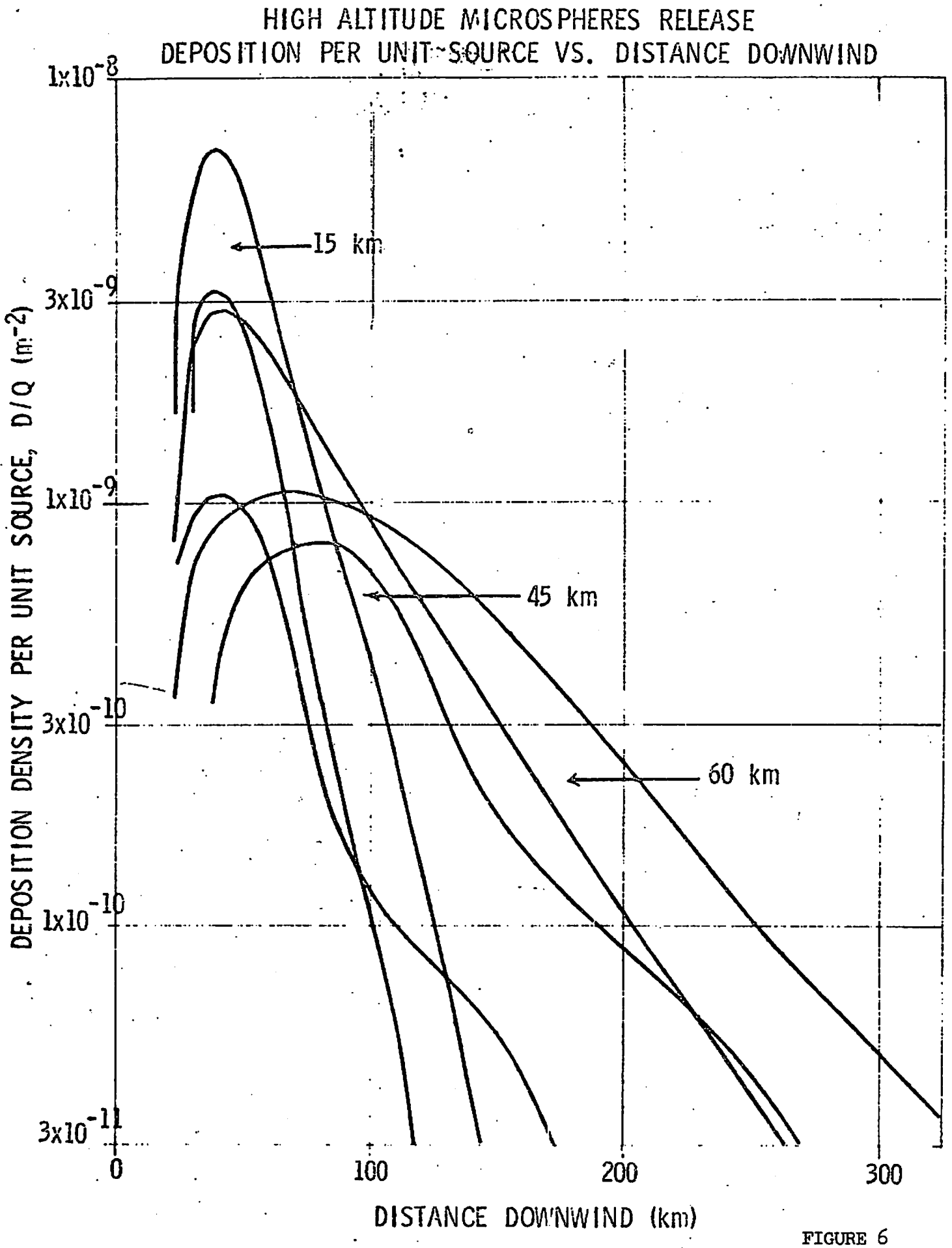
HIGH ALTITUDE MICROSPHERES RELEASE
DEPOSITION PER UNIT SOURCE VS. DISTANCE DOWNWIND
1x10^-8
3x10^-9
1x10^-9
3x10^-10
1x10^-10
3x10^-11
DEPOSITION DENSITY PER UNIT SOURCE, D/Q (m^-2)
15 km
45 km
60 km
0
100
200
300
DISTANCE DOWNWIND (km)

FIGURE 6

MICROSPHERE RELEASE AT 45 km ALTITUDE

AREA COVERED VS. DEPOSITION DENSITY PER UNIT SOURCE

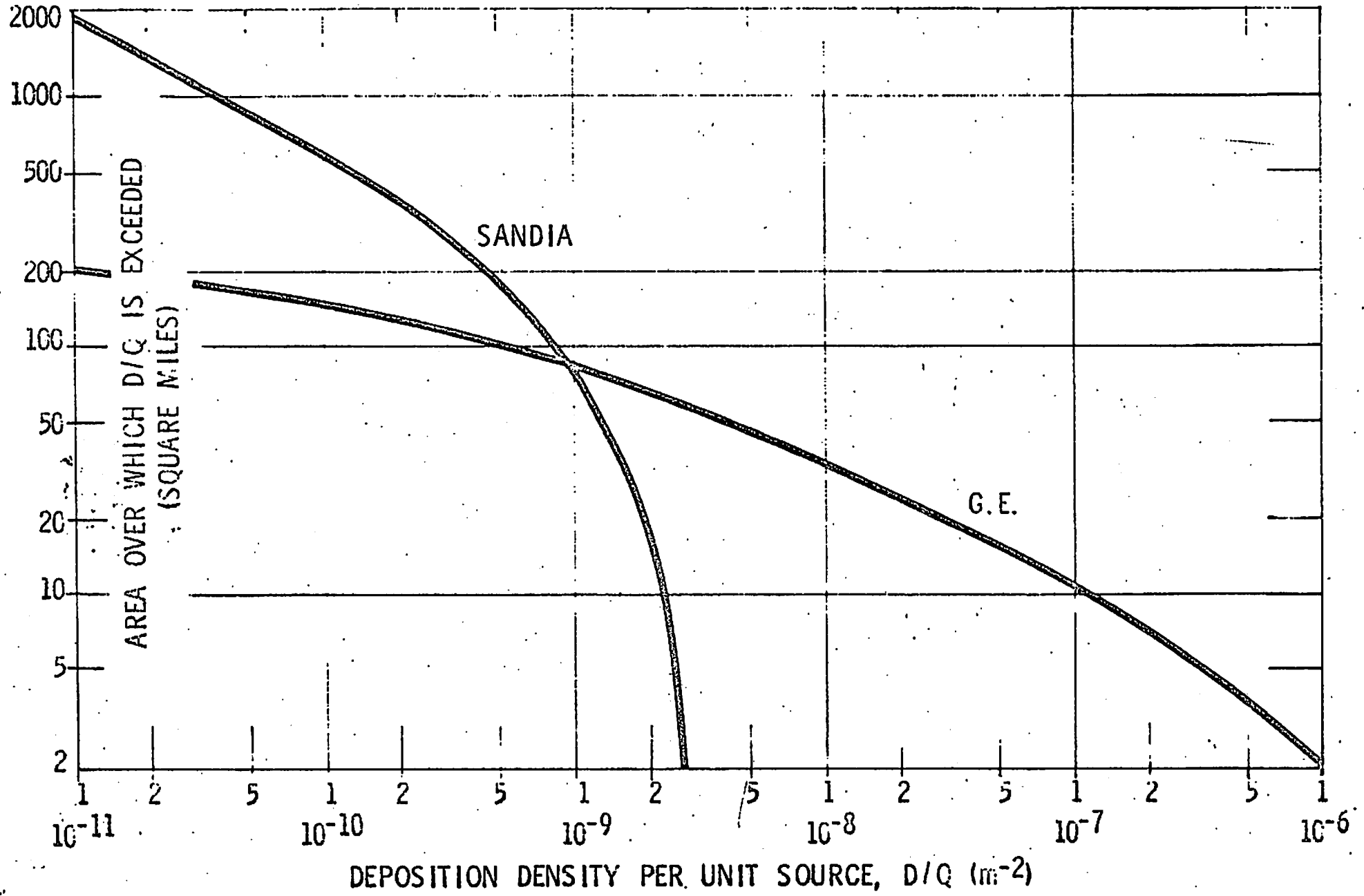

128 :-742

FIGURE 8

RELEASE OF DEGRADED MICROSPHERES AT 45 km ALTITUDE

DEPOSITION DENSITY PER UNIT SOURCE VS. AREA COVERED

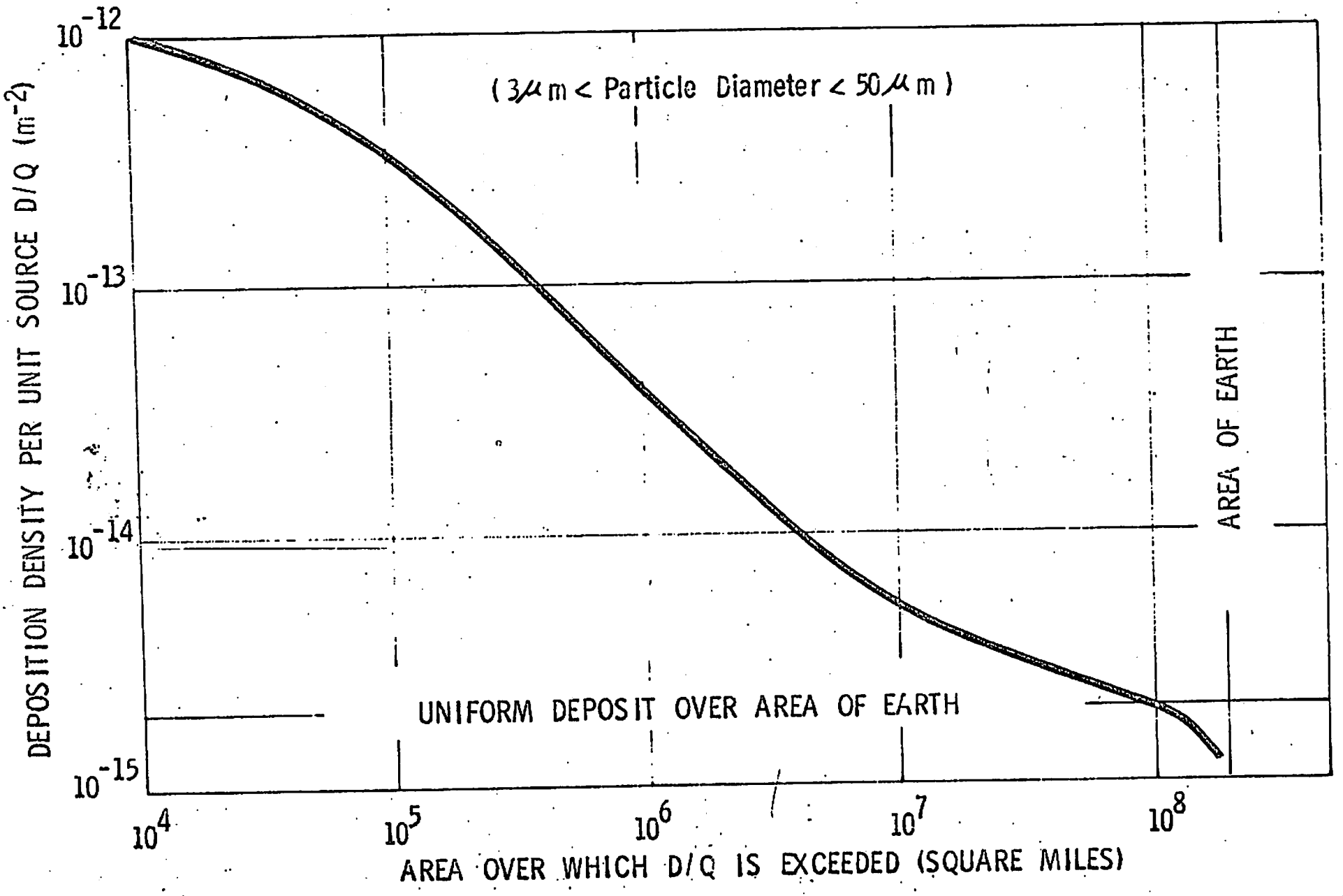

128 :-743

APPENDIX D

REVIEW OF THE MARINE ASPECTS OF SNAP-27 SAFETY ANALYSIS REPORT

REVIEW OF THE MARINE ASPECTS OF SNAP-27 SAFETY ANALYSIS REPORT

The Ad Hoc Marine Subpanel on the Safety Evaluation of SNAP-27/ALSEP met in Seattle, Washington, on September 24-25, 1968. The following persons attended:

Ted Dobry, AEC, Division of Space Nuclear Systems
Ray Klecker, AEC, Division of Reactor Licensing
John Harley, AEC, HASL, New York
Charles Osterberg, AEC, Division of Biology and Medicine
*Allyn Seymour, U. of Washington
Thomas Beasley, U. of Washington
Edward Held, U. of Washington
Richard Foster, Battelle-Northwest, Richland
Col. S. Shwiller, Dept. of Defense, Albuquerque
Arnold Joseph, Marine Resources Council
Saad Mikhail, NRDL, San Francisco
*Donald Pritchard, Johns Hopkins Univ.

*Representing NASCO

After an introduction by Mr. Dobry, results of the research on SNAP-27 at NRDL were presented by Dr. Mikhail. Since the NRDL results seemed to be more realistic than those in the Safety Report, they were adopted as the basis of our report.

Discussion led to the following summary (Table 1) of possible accidents due to aborts in launching or in space.

Table 1. Possible Conditions under Which the Fuel Capsule Might Land in the Sea

	Capsule	Water Depth	Fuel Release
1)	Intact	Shallow (<200m)	None
2)	Split	"	Intact (0.25 Ci/d)
3)	Split	"	Fractured (0.5 Ci/d)
4)	None	"	Dispersed (<100 $\mu Ci/m^2$)
5)	Intact	Intermediate (200-1000m)	None
6)	Split	"	Intact (0.25 Ci/d)
7)	Split	"	Fractured (0.5 Ci/d)
8)	None	"	Dispersed (<100 $\mu Ci/m^2$)
9)	Intact	Deep (>1000m)	None
10)	Split	"	Intact (0.25 Ci/d)
11)	Split	"	Fractured (0.5 Ci/d)
12)	None	"	Dispersed (<100 $\mu Ci/m^2$)

We consider that of the possible events listed above, only two need to be evaluated in terms of potential hazards to man from a release of ^{238}Pu to the marine environment. The two cases considered are: (1) impact of a damaged (split) fuel capsule in the shallow waters over the continental shelf, and (2) release of the fuel particles (microspheres) from the capsule during launch, and subsequent fall-out of the fuel particles into the shallow water of the continental shelf. All other events considered would result in potential hazards to man significantly less then the two cases selected for evaluation.

We have used two approaches in evaluating the possible consequences of the introduction of a damaged fuel capsule into the waters of the continental shelf. In the first approach, we have determined the probable volume of water having concentrations of ^{238}Pu exceeding a derived maximum permissible concentration for sea water (5.4×10^{-6} μCi/ml)1/. The second method of evaluation involves a determination of the probable mean concentration of ^{238}Pu in one year's supply of sea food for one man, and a comparison of the resulting intake rate for that individual with the allowable intake rate for ^{238}Pu for a limited population.

1/ The maximum permissible intake for ^{238}Pu is 1.1×10^{-2} μCi/d = 4 μCi/yr. Assume that a man eats 75×10^3 grams (protein intake for standard man) of edible sea food/yr (from 150×10^3 grams raw seafood/yr.)

$$\frac{4\mu Ci}{75 \times 10^3 g} = 5.4 \times 10^{-5}\ \mu Ci/g = MPC\ (seafood)$$

Assuming a concentration factor of 10 in going from sea water to sea food then, MPCC = 5.4×10^{-6} μCi/ml. of seawater

In carrying out this evaluation, we have made the following assumptions:

(1) The rate of solution in sea water of ^{238}Pu from the full 3800 grams of exposed fuel particles in the damaged fuel capsule is 0.5 Ci.day^{-1}. This value is based on the following considerations. The fuel as originally packaged exists as a mix of microspheres of plutonium oxide having a size range from 50 to 250 microns. Extensive studies by NRDL indicate that the steady state rate of solution of the full 3800 grams of plutonium oxide fuel particles as packaged would result in a release to sea water of about 0.25 curies per day. Experiments have shown that a portion of the fuel particles will shatter when the fuel capsule is subjected to a shock from impact or from an external explosion. The resulting altered size distribution of the fuel particles containing components smaller in size than the original distribution, would be associated with an increased rate of solution. From the data now available on the fraction of the microspheres which might be fragmented on impact of the fuel capsule, we conclude that the rate of solution might be increased by a factor of two. We have therefore doubled the experimentally determined value of about 0.25 Ci.day^{-1} for the source strength of the exposed fuel particles.

(2) The appropriate diffusion model to be used for determination of the probable distribution of concentration of ^{238}Pu in the coastal waters off Cape Canaveral is the linear shear-diffusion model proposed by Carter and Okubo (1965). The attached appendix contains a discussion of the modifications made to this model by NRDL to provide for computer computation of the concentration distirbution from a continuous point source. We used the NRDL results in the following evaluation. The values of the pertinent diffusion parameters

and velocity shear terms employed by NRDL are those obtained by Carter and Okubo (1965) from dye diffusion studies in the coastal waters off Cape Canaveral, and hence should be the best available for this evaluation. While NRDL has not at this date run their computer program for exactly the same source strength and boundary conditions considered here, the computations they have made represent conditions sufficiently close to those considered here so that we can, with reasonable confidence, extrapolate their results.

Such an extrapolation indicates that the volume of sea water having concentrations of ^{238}Pu exceeding 5.4×10^{-6} $\mu Ci/ml$, resulting from a continuous release of 0.5 $Ci.day^{-1}$ of ^{238}Pu from a local source on the bottom of the continental shelf off Cape Canaveral, would be on the order of only 25 M^3. This roughly elliptically shaped volume would have a length of about 14 meters, a width of about 12 meters, and a verticle dimension of about 0.3 meters. Due to temporal changes in the current pattern, this plume of activity would extend away from the source over different segments of the bottom in the vicinity of the source for varying periods of time. No sessile benthic organisms are commercially harvested from the continental shelf off Cape Canaveral, and mobile species would occupy this small volume for such a relatively short period of time that the average concentration to which sea food organisms would be exposed would be very much less than the accepted calculated value for ^{238}Pu in sea water. Put another way, this volume is less than 10^{-4}th of the volume of coastal water required to produce a one-year's supply of sea food for a single individual obtaining all of his protein requirement through consumption of such sea food.

The alternate evaluation of the potential hazard from the introduction of a damaged fuel capsule into the waters of the continental shelf off Cape Canaveral involves the determination of the average concentration of ^{238}Pu in

1.5×10^6 cubic meters, which is the volume required to produce one year's supply of sea food for one man who receive all his protein from consumption of such sea food. This volume is determined in the following manner. In order to obtain all his protein requirement from sea food, an individual would consume 75 kg of edible sea food per year which is equivalent to 150 kg of raw sea food. Production of sea food is three metric tons per square kilometer over the coastal shelf (average depth, 30 meters), or 3×10^{-3} kg.m^{-2} ÷ 30 m = 1×10^{-4} kg.m^{-3}. Hence the required volume V = 150 kg/1×10^{-4} kg.m^{-3} = 1.5×10^6 m^3.

Interpolation from the results obtained from the computer program of the Carter-Okubo shear-diffusion model obtained by NRDL indicate that the total ^{238}Pu inventory at any given time in a volume of water of 1.5×10^6 m^3 about a continuous source on the bottom of the continental shelf of strength 0.5 Ci.day^{-1} would be about 1.5×10^{-1} Ci. The average concentration in the sea water within this volume would then be 1.5×10^{-1} Ci/1.5×10^6 m^3 or 1×10^{-7} Ci.m^{-3}. Assuming a concentration factor between sea water and sea food of 10, the mean concentration is sea food harvested from this volume would be 1×10^{-6} μCi per gram. The intake of ^{238}Pu by one man for one year would then be

$$(1 \times 10^{-6}\ \mu\text{Ci.g}^{-1})\ (75 \times 10^3\text{gr}) = 7.5 \times 10^{-2}\ \mu\text{Ci or } 2 \times 10^{-4}\ \mu\text{Ci per day.}$$

The allowable intake of ^{238}Pu for a limited population (1/10 of the dose allowed to occupational workers as established by the ICRP) is 1.1×10^{-2} μCi per day. This value is approximately two orders of magnitude higher than the value calculated above for one individual receiving all his protein requirements from sea food harvested from the most contaminated area associated with the postulated SNAP-27 source, and hence the hazard to man from this type of accident is not deemed to be significant.

Certain conceivable accidents during the launch of the vehicle carrying the SNAP-27 capsule could produce a release of the fuel particles to the

atmosphere and a subsequent downwind spread over the coastal waters and fallout onto the surface of the coastal waters. Evidence available to us at this time indicates that the maximum areal concentration from such a series of events on the sea surface would be about 100 $\mu C.m^{-2}$. Further, this maximum concentration would be associated with the larger particle sizes (100 microns and greater), which would have a minimum sinking rate of 800 meters per day. Thus the particles would rapidly sink to the bottom in the relatively shallow waters of the continental shelf, and insignificant amounts of activity would be released in solution from the falling microspheres en route to the bottom. Conceivably some particles might be ingested by marine organisms and ultimately reach man. However, such particles are most likely to pass through the gut of the sea food organism without absorption and be ejected as fecal pellets which sink quite rapidly. Any such particle which might reach man in sea food would not normally be contained in that portion of the sea food consumed by man. Even when ingested, such a particle would pass through the intestinal tract, producing at worst a short-time exposure to a small segment of the population.

Fuel particles having a surface area density of about 100 $\mu c\ m^{-2}$ (from a burn-up in which the capsule was destroyed) would be spread over the bottom of the continental shelf in an elongated pattern downwind from the launch site having a length of perhaps 40 to 50 km and a width of about 10 km. This pattern would generally be oriented approximately perpendicular to the coast-line, and since the currents over the shelf are generally along the direction of the coastline, the water of the shelf would be transported across the 10 km width of the pattern.

Making the very conservative assumption that the fuel particles on the bottom would have the same solution rate per unit weight as assumed for the

exposed fuel mix in the damaged capsule, then the rate of solution of ^{238}Pu into the overlying sea water from a fuel particle density of 100 $\mu Ci.m^{-2}$ would be 1.2×10^{-9} Ci day^{-1} m^{-2}. Since the source is then a planar source extending some distance along a line at right angles to the probable current flow, only vertical mixing is likely to be important in this case, and we can consider the concentration which would occur in a strip of water one meter wide in a direction perpendicular to the flow, and having a length equal to the 10 km width of the fallout pattern. Assuming that the current velocity over the bottom is about 12 cm. sec^{-1}, or 10^4 m. day^{-1}, the concentration of ^{238}Pu in the water after passing over the full 10 km of the fallout pattern would be given by

$$\frac{1.2 \times 10^{-9}\ \text{Ci.}\ day^{-1}.\ m^{-2} \times 10^4 m^2}{10^4 \times D\ m^3.\ day^{-1}} = \frac{1.2 \times 10^{-9}\ \text{Ci.}m^{-3}}{D}$$

where D is the vertical thickness of the layer into which the ^{238}Pu would be mixed. Even if this vertical thickness was only one meter, the concentration of ^{238}Pu in the water over the bottom resulting from a planar source of fuel particles on the bottom having an areal density of 100 μCi. m^{-2}, would be 1.2×10^{-9} Ci. m^{-3}, which is less than one-thousandth of the acceptable value calculated here.

In summary, the Subpanel does not consider any of the possible fates of SNAP-27 to constitute a health hazard in the marine environment.

The Subpanel is most appreciative of Dr. Pritchard, who played a major role in the preparation of this report.

ADDENDUM 1

The Subpanel discussed the problem of fresh water contamination. It was felt that the problem of fresh water contamination does not appear to be serious in view of the following:

1. The probability of impact of reentering capsule in fresh water is small compared with either land or ocean surface.
2. The solubility rate of $^{238}PuO_2$ in fresh water is slightly less than the rate in ocean water.
3. Indications are that Pu ions are sorbed on sediments and thereby effectively removed from solution.
4. Plutonium entering in a fresh water supply is expected to be sorbed on the walls of the distribution system.
5. Plutonium reaching the treatment plants will be effectively removed by the water treatment systems.

The working group recognizes that effective water treatment is not common in small town water systems, and advises that in the case of an abort resulting in land impact, rivers, lakes and reservoirs in the suspect area should be monitored.

The present state of the art does not lend itself to a more quantitative evaluation of the fresh water situation.

APPENDIX E

BIOMEDICAL HAZARD EVALUATION OF SNAP-27/ALSEP

APPENDIX E

Final Report

BIOMEDICAL HAZARD EVALUATION OF SNAP-27/ALSEP

Biomedical Subpanel Members
Roy Albert, NYU
William Bair, BNWL
Birney Fish, ORNL
Roger McClellan, Lovelace
Thomas Mercer, Univ. of Rochester
Arthur Tamplin, Livermore
Chester Richmond, LASL and DBM/USAEC
H. D. Bruner, DBM/USAEC, Chm.

* * * * * * * * * *

A report of the Biomedical Subpanel was presented to the SNAP-27 Panel on December 9, 1968. This final report is the result of additional information regarding source terms. This report also includes discussions of several points raised by Panel Members.

Introduction:

A discussion of the state of our current knowledge about the biomedical hazards created by aerosols of PuC_2 was presented in "Comments on the SNAP-19 Problem by the DBM Committee on SNS Radiological Safety Matters," Spring 1968. The Subpanel chose to evaluate the effects of exposure on the basis of an individual person at risk. In that document, the Biomedical Subpanel established that inhalation was the route of exposure most likely to lead to potential biological damage or, possibly, to lethality; other tissues at risk (the skin, the conjunctival-nasopharyngeal mucosal system, the gastrointestinal tract and organs or tissues which might retain Pu absorbed from the gut) ought to receive smaller exposures, if any at all, and their responses would be quite unlikely to be lethal.

Several recent reports offer support for these conclusions. Both acute (1) and chronic (2) feeding of actual $_{238}PuO_2$ microspheres to swine and beagles indicate that ingestion of intact microspheres (e.g., many thousands at one time or one-thousand over six-months time) does not constitute a biological hazard. In addition, the review by Thompson (3) of Pu absorption by the gastrointestinal (G.I.) tract concludes that intestinal mucosa presents a very effective barrier to plutonium absorption under the more usually anticipated conditions of exposure. Present Maximum Permissible Concentrations for Pu in water (MPC_W) are calculated on the basis of an absorption of 0.003% from the G.I. tract. Thompson concludes, from the available experimental data, that such a figure appears appropriate for the general contamination of a drinking water supply. Chronic oral administration to rats of $Pu(NO_3)_4$ at pH 2, in concentrations approximating the (MPC_W), resulted in absorption from the G.I. tract to the extent of 0.003% (4). It is significant that $_{238}Pu$ and $_{239}Pu$ were used. Also, work with pigs, presumably more similar to man in structure and function of the G.I. tract, yields absorptions of 0.002% for Pu given as the nitrate at pH 2.

The biomedical considerations, as outlined in the SNAP-19 report, apply to this present effort; there has been no significant change in the state of our knowledge. The Subpanel has confidence in the hazard estimates given below, but hastens to add that the present state of knowledge does not warrant quantification other than order-of-magnitude type estimates.

The Panel provided source term ranges and meteorological evaluations yielding lung burdens and ground concentrations for several potential accident abort zones (Table 2, SER). These, and previous estimates, were used by the Subpanel.

Thus, this Final Report of the Biomedical Subpanel will deal only with evaluation of the pulmonary hazard from inhaling PuO_2 aerosols that would result from certain of the most probable aborts during the mission. Unfortunately, it is precisely the pulmonary route of exposure which is least well understood and for which the fewest data are available.

The Subpanel wishes the reader to keep in mind that there is no accepted scientific procedure which applies specifically to the situation under consideration: the potential hazard to the lung from inhaled fine particulates emitting alpha particles and a low percentage of soft X-rays (13 per 100 alphas) plus a few neutrons and gamma rays. The SNAP-19 report and the "Uranium Miner Problem" have created renewed interest in this problem on the part of research laboratories, the International Commission on Radiological Protection (ICRP), and our Federal Radiation Council (FRC). At present, however, we are without official guidance or standards applicable to the problem at hand.

Evaluations:

Because there is no single standard of evaluation, the Subpanel has employed several possible approaches. Some are quite new, theoretical, and still undergoing evolution; they are included only to show how choice of assumptions and biological models can affect hazard estimates.

I. The ICRP Concept:

The concept stipulated by the ICRP (5) considers the radiation to be applied evenly to all parts of the lung from either an external source of radiation <u>or</u> a radionuclide distributed evenly throughout the lung. Commonly this is called the organ mean dose or the smear dose. However, exposure from inhalation of a PuO_2 aerosol is in no sense evenly distributed. In reality there will be one or more tiny foci of intense radiation, possibly 40 to 50 micrometers in diameter, dispersed over the 75 meters^2 of lung surfaces. This has been called the "point dose."

Over the years, the ICRP has recommended a Maximum Permissible Dose (MPD) for the lung of 15 rem per year for radiation workers with scaled doses of 1.5 rem per year and 0.5 rem per year for off-site (i.e., non-occupationally exposed) and selected portions of the population respectively. The recent ICRP Publication 9 recommends, "Dose Limits" for planned exposures of individual members of the general public and of populations which amount to 1/10 the MPD (i.e., about 1.5 rem per year and corresponds to a sustained lung burden of 0.0016 μCi Pu if one assumes uniform distribution of the energy). This applies to organ doses and not necessarily to air and water concentrations or to overall average intake estimates. To comply with the recommended practice one should be prepared to show that the critical organ dose does not exceed 1/10 of the occupational MPD for a critical group (i.e., highest dose) within the population. The population residing in a specific isopleth can be considered or treated as such a "critical group," in which case the average lung dose should not exceed 1/10 the occupational MPD. Dose Limit, as recommended by the ICRP, recognizes that dose limitation for members of the general public is a theoretical concept intended to provide standards for the design and operation of radiation sources so that it is unlikely that individuals in the public will receive more than a specified dose. Also, the ICRP points out that because of the innate variability within an apparently homogeneous group, some members of the critical group will receive doses somewhat higher than the Dose Limit; however, at the low levels of risk implied, it is likely to be of minor consequence to their health if the Dose Limit is marginally or even substantially exceeded.

Such a reduction of the MPD by a factor of 10 (to 0.0016 μCi Pu) attempts to allow for the following:

1) that exposure of members of the public generally occurs under uncontrolled situations

2) that there exists in the public domain the young, the aged, the sick, and the pregnant--any of whom may be more sensitive to the effects of radiation exposure. Further reduction by a factor of 3 (to about 0.0005 μCi Pu) attempts to account for variation in individual exposures about the average within the exposed population group (e.g., so that no individual within the exposed group exceeds the MPD for individual members of the public). Use of this factor of 3 is an operational procedure recommended by the FRC.

According to a calculation based on energy released, without reference to its distribution, 0.016 μCi of $_{238}$Pu or $_{239}$Pu would give 15 rem per year to the lung (6). The ICRP considers the standard lung to weigh 1000 grams. We should note that the commonly accepted permissible lung burden of 0.016 μCi for Pu would have to be continuously sustained to deliver 15 rem per year (smear dose). However, amounts deposited in human lungs from most accident modes would be essentially a single deposition which would subsequently be lost, according to the recent ICRP lung model (7) with a biological half-life of 500 days. Therefore, the dose delivered to the lung would decrease as a function of time past exposure.

This is essentially the approach reported recently (8) by several Russians attempting to determine maximum permissible burdens for accidentally inhaled Pu. They calculate that a one-time or short-term intake of $_{239}PuO_2$ should not exceed 0.09 μCi, an amount which would produce a dose of 15 rem for the first year following exposure. They conclude that 0.1 μCi be used as a provisional value for the accidental intake of airborne plutonium dioxide. Use of a factor of 0.2 for alveolar deposition would reduce this value to about 0.018 μCi. The Russian report also concludes that oral ingestion is only of third-order consideration in evaluating the radiation effects of Pu for occupational exposure.

At this time we can offer no criteria that have any proven advantage exceeding that established by international agreement and precedent. Although the Subpanel would reject the smear

dose principle, and the ICRP itself recognizes the shortcomings of the principle as applied to situations in which extreme inhomogeneity of dose occurs, we have no alternative concepts which are firmly established. We have no other choice but to use the ICRP criteria while pointing out the deficiencies, possible merits and current status of other approaches to the problem. We must also recognize that the derivation of the occupational exposure criteria was based on a risk assessment by national and international organizations duly constituted for the purpose of establishing radiation protection criteria.

By this method of evaluation no person (Table 2, SER) would receive a lung burden in excess of that now considered to be an acceptable risk for persons employed in plants handling PuO_2 except from impact cases from which fuel is assumed to be released at either the launch site or at some point following reentry. For these latter cases some unknown maximum lung retention could occur at the point of impact or immediately downwind; lung depositions above 0.016 μCi could be experienced over a 20 Km^2 area. It is difficult to assess the possible consequences of this event as the lung burdens range from 0.016 μCi to some unknown maximum. In the case of low-probability upper-limit worldwide impact conditions occurring in densely populated urban areas, a few unprotected individuals could conceivably receive lung burdens greater than 0.1 μCi, and a number of unprotected individuals could receive burdens in excess of 0.016 μCi.

II. The Experimental Analogy

This approach requires the assumption that a concentration of Pu in the lung of the dog is biologically equivalent to that in man; that the tissue reactions, susceptibility to cancer induction by Pu, and latency are the same for the two species.

Also required is the assumption that $_{239}PuO_2$ and $_{238}PuO_2$ would yield similar biological effects. Preliminary experimental data suggest that $_{238}PuO_2$ and $_{239}PuO_2$, on an equal activity basis, cause roughly similar acute biological effects in dogs.

In late 1958 a plutonium-239 toxicology experiment using 40 beagle dogs was initiated. A previous experiment had shown that death due to respiratory insufficiency took place within one year after lung depositions amounting to 0.1 μCi or more per gram of lung. The second experiment was to study the long-term effects for cases in which initial depositions were less than 0.1 μCi per gram. Twenty-two of the dogs were exposed from late 1958 to early 1960 and an additional 18 were exposed in 1962. Twenty-four have died to date and 5 were sacrificed for tissue distribution. Of the 24, 6 died from pulmonary insufficiency prior to 4.5 years beyond exposure; beyond 4.5 years, all deaths but 2 (cardiovascular and encephalitis) were from pulmonary tumors. Of the 11 now remaining, 9 are from the 1962 exposures. Six of the 11 probably have pulmonary tumors based on radiographic data and 4 are prime suspects. At this time 6 to 10 years after exposure virtually every dog has died of pulmonary insufficiency and/or pulmonary tumors. Of special interest is the observation that tumors were found at autopsy in 4 of the dogs that died prior to 4.5 years from pulmonary insufficiency even though tumors were not suspected from radiographic examinations. From 10 to 48×10^{-3} μCi per gram of lung were initially deposited according to estimates from excretion data. It is, therefore, imperative to begin dose-effect studies at still lower exposure levels, but it is obvious that such experiments are of long duration.

From these data one can derive an incomplete dose-response curve which indicates that initial alveolar depositions of 0.5×10^{-9} Ci per gram of bloodless lung approaches the level at which lung carcinomas might develop late in the life span of the dog. Assuming that a concentration of 0.5×10^{-9} Ci per gram bloodless lung would have an equal effect in man, we can estimate that initial alveolar depositions of 0.25 μCi in the lungs of the standard man (the bloodless lungs weigh about 500 grams or about half the 1000 grams for the blood-containing lung tissue of the ICRP Standard Man) might cause tumor development late in life. It is important to realize that the 0.5×10^{-9} Ci per gram reference value was extrapolated from the dog experiment which although some eight years old is still in progress. The beagle data are the best available for the purpose of estimating tumorigenic response.

The 0.25 μCi value, calculated above for human lungs is approximately 15 times the generally accepted lung burden of 0.016 μCi cited in the preceding section.

III. Present Contamination Levels in the Lung Relative to Amounts Injected into the Atmosphere

A considerable amount of Pu has been put into the atmosphere as a result of atmospheric nuclear weapons tests and other sources (i.e., the SNAP 9-A failure and possibly other nuclear power sources of unknown origin that failed). A conservative estimate is that about 0.5 mega Ci of $_{239}$Pu and 25 kilo Ci of $_{238}$Pu have been injected into the atmosphere, of which 2.5 kilo Ci of $_{239}$Pu and 2 kilo Ci of $_{238}$Pu may still remain suspended. The mean particle size is about 0.01 micrometers. If it is assumed that the aerosols from SNAP-27 and the above sources were similar, and that the dispersion-exposure would be similar in the two cases, then estimates of the current lung burden of Pu in the population would give an indication of the lung burden that might be expected if the full 44,500 Ci from SNAP-27 were released into the atmosphere.

Measurements of the Pu lung burdens of normal people from the USSR, UK, and USA give values ranging from about 0.1 to 2×10^{-12} Ci per kilogram of lung (9-12). The analytical data appear reliable but the total number of lungs analyzed is probably less than 100. However, this is a relative measure of existing burdens.

Thus, 500,000 Ci of Pu put into the atmosphere resulted in lung depositions of about 0.1 to 2.0×10^{-12} Ci and the introduction of 44,500 Ci of Pu into the upper atmosphere would by analogy eventually result in an additional lung burden to the population of 0.1 to 2.0×10^{-13} Ci. In terms of increment a person on the average would acquire 10 per cent more Pu than he already had. This total would still be far below the ICRP levels for the population and, using the smear concept, give a lung dose well below background.

Radiation is only one of the numerous insults that the lung must withstand; generally, it is quite a minor contributor. One of its more notorious responses to insults, lung cancer, has a high morbidity rate, now in the neighborhood of 25 per 100,000 per year, which is rising steadily every year; although radiation is recognized as being an agent capable of initiating tumors, lung cancer occurred long before the atomic age and the rapidly increasing morbidity rates of the last three decades cannot be correlated with the introduction of radioactivity

into the environment. No cynicism is intended by stating that it would be impossible by epidemiologic methods to determine whether the introduction of Pu aerosols into the biosphere has changed the morbidity of lung cancer.

IV. Possible Relation Between Lung Cancer and Volume of Tissue Irradiated

It does not necessarily follow that the stated 15 rem per year with its conventionally equated 0.016 μCi Pu adequately expresses a basis for assessing potential biological hazard--and certainly not as well as the Biomedical Subpanel wished. As an expression of the current state of our knowledge it has been employed, but some members of the Subpanel believe that 0.016 μCi of $_{238}PuO_2$ as a single particle represents less of a biological hazard than if the 0.016 μCi were divided into progressively smaller, therefore more numerous, particles.

Table 1 shows the relation between particle diameter and the number of cells irradiated. For each particle diameter shown the total activity is 0.016 μCi. Up to about 1 μ diameter, the number of particles is the more important determinant of the total number of cells irradiated.

Although the cells adjacent to the inhaled radioactive particle may suffer a very high radiation dose, the fall-off in radiation dose as a function of distance from the particle is rapid because of energy absorption by the tissue and of dispersion due to the inverse square effect. Because of the steep energy absorption gradient, the radiation dose will vary greatly from cell to cell within the volume of irradiated tissue exposed to the alpha radiation.

We should also remember that the dose rate <u>per particle</u> decreases as the number of particles comprising a given activity of $_{238}PuO_2$ increases.

Thus, the number of cells in the lung irradiated by a given activity of $_{238}PuO_2$ will increase as the dimensions of the particles in the aerosol decrease, but there will be limits imposed by the behavior of the aerosol with respect to the mechanics of breathing and diffusion. Unfortunately, soundly based experimental knowledge of retention of particles less than 0.1 micron is so fragmentary as not to warrant any confidence. Clearly the problem of the very fine alpha-emitting particle in the lung demands further investigation.

The Biomedical Subpanel has been guided in its thinking by the following generalizations based on animal experiments:

1) The probability of lung cancer appears to increase as the volume of irradiated lung tissue increases and inversely with the rate of energy absorption,

2) Continued exposure of a large fraction of the lung is more likely to produce cancer than is the same total amount of absorbed energy delivered to a small volume of tissue over a short interval.

Based on these considerations it is possible that 0.016 μCi of $_{238}$Pu retained in the lung as particulates may be a lesser biological insult, from the standpoint of carcinogenesis, than the 15 rem per year "smeared" over the entire lung. It follows, therefore, that the ICRP organ-mean dose concept and application may be conservative and hence the hazard estimates based on it are proportionally conservative.

V. Theoretical Assessment of Tumorigenic Risk from Particulates Deposited in the Lung

Because of dissatisfaction with the ICRP technique for estimating lung exposure from inhaled alpha-emitting particles, the Los Alamos Biomedical Group is developing a theoretical approach intended to identify the variables which influence dose to a given cell. A model lung has been constructed and programmed for computer analysis in such a way that ogives of cell doses can be read out with respect to any combination of input exposure parameters, such as number, size, specific activity and movement of the alpha-emitting particle, size of lung cell, etc. The cell doses obtained in this way are then compared with data on the radiation dose to an epithelial cell of the rat skin which is associated with a skin cancer during the subsequent life of the rat. The tumor probabilities for each ogive of cells exposed to the alpha emitting particle are then summed to arrive at an integrated tumor probability for that particle; any number of such exposure units (point exposures) can then be added to give the total tumor probability.

This technique is attractive and has great promise for analyzing the effects of the input variables separately and in combination. As an example of the error that can be made by the "smear technique," the dose from 0.016 μCi of $_{238}$Pu averaged

The Biomedical Subpanel has been guided in its thinking by the following generalizations based on animal experiments:

1) The probability of lung cancer appears to increase as the volume of irradiated lung tissue increases and inversely with the rate of energy absorption,

2) Continued exposure of a large fraction of the lung is more likely to produce cancer than is the same total amount of absorbed energy delivered to a small volume of tissue over a short interval.

Based on these considerations it is possible that 0.016 μCi of $_{238}$Pu retained in the lung as particulates may be a lesser biological insult, from the standpoint of carcinogenesis, than the 15 rem per year "smeared" over the entire lung. It follows, therefore, that the ICRP organ-mean dose concept and application may be conservative and hence the hazard estimates based on it are proportionally conservative.

V. Theoretical Assessment of Tumorigenic Risk from Particulates Deposited in the Lung

Because of dissatisfaction with the ICRP technique for estimating lung exposure from inhaled alpha-emitting particles, the Los Alamos Biomedical Group is developing a theoretical approach intended to identify the variables which influence dose to a given cell. A model lung has been constructed and programmed for computer analysis in such a way that ogives of cell doses can be read out with respect to any combination of input exposure parameters, such as number, size, specific activity and movement of the alpha-emitting particle, size of lung cell, etc. The cell doses obtained in this way are then compared with data on the radiation dose to an epithelial cell of the rat skin which is associated with a skin cancer during the subsequent life of the rat. The tumor probabilities for each ogive of cells exposed to the alpha emitting particle are then summed to arrive at an integrated tumor probability for that particle; any number of such exposure units (point exposures) can then be added to give the total tumor probability.

This technique is attractive and has great promise for analyzing the effects of the input variables separately and in combination. As an example of the error that can be made by the "smear technique," the dose from 0.016 μCi of $_{239}$Pu averaged

over the entire lung for a period of 720 days is 3.24 rads, whereas the model shows that 3×10^5 cells actually absorb over 95% of the total radiation for a dose of 1.6×10^6 rads. However, the model technique has not yet been published and subjected to the critical scrutiny of the scientific community.

The tumorigenic risk data are presented here with reservations. One of the more obvious assumptions required is that the neoplastic response of an epidermal cell in the hair follicle of the skin of a rat is the same as that of any of the various cell types of the human respiratory tract. Many of the biological parameters are poorly defined or are merely assumptions. In its present form the model maximizes the number of cells exposed and consequently overestimates the tumor probability for the average case. Also, the tumor probability versus dose-response curve used in the model was obtained from white rats which are very sensitive to skin tumor formation. It is premature to use such theoretic models in hazards analysis for Pu; this is not to say, however, that models will not be helpful after refinement and experimental verification.

This model was used to calculate tumorigenic risk probabilities with respect to particle size and number for several retained lung burdens (Table 2).

VI. Summary:

1. The Biomedical Subpanel wishes to note again that it has been requested to deal with dose-effect relations in the lung for which there are no accurate standards or final criteria.

2. The system recommended by the ICRP was deemed not well suited to the problem at hand, but nevertheless calculations were made with respect to it because the scientific community has used it in the past, and for want of something better continues to use it.

3. The direct comparison of human lung exposures with experimental exposures in dogs under conditions simulating human exposures is a method of evaluation which the Subpanel found quite acceptable. The conclusions drawn from these comparisons are given credence.

4. A comparison was made of the lung burdens of Pu in the population from weapon tests and other sources, and on this basis an estimate was made of the effect of adding to the atmosphere another batch of PuO_2 amounting to about 10% of what had been put up before. This system provides an evidential check on the calculated dispersions from high altitude aborts. The Subpanel attached weight to the implications of the factual data. This, of course, is not applicable to a launch pad abort.

5. For launch abort failures the area of possible concern in which 0.016 μCi lung burdens might be exceeded for off-site populations would be the impact release. Impact release is also the possible area of concern for early ascent aborts and reentry. The latter situation could occur outside the continental United States. As indicated earlier, these situations are difficult to evaluate as lung burdens can increase up to some unknown maximum as one approaches the point of impact.

6. A theoretical examination of the relation of PuO_2 sizes to carcinogenicity indicates that a few large particles might offer less overall biomedical hazard than the equivalent radioactivity divided into many finer particles. While the spectra of PuO_2 particle sizes are not at hand for all types of aborts, this observation suggests that the ICRP value, which is based on "smear dose," may be conservative. Also, the smear dose concept, implicit in the ICRP approach, is easier to rationalize as particle size, and number, decrease for a given lung burden.

7. A theoretical model now being developed has been included because it attempts to apportion and appraise the influences of the several variables that determine the radiation exposures of the lung cells. It is instructive but does not merit being a major determinant in the Biomedical Subpanel's judgment. At this point it serves only to focus attention on the relation of particle size vis à vis numbers of particles.

8. The Subpanel has not considered in great detail the possible risk from the uptake of Pu by ecological systems; ecological uptake is usually considered to represent second or third order risks. Discrimination factors from soil to plants are of the order of 10^{-4} to 10^{-6} and vary with species, soil type, climate, and physical state of the Pu. Certain aquatic biota, however, are capable of concentrating Pu from the environment by factors up to 10^{3}. These would not present a problem to man if eaten because, as indicated earlier, of the poor absorption of Pu from the G.I. tract.

Ground contamination is another complicated problem as no official or realistic standards exist for guidance except for DoD-AEC agreements for weapons accidents. To assess the biomedical risk resulting, for example, from continuous occupancy we must know and apply resuspension and attenuation factors to surface depositions. The resuspension factor (RS) is the ratio of air concentration above the surface ($\mu Ci/m^3$) to the surface concentration ($\mu Ci/m^2$); the attenuation factor (AF) reduces the amount of Pu available for resuspension as a function of time following deposition. Unfortunately, values of the RS vary by as much as 10^5 depending upon numerous conditions. Also, values of the AF are imprecise and variable. Some estimates conclude that areas initially contaminated to the extent of about 7 $\mu Ci/m^2$ ($_{239}PuO_2$) were safely inhabitable for a lifetime without decontamination. This estimate (13) was based on a permissible lung burden of 0.02 μCi, a 70-year lifetime occupancy, an AF of 0.10 per year, and several values for the RS.

Other data from Nevada (Plumbob Roller Coaster) suggest that initial contamination levels of 70 $\mu Ci/m^2$, or more, might be safely inhabitable for a lifetime without decontamination. Unfortunately, application of these data are complicated by the fact that they were obtained under arid desert conditions.

* * * * * * * * * * * *

The Subpanel, therefore, is of the opinion that aborts which release PuO_2 to the atmosphere or land would on the average give exposures in the range of those accepted in the atomic industry and generally they are distinctly less or negligible.

In the case of reentry, where the capsule releases particulate PuO_2 upon impact with the surface, persons in the path of the ensuing cloud might acquire a lung burden somewhat in excess of the occupational limit. This would apply most to those who happened to be at the impact point or within a small ovoid shaped area downwind of the point of impact; persons to the side or still further downwind would retain lesser amounts. The Subpanel is aware that the above judgments apply to the average person taking an average exposure; the source terms are not concerned with unevenness of concentration within an isopleth or other space.

The Subpanel originally suggested that the following be considered because of the possibility of abort on the pad with release of fuel:

1) Exclusion of non-essential personnel from the launch area;

2) Examination of the LCC and VAB air-handling system for measures to preclude intake of PuO_2 aerosols; and

3) Standby airborne radiological monitoring system with long-range overwater capability for PuO_2.

The Subpanel is now aware that contingency plans are being prepared for the launch abort situation and that normal precautions associated with potential releases of nuclear material will be taken.

REFERENCES

1. C. R. Richmond, J. E. London, J. S. Wilson, and J. Langham. Biological Response to Small Discrete Highly Radioactive Sources - I. Observations on Gastrointestinal Transit, Histological Change, and Tissue Deposition in Beagles Fed One-Half Curie $_{238}PuO_2$ for Six Months. Health Physics 15: 487 (1968).

2. V. H. Smith, H. A. Ragan, B. J. McClanahan, J. L. Beamer, and J. L. Palotay. The Passage Time of Plutonium Oxide in Pigs. In Gastrointestinal Radiation Injury. M. F. Sullivan, Ed. Excerpta Medica Foundation Monographs on Nuclear Medicine and Biology, Number 1. pps. 518-523 (1968).

3. R. C. Thompson. Biological Factors Chapter 25 in Plutonium Handbook, Volume 2. O. J. Wick, Ed. Gordon and Breach, N. Y.

4. M. H. Weeks, J. Katz, W. D. Oakley, J. E. Ballou, L. A. George, L. K. Bustad, R. C. Thompson, and H. A. Kornberg. Further Studies on the Gastrointestinal Absorption of Plutonium. Radiation Research 4: 339 (1956).

5. Recommendations of the International Commission on Radiological Protection. Report of Committee II on Permissible Dose for Internal Radiation. Publications 2 (1959), 6 (1962), and 9 (1965).

6. J. R. Mann and R. A. Kirchner. Evaluation of Lung Burden. Following Acute Inhalation Exposure to Highly Insoluble PuO_2. Health Physics 13: 877 (1967).

7. Deposition and Retention Models for Internal Dosimetry of the Human Respiratory Tract. Task Group on Lung Dynamics. Health Physics 12: 173 (1966).

8. V. I. Malykhin, V. P. Shamov, N. A. Isanin, and L. A. Bogdanova. Tissue-Dosimetry Characteristics of Plutonium (Preliminary Data Relating to the Determination of Maximum Permissible Levels for the Accidental Intake of Plutonium. Presented at the IAEA Panel Meeting on Detection and Assessment of Uranium and Plutonium in the Whole Body and in Critical Organs. Vienna, 11-15 November, 1968.

9. R. V. Osborne. Plutonium-239 and Other Nuclides in Ground-Level Air and Human Lungs During Spring 1962. Nature 199: 143 (1963).

10. P. W. Krey, D. Bogen, and E. French. Plutonium in Man and His Environment. Nature 195: 263 (1962).

11. P. J. Magno, P. E. Kauffman, and B. Shleien. Plutonium in Environmental and Biological Media. Health Physics 13: 1325 (1967).

12. Smorodintseva, et al. Study of the Uptake of Airborne Pu-239 by the Human Organism. Unpublished translation of United Nations Scientific Committee on the Effects of Atomic Radiations, 1968. (Data provided by J. Harley, HASL).

13. W. H. Langham. The Problem of Large-Area Plutonium Contamination. Presented at The National Center of Radiological Health. Dec. 6, 1968.

Table 1

Relation Between Particle Diameter, Particle Number and Number of Cells Irradiated For a Lung Burden of 0.016 μCi $_{238}PuO_2$

Diameter (μ)	Number Particles	Number Cells Irradiated*
0.01	2.0×10^8	5.2×10^{10}
0.1	2.0×10^5	5.4×10^7
1.0	2.0×10^2	5.6×10^4
10	2.0×10^{-1}	1.4×10^3 **

* For each particle the number of cells exposed within the 40 μ alpha particle range are estimated. The total number of cells irradiated becomes the product of the number of cells irradiated per particle and the number of particles. A cell volume of 10^3 μ^3 was assumed.

** Number of cells for a single 10 μ particle in this case.

TABLE 2

Calculated Tumor Probability per Person as a Function of Particle Size of the Retained Lung Burden

Amount Retained per Person (μCi)	Tumor Probability if Particles were of Indicated Diameter (in microns) 1.0	0.5	0.1	0.01
0.03	1.0	1.0	1.0	5×10^{-5}
0.0015	0.9	1.0	0.9	2.5×10^{-6}
0.0005	0.5	0.9	0.5	8.3×10^{-7}
7×10^{-7}	0	0	4.5×10^{-4}	0